

FLOW VISUALIZATION AND DETERMINATION OF TEMPERATURE  
DISTRIBUTION IN INCLINED CHANNELS

A THESIS SUBMITTED TO  
THE GRADUATE SCHOOL OF NATURAL AND APPLIED SCIENCES  
OF  
MIDDLE EAST TECHNICAL UNIVERSITY

BY

ABDÜLAZİZ MEHMET SAĞLAMCI

IN PARTIAL FULFILLMENT OF THE REQUIREMENTS  
FOR  
THE DEGREE OF MASTER OF SCIENCE  
IN  
MECHANICAL ENGINEERING

MARCH 2018



Approval of the thesis:

**FLOW VISUALIZATION AND DETERMINATION OF TEMPERATURE  
DISTRIBUTION IN INCLINED CHANNELS**

submitted by **ABDÜLAZİZ MEHMET SAĞLAMCI** in partial fulfillment of the requirements for the degree of **Master of Science in Mechanical Engineering Department, Middle East Technical University** by,

Prof. Dr. Halil Kalıpçılar  
Dean, Graduate School of **Natural and Applied Sciences**

\_\_\_\_\_

Prof. Dr. M. A. Sahir Arıkan  
Head of the Department, **Mechanical Engineering**

\_\_\_\_\_

Asst. Prof. Dr. Özgür Bayer  
Supervisor, **Mechanical Engineering Dept., METU**

\_\_\_\_\_

**Examining Committee Members**

Assoc. Prof. Dr. Ahmet Yozgatlıgil  
Mechanical Engineering Dept., METU

\_\_\_\_\_

Asst. Prof. Dr. Özgür Bayer  
Mechanical Engineering Dept., METU

\_\_\_\_\_

Assoc. Prof. Dr. Cemil Yamalı  
Mechanical Engineering Dept., METU

\_\_\_\_\_

Prof. Dr. Selin Aradağ Çelebioğlu  
Mechanical Engineering Dept., TOBB ETU

\_\_\_\_\_

Asst. Prof. Dr. Ece Aylı İnce  
Mechanical Engineering Dept., ÇANKAYA ÜNİ.

\_\_\_\_\_

**Date: 09.03.2018**

**I hereby declare that all information in this document has been obtained and presented in accordance with academic rules and ethical conduct. I also declare that, as required by these rules and conduct, I have fully cited and referenced all material and results that are not original to this work.**

Name, Surname: Abdülaziz Mehmet SAĞLAMCI

Signature:

## **ABSTRACT**

### **FLOW VISUALIZATION AND DETERMINATION OF TEMPERATURE DISTRIBUTION IN INCLINED CHANNELS**

Sağlamcı, Abdülaziz Mehmet  
M.S., Department of Mechanical Engineering  
Supervisor: Asst. Prof. Dr. Özgür Bayer

March 2018, 86 Pages

Subway transportation systems play an important role in human life in this century. Millions of people make use of subway transportation every day in metropolises. In subways, there is a very crucial situation "case of fire and smoke generation" that must be prevented. In subway areas, it is known that stairs are used to connect the ground with the subway area, metro stations in other words. Stairs have an angle with the ground horizontal called as tilt angle. The most important case of smoke movement in case of a fire occurs in the area of the subway constructions as being fresh air access for people.

Originating a metro tunnel and simulating the case of fire, the objective of this thesis is to understand the smoke flow and temperature distribution characteristics in a combined tunnel composed of horizontal and inclined parts. Many researches have been made so far to lower the risk of poisoning cases due to smoke.

In this study, both experimental and numerical investigations were made having larger tilt angles for the inclined parts of the domain varying from 25 to 40 degrees. The smoke flow patterns were observed by means of a CFD (Computational Fluid Dynamics) program. Velocity fields and the temperature distributions were investigated through the tunnel. In experiment, a controlled fire was started by burning mixture of propane-butane mixture and temperature distribution data was collected throughout the experimental tunnel using thermocouples attached in six planes located in the setup cross-sections. The experimental results were used to verify the CFD solution. Temperature trends shows indicative manner so that velocity profiles were investigated numerically. Effects of the ventilation velocity, inclination angle and fire location on the temperature and velocity profiles in the tunnel were investigated.

**Keywords:** Smoke flow, inclined tunnels, temperature distribution.

## ÖZ

### EĞİMLİ KANALLARDA AKIŞ GÖRÜNTÜLENMESİ VE SICAKLIK DAĞILIMININ İNCELENMESİ

Sağlamcı, Abdülaziz Mehmet  
Yüksek Lisans, Makina Mühendisliği Bölümü  
Tez Yöneticisi: Y. Doç. Dr. Özgür Bayer

Mart 2018, 86 Sayfa

Günümüzde yeraltı ulaşım sistemleri insan hayatında önemli bir rol oynamaktadır. Büyük şehirlerde, her gün milyonlarca insan yer altı ulaşımını kullanmaktadır. Yeraltında doğabilecek en büyük problemlerden biri çıkabilecek bir yangın ve neticesinde oluşacak zehirli gaz salınımıdır ki bu durum için önlemler alınmalıdır. Yer altı istasyonlarında açık havaya çıkışlar merdivenler aracılığı ile gerçekleşmektedir. Söz konusu merdivenlerin yer düzlemi ile yaptığı açılı eğim açısı olarak adlandırılmaktadır. Yangın durumunda dikkate alınması gereken en önemli bölge de insanların açık havaya tahliyesinin sağlandığı merdivenlerdir.

Bu çalışmanın amacı, metro tünellerinden esinlenerek yapılmış yatay ve eğimli bölümlerden oluşan bir tünelde, yangın anında duman akışının ve sıcaklık dağılımının karakteristik özelliklerini incelemektir. Bu güne kadar benzer durumlarda insanların zehirli gazdan etkilenme riskini azaltmak için birçok çalışma yapılmıştır.

Bu çalışmada, 25 derece ile 40 derece arasında olacak şekilde, daha yüksek eğim açılarında tünel içi hava akışı ve sıcaklığının karakterizasyonunu belirlemek için hem deneysel, hem de sayısal analizler yapılmıştır. Duman akışı bir HAD (Hesaplamalı Akışkanlar Dinamiği) programı ile incelenmiştir. Duman dağılışı, hız vektörleri ve tünel boyunca sıcaklık dağılımı analizi yapılmıştır.

Deneysel çalışmada, tünel boyunca belirlenen altı kesit alanına ısı çiftleri yerleştirilerek sıcaklık dağılımı ölçülmüş ve bu sonuçlar HAD çözümünü doğrulamak amacıyla kullanılmıştır. Deneysel çalışmada, yakıt olarak propan-bütan karışımı kullanılarak oluşturulan kontrollü yangın çıkarılmış, ısı çiftleri kullanılarak tünel boyunca belirlenen noktalardan sıcaklık verileri toplanmıştır. Bunun yanı sıra, deneysel ve sayısal çalışmaların sonuçları karşılaştırılmış olup sıcaklık datalarındaki trendlerin birbiri ile uyum içinde olduğu görülerek hız profillerinin incelenmesi sayısal olarak yapılmıştır. Havalandırma hızının, eğim açısının ve yangın konumunun tünel içerisindeki sıcaklık ve hız profillerine etkileri belirtilmiştir.

Anahtar Kelimeler: Duman akışı, eğimli tüneller, sıcaklık dağılımı.



## **ACKNOWLEDGMENTS**

I would like to express my sincere thanks to my supervisor Asst. Prof. Dr. Özgür BAYER for his guidance and support.

I would like to express my thanks TOBB University of Economics and Technology Hydro Laboratory for providing access to commercial CFD program used for the numerical analysis.

I would like to thank my friend and colleague from Middle East Technical University, Salim SANIOĞLU for their suggestions and comments in this thesis.

Lastly, I would like to give my special thanks to my family for their experience sharing, material aid, spritrial support, guidance, and amazing motivation to stare down the hard period of the thesis progress.

## TABLE OF CONTENTS

ABSTRACT.....	v
ÖZ.....	vii
ACKNOWLEDGMENTS.....	ix
TABLE OF CONTENTS.....	x
LIST OF TABLES.....	xii
LIST OF FIGURES.....	xiii
LIST OF SYMBOLS.....	xvii
LIST OF ABBREVIATIONS.....	xviii

### CHAPTERS

1. INTRODUCTION.....	1
1.1 General.....	1
1.2 Natural Ventilation.....	3
1.3 Mechanical Ventilation.....	3
1.4 Literature Review.....	3
1.4.1 Numerical Studies.....	3
1.4.2 Experimental Studies.....	6
1.5 Objective of the Thesis.....	11
1.6 Thesis Outline.....	12
2. METHODOLOGY.....	13
2.1 Governing Equations.....	13
2.2 Experimental Work.....	14
2.3 Experimental Procedure.....	17
2.4 Numerical Procedure.....	20
3. RESULTS AND DISCUSSION.....	25

3.1 Results of Midpoint Temperature on Planes.....	25
3.1.1 Midpoint Temperature Trends for Different Inclination Angles.....	27
3.1.2 Midpoint Temperature Trends for Different Ventilation Velocities.....	30
3.2 Results of Maximum Temperature on Planes.....	35
3.2.1 Maximum Temperature Trends for Different Inclination Angles.....	35
3.2.2 Maximum Temperature Trends for Different Ventilation Velocities.....	38
3.3 Results of Numerical Midpoint Velocity on Planes .....	43
3.3.1 Midpoint Velocity Trends for Different Inclination Angles.....	43
3.3.2 Midpoint Velocity Trends for Different Ventilation Velocities.....	46
3.4 Numerical Streamline Results.....	51
3.5 Numerical Streamline Results for Lower Ventilation Velocity..	53
4.CONCLUSION.....	57
4.1 Conlusions.....	57
4.2 Recommendations for Future Work.....	59
REFERENCES.....	61
APPENDICES	
A. CONTOUR RESULTS OF CFD.....	65
B. DATA TAKEN IN STUDIES .....	77
C. BOUNDARY CONDITIONS AND CFD SETTINGS.....	83

## LIST OF TABLES

### TABLES

Table 2.1 Experiment and numerical work matrix.....	19
Table 2.2 Locations of the planes (cm) in x-direction for inclination angles.....	19
Table 2.3 Properties of the model.....	20
Table 2.4 Mesh properties.....	21
Table 2.5 Boundary conditions... ..	23
Table 2.6 Numerical settings.....	23
Table 3.1 Key results.....	53

## LIST OF FIGURES

### FIGURES

Figure 1.1 Fire in Daegu Subway Station, South Korea, in 2003.....	1
Figure 1.2 Back-layering.....	10
Figure 1.3 Smoke flow patterns for different angles.....	11
Figure 2.1 Experimental set-up.....	14
Figure 2.2 Planes with thermocouples attached.....	15
Figure 2.3 Fire in the tunnel.....	16
Figure 2.4 Discharge fan.....	16
Figure 2.5 AC to DC converter unit and fan speed controller.....	17
Figure 2.6 Experimental setup drawing.....	18
Figure 2.7 Representation of thermocouple positions.....	19
Figure 2.8 Numerical domain.....	20
Figure 2.9 (a) Mesh, (b) a randomly cut plane for the model .....	21
Figure 2.10 Mesh independency analyses results.....	22
Figure 3.1 Profiles of midpoint temp. on planes in case A for 2.0m/s.....	27
Figure 3.2 Profiles of midpoint temp. on planes in case A for 2.5m/s.....	27
Figure 3.3 Profiles of midpoint temp. on planes in case A for 3.0m/s.....	28
Figure 3.4 Profiles of midpoint temp. on planes in case B for 2.0m/s.....	29
Figure 3.5 Profiles of midpoint temp. on planes in case B for 2.5m/s.....	29
Figure 3.6 Profiles of midpoint temp. on planes in case B for 3.0m/s.....	30
Figure 3.7 Profiles of midpoint temp. on planes in case A for 25°.....	31
Figure 3.8 Profiles of midpoint temp. on planes in case A for 30°.....	31
Figure 3.9 Profiles of midpoint temp. on planes in case A for 35°.....	32
Figure 3.10 Profiles of midpoint temp. on planes in case A for 40°.....	32

Figure 3.11 Profiles of midpoint temp. on planes in case B for 25°.....	33
Figure 3.12 Profiles of midpoint temp. on planes in case B for 30°.....	33
Figure 3.13 Profiles of midpoint temp. on planes in case B for 35°.....	34
Figure 3.14 Profiles of midpoint temp. on planes in case B for 40°.....	34
Figure 3.15 Profiles of maximum temp. on planes in case A for 2m/s.....	35
Figure 3.16 Profiles of maximum temp. on planes in case A for 2.5m/s.....	36
Figure 3.17 Profiles of maximum temp. on planes in case A for 3m/s.....	36
Figure 3.18 Profiles of maximum temp. on planes in case B for 2m/s.....	37
Figure 3.19 Profiles of maximum temp. on planes in case B for 2.5m/s.....	37
Figure 3.20 Profiles of maximum temp. on planes in case B for 3m/s.....	38
Figure 3.21 Profiles of maximum temp. on planes in case A for 25°.....	39
Figure 3.22 Profiles of maximum temp. on planes in case A for 30°.....	39
Figure 3.23 Profiles of maximum temp. on planes in case A for 35°.....	40
Figure 3.24 Profiles of maximum temp. on planes in case A for 40°.....	40
Figure 3.25 Profiles of maximum temp. on planes in case B for 25°.....	41
Figure 3.26 Profiles of maximum temp. on planes in case B for 30°.....	41
Figure 3.27 Profiles of maximum temp. on planes in case B for 35°.....	42
Figure 3.28 Profiles of maximum temp. on planes in case B for 40°.....	42
Figure 3.29 Numerical midpoint x-velocity profiles in case A for 2.0m/s.....	43
Figure 3.30 Numerical midpoint x-velocity profiles in case A for 2.5m/s.....	44
Figure 3.31 Numerical midpoint x-velocity profiles in case A for 3.0m/s.....	44
Figure 3.32 Numerical midpoint x-velocity profiles in case B for 2.0m/s.....	45
Figure 3.33 Numerical midpoint x-velocity profiles in case B for 2.5m/s.....	45
Figure 3.34 Numerical midpoint x-velocity profiles in case B for 3.0m/s.....	46
Figure 3.35 Numerical midpoint x-velocity profiles in case A for 25°.....	47
Figure 3.36 Numerical midpoint x-velocity profiles in case A for 30°.....	47
Figure 3.37 Numerical midpoint x-velocity profiles in case A for 35°.....	48
Figure 3.38 Numerical midpoint x-velocity profiles in case A for 40°.....	48
Figure 3.39 Numerical midpoint x-velocity profiles in case B for 25°.....	49

Figure 3.40 Numerical midpoint x-velocity profiles in case B for 30°.....	49
Figure 3.41 Numerical midpoint x-velocity profiles in case B for 35°.....	50
Figure 3.42 Numerical midpoint x-velocity profiles in case B for 40°.....	50
Figure 3.43 Numerical streamline results for case A.....	51
Figure 3.44 Numerical streamline results for case B.....	52
Figure 3.45 Numerical streamlines of $VV= 0.1\text{m/s}$ for case A.....	54
Figure 3.46 Numerical streamlines of $VV= 0.1\text{m/s}$ for case B.....	55
Figure A.1 Temperature contours for case A.....	65
Figure A.2 Temperature contours on plane horz1 for case A.....	66
Figure A.3 Temperature contours on plane horz2 for case A.....	67
Figure A.4 Temperature contours on plane inc1 for case A.....	68
Figure A.5 Temperature contours on plane inc2 for case A.....	69
Figure A.6 Temperature contours on plane inc3 for case A.....	70
Figure A.7 Temperature contours on plane inc4 for case A.....	71
Figure A.8 Temperature contours for case B.....	72
Figure A.9 Temperature contours on plane inc1 for case B.....	73
Figure A.10 Temperature contours on plane inc2 for case B.....	74
Figure A.11 Temperature contours on plane inc3 for case B.....	75
Figure A.12 Temperature contours on plane inc4 for case B.....	76
Figure B.1 Temperature results of experiments for case A with $\alpha=25^\circ$ .....	77
Figure B.2 Temperature results of experiments for case A with $\alpha=30^\circ$ .....	77
Figure B.3 Temperature results of experiments for case A with $\alpha=35^\circ$ .....	78
Figure B.4 Temperature results of experiments for case A with $\alpha=40^\circ$ .....	78
Figure B.5 Temperature results of experiments for case B with $\alpha=25^\circ$ .....	78
Figure B.6 Temperature results of experiments for case B with $\alpha=30^\circ$ .....	79
Figure B.7 Temperature results of experiments for case B with $\alpha=35^\circ$ .....	79
Figure B.8 Temperature results of experiments for case B with $\alpha=40^\circ$ .....	79
Figure B.9 Temperature results of numerical work for case A with $\alpha=25^\circ$ .....	80
Figure B.10 Temperature results of numerical work for case A with $\alpha=30^\circ$ .....	80
Figure B.11 Temperature results of numerical work for case A with $\alpha=35^\circ$ .....	80
Figure B.12 Temperature results of numerical work for case A with $\alpha=40^\circ$ .....	81

Figure B.13 Temperature results of numerical work for case B with $\alpha=25^\circ$ .....	81
Figure B.14 Temperature results of numerical work for case B with $\alpha=30^\circ$ .....	81
Figure B.15 Temperature results of numerical work for case B with $\alpha=35^\circ$ .....	82
Figure B.16 Temperature results of numerical work for case B with $\alpha=40^\circ$ .....	82
Figure C.1 Mass flow rate into the system through inlet.....	83
Figure C.2 Mass flow rate into the system through the beginning of the horizontal part.....	84
Figure C.3 Mass flow rate into the system through the end of the inclined part.....	84
Figure C.4 Mass flow rate leaving the system through the fan.....	85
Figure C.5 General setup for numerical analyses.....	85
Figure C.6 Turbulent model for numerical analyses.....	86
Figure C.7 Solution methods for numerical analyses.....	86



## LIST OF SYMBOLS

- V: velocity [m/s]  
 $\alpha$ : inclination Angle [degrees]  
 $\dot{m}$ : mass Flow Rate of the LPG [kg/h]  
 $D_{\vec{v}}$ : material derivative for moving frame with velocity V  
T: temperature [°C]  
 $V_f$ : velocity of the fluid [m/s]  
t: time [s]  
 $\rho$ : density of the fluid [kg/m<sup>3</sup>]  
 $\sigma$ : stress [N/m<sup>2</sup>]  
g: gravitational acceleration [m/s<sup>2</sup>]  
k: turbulent kinetic energy [J/kg]  
 $\mathcal{E}$ : dissipation rate of turbulence kinetic energy [J/kg-s]  
 $\vec{\sigma}$ : stress tensor [N/m<sup>2</sup>]  
 $\vec{u}$ : velocity vector [m/s]  
 $\sigma_k$ : turbulent Prandtl number of turbulence kinetic energy  
 $\sigma_{\mathcal{E}}$ : turbulent Prandtl number of dissipation rate

## **LIST OF ABBREVIATIONS**

Mid: Middle

Num: Numerical

Exp: Experimental

LPG: Liquefied Petroleum Gas

CFD: Computational Fluid Dynamics

HRR: Heat Release Rate

CVV: Critical Ventilation Velocity

VV: Ventilation Velocity

CFL: Courant-Fredrichs-Levy

Temp: Temperature

## CHAPTER 1

### INTRODUCTION

#### 1.1 General

In recent years, mass transportation has become an important subject for life. Due to heavy traffics in metropolises, giving preference to public transportations, especially subway transportation, seems logical. However, due to some accidents causing fire in such subway areas may result in severe problems for people. Due to fire, toxic gases like carbon monoxide and temperature increase in tunnels may lead people to die. A very striking accident event in Figure 1.1, resulted in 192 dead, 151 injured in Daegu Subway station, South Korea, in 2003.



**Figure 1.1 Fire in Daegu Subway Station, South Korea, in 2003[1]**

Being inspired by such a case, fire scenarios in underground systems that may result in disasters are investigated in scaled and real tunnels by means of experiments and numerical approaches, originated from subway systems. Evacuation routes are investigated to be clearly determined. Furthermore, in different cases, the routes are to be analyzed in terms of temperature distributions and smoke flow patterns. Researchers try to analyze and compare the different case of fires in terms of fire locations, dimensions of the tunnels, the effects of subway transportation vehicles passing through or stopping at the stations, and the ventilation systems sitting on the subway systems.

Ventilation systems are very significant units in the tunnels supplying fresh air inside and exhausting poor quality air. Besides the main function in daily conditions, ventilation systems have a very important role in case of a fire scenario. People in subways must be prevented from the resultant toxic gases during the evacuation. Therefore, ventilation systems are to be designed to discharge the toxic gases without affecting people.

Furthermore, a common problem that comes to the forefront is the back-layer formation. Back-layer is a phenomenon that is the back flow formation to the opposite direction of the flow going through the intended direction of combustion gases to be discharged outside. Many researches have been conducted so far and observation revealed that this phenomenon depends on different parameters such as velocity, inclination angles of tunnel, temperature etc. Especially critical ventilation velocity (CVV) that is the minimum air velocity required to suppress the smoke spreading against the longitudinal ventilation flow during tunnel fire situations is a crucial parameter. Analyses clarified that back-layer formation must be prevented by improving the conditions in tunnels with optimizing the related parameters.

## **1.2 Natural Ventilation**

Natural ventilation in subway systems is generally worked by using the vent shafts. Air flow passing through tunnels by means of train piston effect leads moving the low quality air inside to outside throughout the vent shafts. Trains push the air forward and drawn the air behind, called as train piston effect [2].

These shafts placed at the beginning and the end of stations, provide ventilation and also cool the air inside. Natural ventilation systems are to be well-designed in terms of dimensions and placing regions to avoid short circuiting of air.

## **1.3 Mechanical Ventilation**

Mechanical ventilation is a necessity in subway stations in case of the incapability of natural ventilation systems. As natural ventilation depends on the train movement, capacity changes with the passing frequency of trains. Fans are attached to shafts to overcome this kind of incapability of air exchange between outside and inside. Not only in the incapability situation but also in case of a subway fire scenario, fans are very important units to get rid of gases. At that, people should be prevented from gas poisoning, and visibility inside should be kept in a reasonable value. Accordingly, fans are to be operated in such a way that they all lead the air flow through the desired direction to exhaust smoke outside.

## **1.4 Literature Review**

### **1.4.1 Numerical Studies**

Blanco et al. [3] studied fire scenario in longitudinal tunnels to avoid back-layer formation of combustion gases by means of numerical work using a CFD program

considering natural ventilation. Numerical work was based on transient analyses. Smoke propagation in road tunnels was investigated constructing a model. The model was tested by comparing the results with the data taken from the Memorial Tunnel Fire Ventilation Test Program in which fire scenarios had been investigated previously.

Numerical model used in the study overestimated critical ventilation velocities for higher heat release rates. Thus, it was stated that the values of the temperature and mass flow rates of the fire source should be offset with respect to heat release rates to see the ventilation effect on back-layer formation.

Yang et al. [4] numerically investigated the effect of initial velocity fields on smoke diffusion characteristics by means of two cases. One of them was simulating a train that was standing in a station and as the second one, a train decelerating in a fire scenario taking place below the under plate of the head of a train. The possible routes for passenger to evacuate were revealed. Temperature and visibility results towards the back of the train are safe for six minutes without any ventilation. For the second one, it was four minutes safe for leaving the tunnel towards platform ahead.

Ji et al. [5] have made a study to investigate the upstream maximum centerline temperature in inclined urban road tunnel fires. Fire scenarios with different inclination angles of  $5^{\circ}$ - $15^{\circ}$  were simulated. Results of this study clarified that peak temperature occurs at the downstream region rather than right above the fire source. The points where peak temperatures showed up were called as virtual fire sources. Furthermore, it was observed that back-layer length did not reach the left side of the tunnel end at the inclination angles of  $7^{\circ}$  and higher.

Aradağ [2] studied the train piston effect on the underground transportation system ventilation. Trains entering a tunnel cause air in front displace through and it was stated that pressure wave occurs in front of the train, therefore the wave at issue disturbing passengers standing in station. Phenomenon is called as train piston effect.

The subject was examined focusing on transient pressure and velocity distributions along the tunnel and Ankara Metro Third Phase Project was taken as basis. Since the considered variables of unsteady processes might be fluctuating in an uncontrollable manner in case of more than one train approaching to the station, a single track tunnel was examined in the study. In progress, a computer program called Trapac (Train Piston Action) was developed. Partial differential equations governing unsteady flow were converted to ordinary differential equations and program was coded accordingly to solve the equations numerically.

In the study including constant and variable train speed, and tunnels with and without ventilation shafts states the importance of defining boundary conditions and choosing time steps carefully to observe the transient process in the system clearly. Therefore, the CFL number proposed by Courant-Fredrichs-Levy stability criterion was taken into consideration. Moreover, number of grid points and time steps were kept in sight together for the stability of the solution. The final results were compared with the related literature and verified. Suggestions on how to reduce steepness of primary air wave front were given.

Kayılı [6] numerically researched the flow patterns, smoke propagation and temperatures on escape routes of passenger in case of a fire in underground transportation systems. Three scenarios of transient analyses were performed in two different CFD programs.

For the scenario with jet fans satisfied the requirements for a successful evacuation with respect to other scenarios in which smoke filled the path of passenger according to the time elapsed of 6 minutes.

Musluoğlu [7] investigated the tunnel geometry effects, ventilation and evacuation strategies in case of a fire in underground trains. Two different scenarios of a small size arson fire and a severe baggage fire were studied. Results of two different CFD programs used for the study were compared.

It was stated that, different effects existing such as windows fails, open doors have different impacts on flame spread and effective ventilation of smoke. For this reason, the preferred routes of evacuation show an alteration for different cases. Yazıcı [8] seek out the effect of geometry on the hot air flow discharge. Besides, the fire emergency ventilation systems are criticized using ANSYS software with a model of Ümraniye Metro Station. It was claimed that simple additions to station geometry like fire screens is more effective than increasing ventilation capacity to stop fire propagation.

Altay [9] researched the effect of forced ventilation on heat releasing rates in case of a fire in longitudinal road tunnels using fire dynamics simulator software for analyses. Different fan groups were settled on different locations for power of ten and fifty megawatts fires of vehicle and pool fires. It was claimed that improvements on the existing tunnel constructions look better in exhausting resulted gases of fire than revolutionizing the whole system and suggested axial mobile fan installations to the tunnels as a solution for the cases analyzed.

Yüzücü [10] concentrated on the evacuation strategies from a building in case of a fire. A software was used and six different buildings of Sakarya were modeled for numerical analyses. Different scenarios for ventilations were investigated by means of fans and without fans as natural ventilation. It was revealed that for one of the scenarios studied, an evacuation may results in a better way without using fans to discharge the smoke for buildings.

#### **1.4.2 Experimental Studies**

Wu et al. [11] investigated the effect of slope on critical ventilation velocity that is the minimum air velocity required to suppress the smoke spreading against the longitudinal ventilation flow during tunnel fire situations to control the back-layering of the smoke. Downhill slopes of zero to ten degrees were investigated. It was stated that the effect of the slope was modest and a formulae was suggested for predicting



the critical ventilation velocity.

Wu and Bakar [12] conducted an experiment and made a CFD analysis to investigate critical ventilation velocity and its dependence on the dimensions of the tunnel. They have changed the cross-section of the tunnel and observed the effect of aspect ratios, height on the critical ventilation velocity. Besides the dimensional effects, the results give the proportionality between HRR and CVV was suggested with a relation that critical ventilation velocity is proportional with the one third of heat release rate.

Tsai et al. [13] seek out the effects of dimensions on the tunnel fires and studied the subject of critical ventilation velocity for tunnel fires occurring near tunnel exits. In this work, a tunnel of 4m long, square cross-section of width and height of 0.6m was built, and parameters were chosen as fire size and distance of fire to the tunnel exit. Fire locations were determined at 0.5, 1.0, 1.5 m from the tunnel exit. The fire was set as making use of 6.3\*6.3 cm and 9.0\*9.0 cm square gasoline fuel pans. Result of this study stated that CVV decreases as fire approaches the tunnel exit.

Tanaka et al. [14] analyzed the smoke propagation of a fire in a tunnel when a concentrated exhaust ventilation system stands for. A one over five scales of a real tunnel was used for the experimentation. Smoke discharge increase leads to an improvement on the evacuation environment on the downstream side of the concentrated smoke ventilation.

Additionally, changing position of the fire sources does not influence the evacuation environment of the downstream side of the concentrated smoke ventilation. Some of the experimental studies are concentrated on the heat release rate parameter on ventilation characteristics [15] – [21].

As a continuation study of his master work, Kayılı [15] carried out an experimental research to investigate the effect of vehicle blockage in tunnels on heat releasing rates and temperature distributions with different longitudinal ventilation velocities. In the

setup wooden materials were burned and mass loss of the materials was measured by means of a sensitive balance. It is revealed that increase of ventilation velocity led to temperature inside the tunnel decrease and heat release rate increase. It was also stated that velocities higher than 2m/s did not affect the heat releasing rate.

Yamalı [16] investigated the heat release rates on tunnels and seek out the effect of ventilation velocity, fuel content and pan geometry on the combustion characteristics of heat release rates, burning rates and ceiling gas temperatures in case of fire in a longitudinal tunnel. Ventilation velocities were changed from 0.5 m/s to 2.5 m/s with the increments of 0.5 m/s and the volumetric fractions of ethanol blended heptane fuel mixtures were varied in the study.

Ventilation velocity has a significant effect on heat releasing rates, burning rates and ceiling gas temperatures. The same effect of ventilation velocity was stated by Shafee et al. [17].

Shafee et al. [18] investigated the effects of ventilation velocity on burning rates of ethanol pool fires in different size and depth. Results revealed that ventilation velocity affects the burning rates.

Kayılı et al. [19] worked on the blockage ratio and ventilation velocity effects on the heat releasing rates of fires by wood sticks. The results show ventilation velocity and area of burning substances affect the heat releasing rates in different manners.

Kayılı et al. [20] research the geometrical parameters of the burning object on heat releasing rates with different ventilation velocities by means of analysis of variance method. Results state that increase of ventilation velocity increases the heat release rates of burned vehicles; however, this effect is valid to the velocity of 2m/s. After this, heat releasing rate is not affected by ventilation velocity.

Çelik [21] studied on the heat release rates and effects of fuel sources on the average

mass loss rates, peak mass loss rates and heat release rates of pool fires. There were three different fuel sources of ethanol, gasoline and mixture of them. Ethanol was used due the fact that it is an alternative fuel source having renewable characteristics. Changing ventilation velocities, pan geometries and initial fuel thicknesses results were taken.

It was stated that increase of amount of fuel leaded mass loss rate increasing and also, peak heat release rates for ventilation velocity of 0.5 m/s were very smaller than 1.5 and 2.5 ones due to deflection of flame for gasoline and mixture.

Wu et al. [22] worked through the interaction of fire plume with inclined surface experimentally using a system with CCD camera and computer system. With a fire produced, sequences of images of fire plumes at inclination angles of 0°-40° were taken and the effect of inclination angle of the surface was investigated. Surfaces taken into account were both isothermal and adiabatic to which both flame and buoyant flow attached near burner.

There was a point plume detached from the surface and rose at an angle to the surface. The length of the fire attachment is measured and it was seen that fire plume attachment length increase sharply after 24° of inclination angle and critical angle is not sensitive to the fire HRR and surface conditions.

Vauquelin and Wu [23] looked for the influence of tunnel width on longitudinal smoke control. In this study, in which a longitudinal tunnel which was horizontal to ground was investigated, height of tunnel (H) was kept as constant and weight of the tunnel (W) was taken as variable to observe the influence of W on CVV.

Study results showed that for aspect ratio (W/H) greater than unity, CVV is seen as decreasing with increase of W and for W/H lower than unity, CVV is increasing with increase of W. Furthermore, back-layer formation was observed and shown.

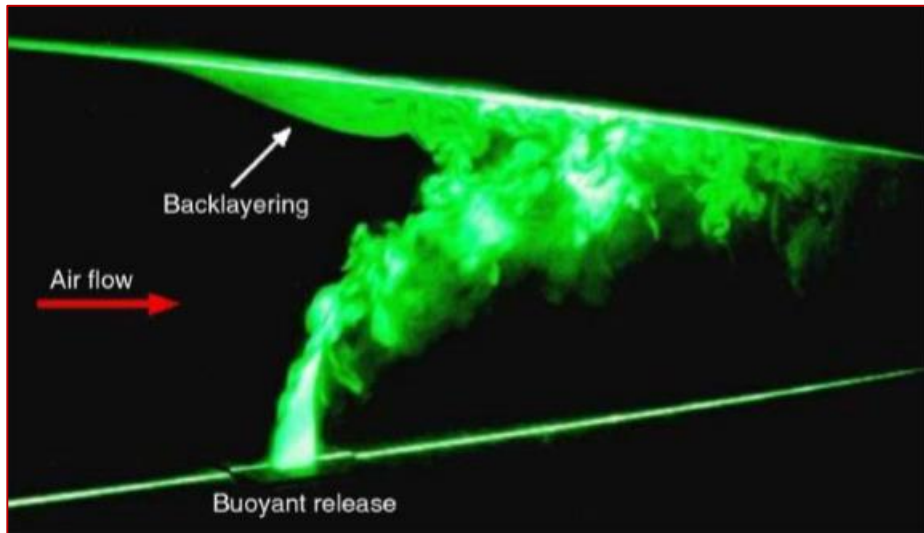


**Figure 1.2 Back-layering [23]**

Hu et al. [24] worked through the CO concentration and smoke spread by fire in a long tunnel. Study included both numerical and experimental works in which results showed that numerical results were in a good agreement with experimental ones. It was revealed that CO concentration linearly increases with the height and exponentially decreases with the distance away from the fire source.

Zhang et al. [25] investigated the inclination effect on CO generation and smoke movement pattern in inclined tunnel fires. Different inclination angles of  $-10^\circ$ ,  $-5^\circ$ ,  $0^\circ$ ,  $5^\circ$ ,  $10^\circ$  were set for the study, and a fire sources was set by n-heptane pool fires. It was stated that while smoke layer thickness with the increase of inclination angle, CO concentration decreases. Furthermore, it is reported that outflow rate increases with the increase of inclination angle.

For a further investigation, Hu et al [26] researched the back-layer length and the critical ventilation velocity of longitudinal ventilation in case of fire in tunnels. Critical ventilation velocity to make back-layer length zero, was investigated by experiments and numerical works by means of a CFD program. It was stated that back-layer length is increasing with the increase of the fire size and decreasing with

the increase of the tunnel height and ventilation. Moreover, a semi-empirical model was formulated to predict the length of back-layer.

Chow et al. [27] studied the subject of longitudinal ventilation for smoke control in a tilted tunnel by modeling scale saying that many tunnels in big cities are inclined. In this study, claiming that smoke movement in tilted tunnels is not fully understood and a tunnel of 2m length was constructed as 1/50 scaled model with a material of acrylic plastic. 0.00097 kW propanol fire was set combined with burning pellets generating smoke. Experiments were performed till 30° of inclination angle and a fan was used for longitudinal ventilation. Obtained results in the study clarifies that increase of tunnel inclination angle resulted on larger amount of smoke flow and more importantly, a larger tilt angle of 25° would give larger flow in the tunnel as observed from the smoke pattern.

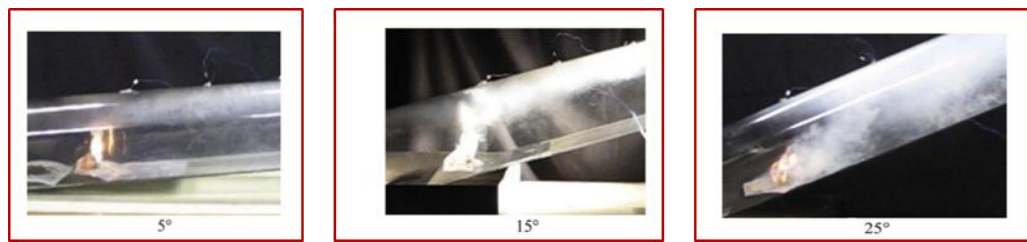


**Figure 1.3 Smoke flow patterns for different angles [27]**

### **1.5 Objective of the Thesis**

Literature and the past events show that smoke flow and temperature distributions in subway stations in case of a subway fire are very crucial. Passengers inside must be evacuated without harmed. For such a fire scenario, people totally tend to take the stairs immediately and the route of almost all people would be the same. Studies so far clearly show that dimensions of tunnel, size, power and locations of fire, movement of the vehicles inside, ventilation velocities and inclination angles of the

tunnels are very important parameters affecting the flow patterns in the tunnels.

In present thesis work, both experimental and numerical studies were performed. To seek through the effects of the ventilation velocity, inclination angle and fire location on temperature distribution and velocity field in inclined tunnels in case of fire, two different fire case scenario as case A (away from the inclined tunnel simulating stairs) and case B (fire start-up neighbor on the stairs) was created. On the basis of the researches [13] and [24], CO concentration and necessary ventilation velocities decrease with the increasing distance to the fire sources. For this reason, in this study, there will be two different sources on different locations in a horizontal tunnel with same heat release rates to observe the differences of temperature distribution and flow patterns keeping up with the back-layer formation.

Different from the literature [11], [23], [27], this work is dealing with larger tilt angles to be investigated to observe how the smoke patterns could be. Besides, studies so far did not check up on a combined tunnel composed of two tunnels, one is horizontal and the other is inclined. Only one of them has been investigated as a model. This thesis reveals the results originating from inclination angles of stairs taken by passenger. Past researches presents the inclination angles of the train rails. Thus, the study covers an original scenario comparing to the literature. Furthermore, the ventilation velocities were chosen with respect to the experimental limitations to compare the temperature, velocity and backflow formations for different cases. For a specific study on real tunnels, velocities should be taken relatively smaller. The main objective of this study is to visualize the smoke flow and determine the temperature distribution in the combination of horizontal and inclined tunnels in case of a fire.

## **1.6 Thesis Outline**

In the first chapter, introduction and literature review were presented. The next chapter gives information about the methodology. After, results are revealed and discussed in Chapter 3. Lastly, the conclusions are discussed in Chapter 4.

## CHAPTER 2

### METHODOLOGY

#### 2.1 Governing Equations

The governing equations used in the numerical study are provided in this section.

The mass conservation is given as:

$$\frac{\partial \rho}{\partial t} + \vec{\nabla} \cdot (\rho \vec{V}_f) = 0 \quad (2.1)$$

The momentum conservation equation is:

$$\frac{\partial \vec{V}_f}{\partial t} + (\vec{V}_f \cdot \vec{\nabla}) \vec{V}_f = \frac{1}{\rho} \vec{\nabla} \cdot \vec{\sigma} + \vec{g} \quad (2.2)$$

Since temperature gradients are also important, the energy conservation equation is used as:

$$\frac{D_{\vec{V}_f} T}{Dt} = \frac{\partial T}{\partial t} + \vec{V}_f \cdot \vec{\nabla} T \quad (2.3)$$

Standard k- $\epsilon$  model used as the turbulence model in numerical analysis is given as:

$$\frac{\partial k}{\partial t} + \nabla \cdot \left( k \vec{u} - \frac{\nu_T}{\sigma_k} \nabla k \right) = P_k - \epsilon \quad (2.4)$$

$$\frac{\partial \varepsilon}{\partial t} + \nabla \cdot \left( \varepsilon \vec{u} - \frac{\nu_T}{\sigma_\varepsilon} \nabla \varepsilon \right) = \frac{\varepsilon}{k} (C_1 P_k - C_2 \varepsilon) \quad (2.5)$$

$$\nu_T = C_\mu \frac{k^2}{\varepsilon} \quad (2.6)$$

where,

turbulent constants for turbulence models are,  $C_\mu = 0.09$ ,  $C_1 = 1.44$ ,  $C_2 = 1.92$ ,

$\sigma_k = 1.0$ ,  $\sigma_\varepsilon = 1.3$

## 2.2 Experimental Work

The experimental set-up is constructed as seen in Figure 2.1 to demonstrate a metro station and its stairs opening to atmosphere. The set-up is composed of two different tunnels, one is horizontal and other one stands with an inclination angle to the ground.

The inclined tunnel is adjusted with pins. Two tubular metal with different perimeters are fitted into each other. Both are drilled in specific points. Points are calculated so that pins can be passed through at the same locations. The positions of the holes let the tunnel stand with desired angle.



**Figure 2.1 Experimental set-up**



There is a linkage between the tunnels not to let any leakage on the system. This linkage is made of a black fireproof fabric. The fabric is attached to the system by means of aluminum tapes to ensure the impermeability. System is covered by using polyurethane foam to insulate the whole system not to let heat loss as much as possible.

Before the system was fully constructed, six planes onto which five thermocouples had been attached were prepared as illustrated in Figure 2.2. After all the planes had been ready and themocouples were numbered, the planes were attached to the set-up.



**Figure 2.2 Planes with thermocouples attached**

Two holes were drilled at the bottom side of the horizontal tunnel to supply the gas inside to set a fire as shown in Figure 2.3. An LPG tank was provided as a gas source for the fire. Lastly, a burner was integrated the system.

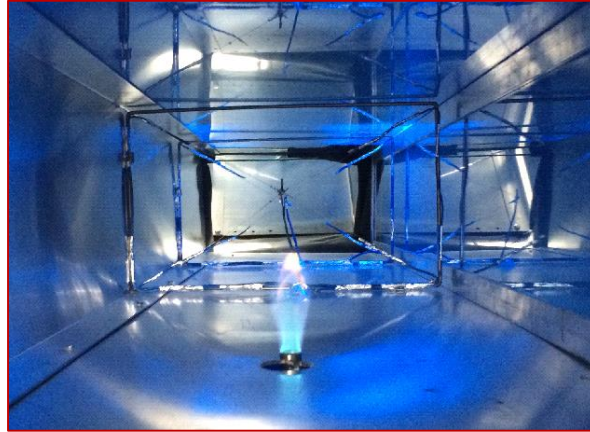


**Figure 2.3 Fire in the tunnel**

Mass flow rate through the gas burner was measured by means of a balance as used in reference study [15]. Besides the fire part of the system, another critical unit is the ventilation system of the setup, composed of two main parts, a fan and a current converter. The square DC fan shown in Figure 2.4, is attached to ceiling midline at end of the inclined tunnel to provide the air flow from the inside of the tunnel to discharge the burned gas products and air to outside. A speed controller of the fan and the AC to DC converter unit to run the DC fan were included to the system presented in Figure 2.5. Constant mass flow discharge rate of the fan is set and checked by means of an anemometer.

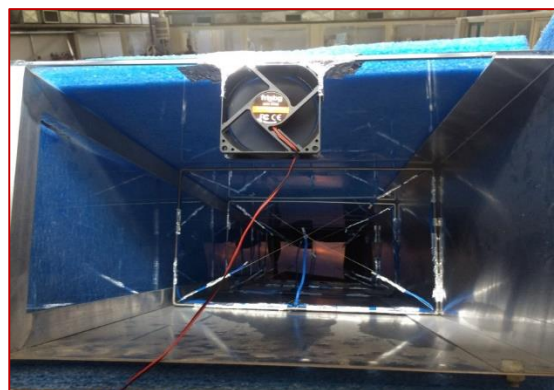


**Figure 2.4 Discharge fan**

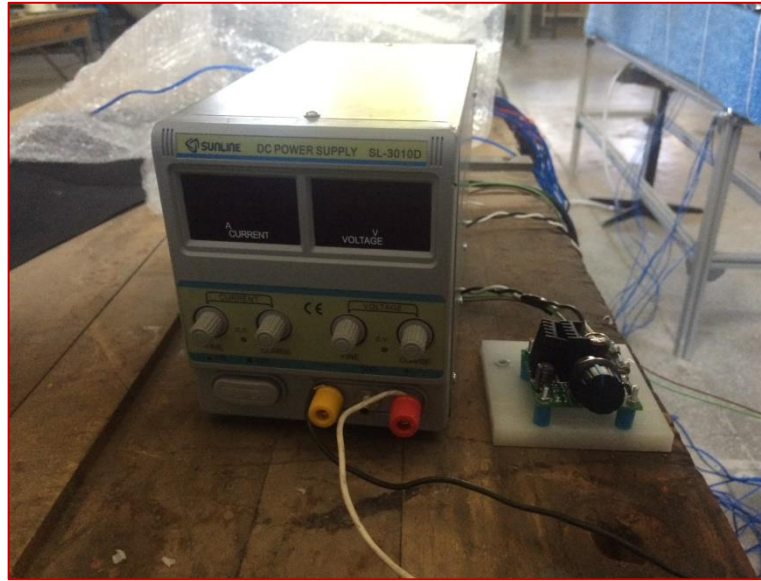


**Figure 2.5 AC to DC converter unit and fan speed controller**

### **2.3 Experimental Procedure**

The features of the experimental setup are shown in Figure 2.6. One horizontal and one inclined tunnel, each are 2m long and have rectangular cross-section of 0.25m height and 0.42m width, were combined and the experimental tunnel was constructed. Six cross-section planes called as horz1, horz2, inc1, inc2, inc3, and inc4 were attached to the system. In horizontal tunnel, fire gas burner was placed 50cm far from the left opening side of the tunnel as case A and it was placed secondly 25cm far behind from the linkage side of the horizontal tunnel as case B. Planes were set with the distance of 50cm beginning from the fire location in case A. In the inclined tunnel, all the planes were set with distance of 40 cm to each other.

In experiment, temperature distribution is investigated using six cross-sectional planes to which five thermocouples attached. All planes and thermocouple positions are represented by means of different colors in Figure 2.7. Total pieces of 30 thermocouples were set to collect temperature data. A velocity controlled fan having 8\*8 cm was attached to the ceiling at the end of the inclined tunnel.

LPG (70%-Butane & 30% Propane Mixture) was burned with the adiabatic flame temperature of 2243K to set fire by means of a gas cylinder. A constant flow rate of gas burned ( $\dot{m}$ ) was set as 0.15 kg/h. Flow rate of LPG was adjusted by means of a balance as in Kayılı’s work measuring the mass loss of the gas cylinder in a time period [15]. Inclinations angle of the tunnel ( $\alpha$ ) was variable and set as 25, 30, 35, 40 degrees. Discharge velocity ( $V$ ) was another parameter and was set in order of 2, 2.5, 3 m/s. The reason why these velocities are chosen is the fact that backflow formations can be observed in this range in the numerical study as the constant flow rate used in the experimental part can be successively provided.

Within the explained features of the experimental setup, temperature data was taken for each combination of  $\alpha$  and  $V$  in the case of steady state conditions of the flow. For the experiment, there were 24 different combinations of discharge velocity “ $V$ ” and inclination angle “ $\alpha$ ” as seen in experiment matrix, Table 2.1. Locations of planes on x plane to which thermocouples attached are represented in Table 2.2 in cm with respect to the coordinate system in Figure 2.6.

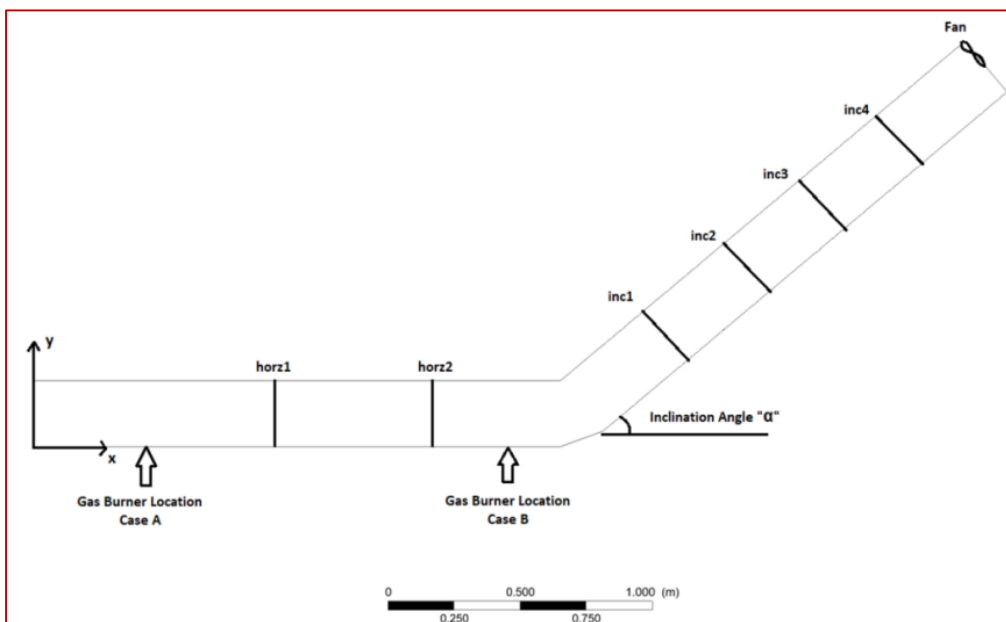


**Figure 2.6 Experimental setup drawing**

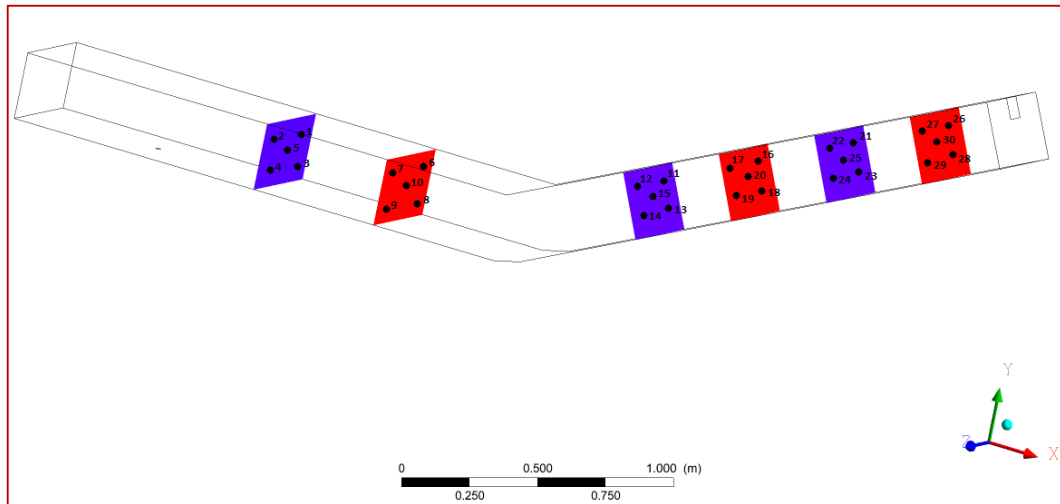


**Figure 2.7 Representation of thermocouple positions**

**Table 2.1 Experiment and numerical work matrix**

<b>CASE A</b>				<b>CASE B</b>			
$\alpha$	$V_1= 2\text{m/s}$	$V_2= 2.5\text{m/s}$	$V_3= 3\text{m/s}$	$\alpha$	$V_1= 2\text{m/s}$	$V_2= 2.5\text{m/s}$	$V_3= 3\text{m/s}$
$25^\circ$				$25^\circ$			
$30^\circ$	<b>12 DIFFERENT</b>			$30^\circ$	<b>12 DIFFERENT</b>		
$35^\circ$	<b>COMBINATIONS</b>			$35^\circ$	<b>COMBINATIONS</b>		
$40^\circ$				$40^\circ$			

**Table 2.2 Locations of the planes (cm) in x-direction for inclination angles**

Planes	$\alpha= 25^\circ$	$\alpha= 30^\circ$	$\alpha= 35^\circ$	$\alpha= 40^\circ$
horz1	100	100	100	100
horz2	150	150	150	150
inc1	236	234	232	230
inc2	272	269	265	261
inc3	308	303	298	291
inc4	345	338	331	322

## 2.4 Numerical Procedure

The geometry for the numerical model is shown in Figure 2.8. Every parameter was set one to one with the experiment presented in Table 2.3 with respect to the coordinate system in Figure 2.6.

**Table 2.3 Properties of the model**

Properties	Case A	Case B
Location (x-direction)	50 cm	175cm
Source type	Air	Air
Source temperature	2243 K	2243 K
Source mass flow rate	0.15 kg/h	0.15 kg/h
Tilt angles	25°, 30°, 35°, 40°	25°, 30°, 35°, 40°
Ventilation velocities(m/s)	2.0, 2.5, 3.0	2.0, 2.5, 3.0

Points are selected as equally spaced nodes from inlet to outlet boundary including both horizontal and inclined parts of the domain and presented in Figure 2.8.

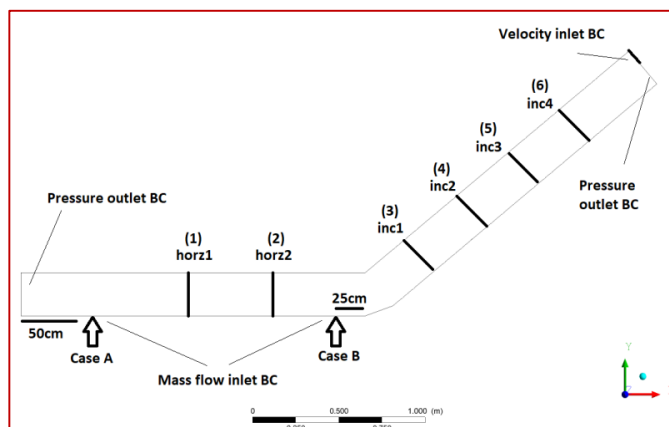


**Figure 2.8 Numerical domain**

Meshed model and a random cross-sectional plane cut to see the meshes are shown in Figure 2.9.

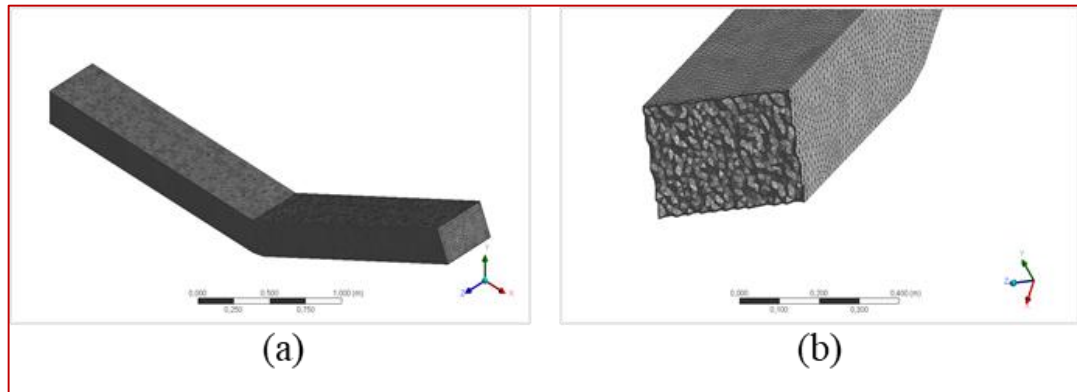


**Figure 2.9 (a) Mesh, (b) a randomly cut plane for the model**

Analyses lead to the usage of 1 million mesh domain. Mesh properties are given in Table 2.4.

**Table 2.4 Mesh properties**

<b>Property</b>	<b>Description</b>
Max. Face size (m)	1.65E-02
Inflation	Smooth transition
Nodes	248794
Elements	997855

Mesh independency is achieved by means of comparing temperature values of eight chosen points in the tunnel system as shown in Figure 2.10.

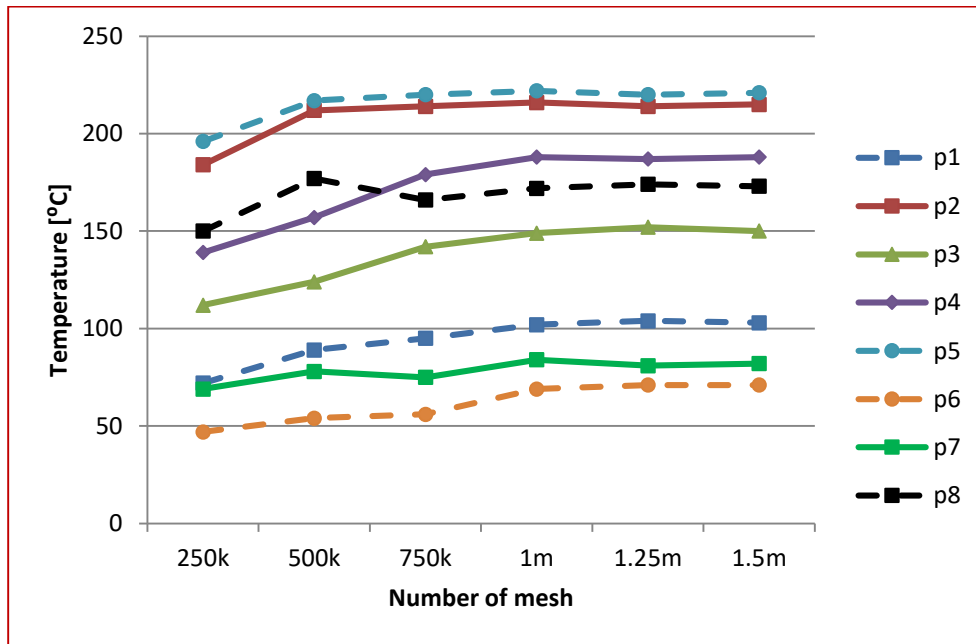


**Figure 2.10 Mesh independency analyses results**

For the sake of reliability of the numerical analyses, mass conservation was justified via calculating mass inlets to the system and the mass exhaust to outside of the system with the fan. An area of 8\*8 cm at the end of inclined tunnel shown in Figure 2.8 was split from the whole plane and defined as velocity inlet entering the negative value of the discharge velocity to let air go through outside. As the only different feature from the experimental study, boundary conditions (BC) for walls were chosen as “wall BC “ and set to be totally insulated via no heat flux to reach the maximum possible conditions of the soil around the metro tunnels in reality. BC at the exit of the inclined tunnel was set to be velocity inlet, and velocity values were entered as negative to set a discharge velocity. Other openings to the atmospheric conditions were defined as pressure outlet BCs. Numerical model was solved with pressure-based type, absolute velocity formulation and steady state. Pressure velocity coupled solution method with least squares cell based. All equations, i.e. pressure, momentum, energy etc., were chosen as second order and second order upwind. Viscous model with standard k-epsilon was set, and near wall treatment was chosen as standard wall functions. Boundary conditions and all the settings proposed in Tables 2.5 and 2.6.



**Table 2.5 Boundary conditions**

<b>Boundary</b>	<b>Boundary Condition</b>
Walls	Wall (with no heat flux)
Fan	Velocity inlet
Air inlet (source)	Mass flow inlet
Openings to atmosphere	Pressure outlet

**Table 2.6 Numerical settings**

<b>Settings</b>	<b>Description</b>
Solver type	Pressure based
Time	Steady state
Gravity	On
Gradient	Least square cell based
Pressure	Second order
Momentum	Second order upwind
Turbulent kinetic energy	Second order upwind
Turbulent dissipation rate	Second order upwind
Energy	Second order upwind

There were two different cases leading two different mass flow inlet locations. For case A, mass flow rate entering into the tunnel through the hole was defined in 50 cm away from beginning of the horizontal tunnel. For case B, the hole was set 25 cm away from the intersection of the tunnels through the  $-x$  direction. For simulating fire, hot air mass flow was given to the inlet of the tunnels at the temperature of adiabatic flame temperature of LPG as 2243K with the mass flow rate of 0.15 kg/h, as in the experiment.

All runs of CFD calculations were accomplished in the case of steady-state conditions. Temperature data and temperature contours taken for each combination of  $\alpha$  and V for each case as shown in Table 2.1.



## CHAPTER 3

### RESULTS AND DISCUSSION

In this chapter, experimental and numerical results are presented and discussed. Experimental and numerical results of temperature and velocity data are available in the same graphics.

All cases were studied and evaluated. Results of case A and case B are presented. All the presentations have been made in terms of experiment matrix in Table 2.1 and the model constructed for numerical study identical to experiments.

The plane names used in Appendix A that show the figures of temperature contours on the planes represented in Figure 2.8. Experimental and numerical temperature data used for resulted graphics are presented in Appendix B. Numerical models were also checked with the conservation of mass flow rates, shown in Appendix C. It is observed that there are logical variations between the results of different inclination angles and velocities. Differences between the numerical and experimental temperature values are due to the fact that wall boundary conditions in numerical part was defined as “wall” with no heat flux through as aiming to construct a real case scenario for a tunnel system surrounded by soil under the ground.

Furthermore and more important reason of the temperature differences in the results is the chosen source temperature of hot air in numerical analyses as temperature is defined as adiabatic flame temperature of the LPG that may differ 500°C at the very beginning of a real flame.

### **3.1 Results of Midpoint Temperature on Planes**

Experimental and numerical midpoint temperature profiles for each plane are shown in this section. Results are presented for two main variables of ventilation velocity and inclination angle.

To see the effects of inclination angles and ventilation velocity on midpoint temperature profiles on preset normal planes related figures are presented.

Figures in this chapter were prepared so that one can see the midpoint temperature trends with the same ventilation velocities and the variations of the inclination angles; and vice versa, with the same inclination angles and the variations of the ventilation velocities for case A and B. The change in the temperature results are given in Figures 3.1-14.

The reason of choosing midpoints of the planes to be taken into consideration is the fact that midpoint temperature values were decided as the most critical ones as heads of people taking stairs stands around these positions in the underground exits. Since that, temperature data on these points for each case are presented.

Comparing the results of the experimental and numerical results, it is clearly seen in figures that there is a pretty much perfect match-up of temperature trends between the these studies.

Sections 3.1, 3.2, 3.3 are divided into two subsections “for different inclination angles” and “for different ventilation velocities”. The figures are sharing the same data for each section. However, this is a necessity to simplify the comparison between the effects of inclination angle with constant ventilation velocity and, vice versa, the effects of ventilation velocity with constant inclination angle.

### 3.1.1 Midpoint Temperature Trends for Different Inclination Angles

In this section midpoint temperature trends are presented for analogy on inclination angles in Figures 3.1-3.6.

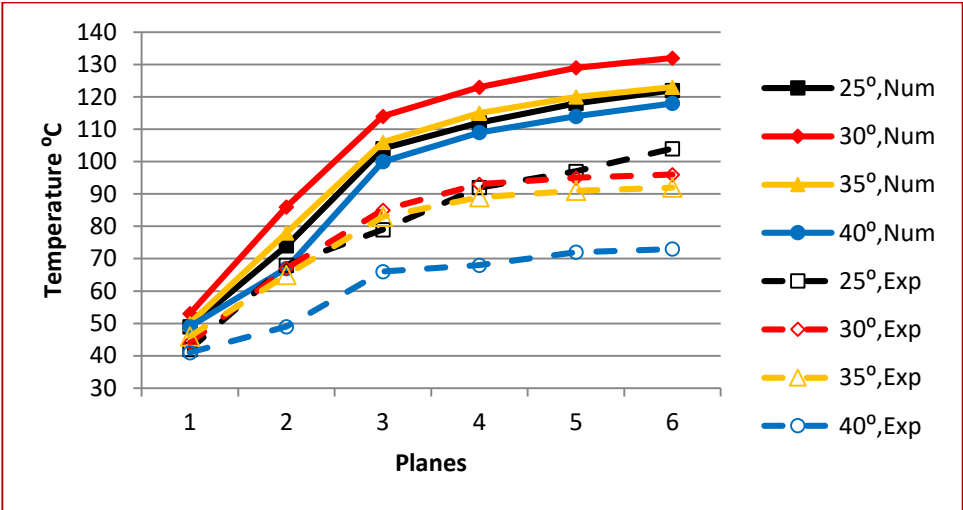


Figure 3.1 Profiles of midpoint temp. on planes in case A for VV=2.0m/s

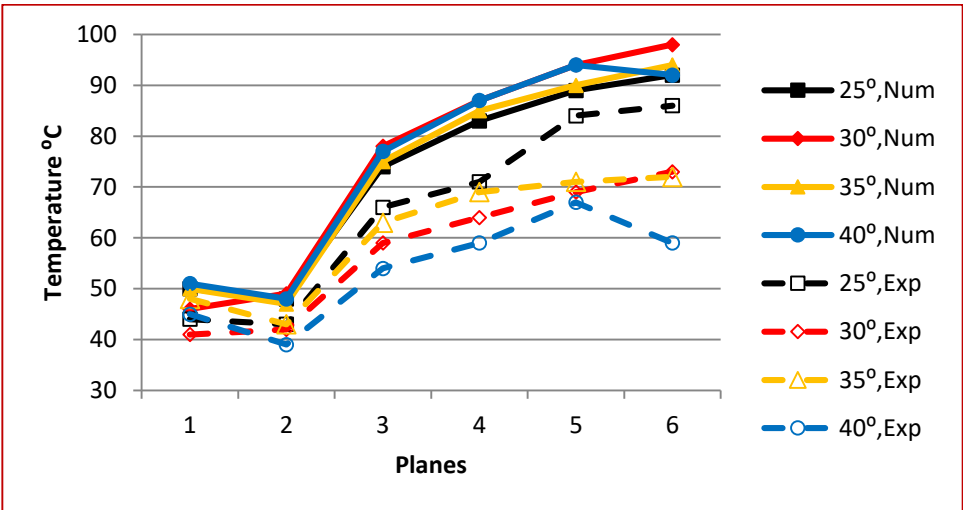
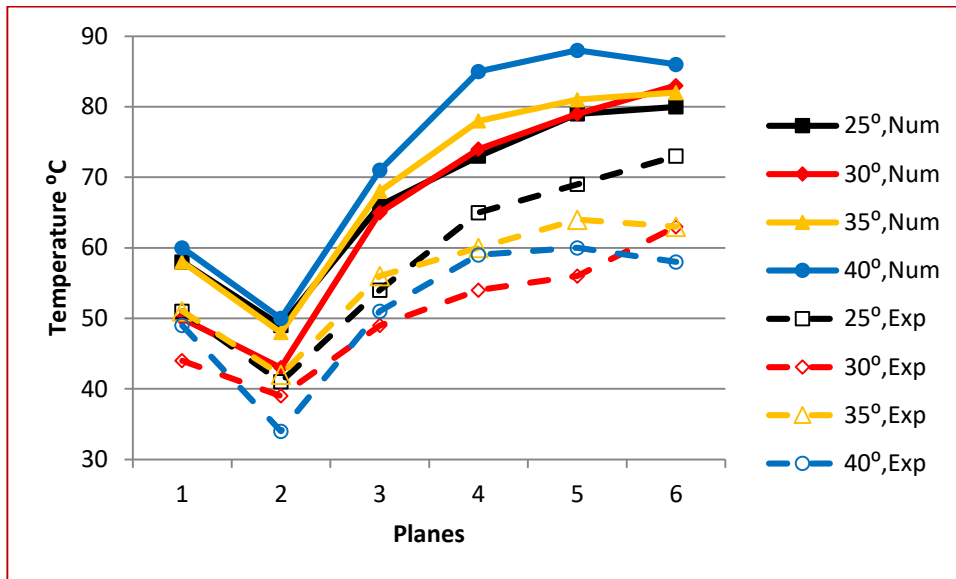


Figure 3.2 Profiles of midpoint temp. on planes in case A for VV=2.5m/s



**Figure 3.3 Profiles of midpoint temp. on planes in case A for  $VV=3.0\text{m/s}$**

For case A, increase of inclination angle results in decrease in midpoint temperatures on the planes. Increase of midpoint temperatures is sharp until third plane, and after this plane temperature increase is smoother. This manner is on account of the linkage of the tunnels standing between second and third plane.

Hot gases crossing over that region hitting on the boundaries results in a transition. Thus, hot and cold air zones changes leading changes in temperature trends on the midpoint locations. While trends of temperature results from numerical analyses are in a stable rise, experimental ones have trivial fluctuations. The situation is in virtue of experimental errors.

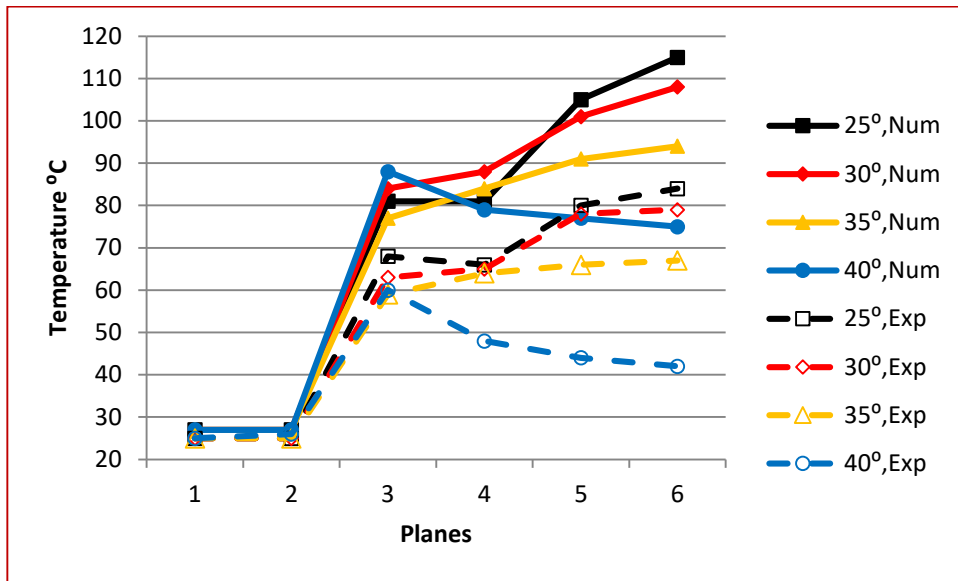


Figure 3.4 Profiles of midpoint temp. on planes in case B for  $VV=2.0\text{m/s}$

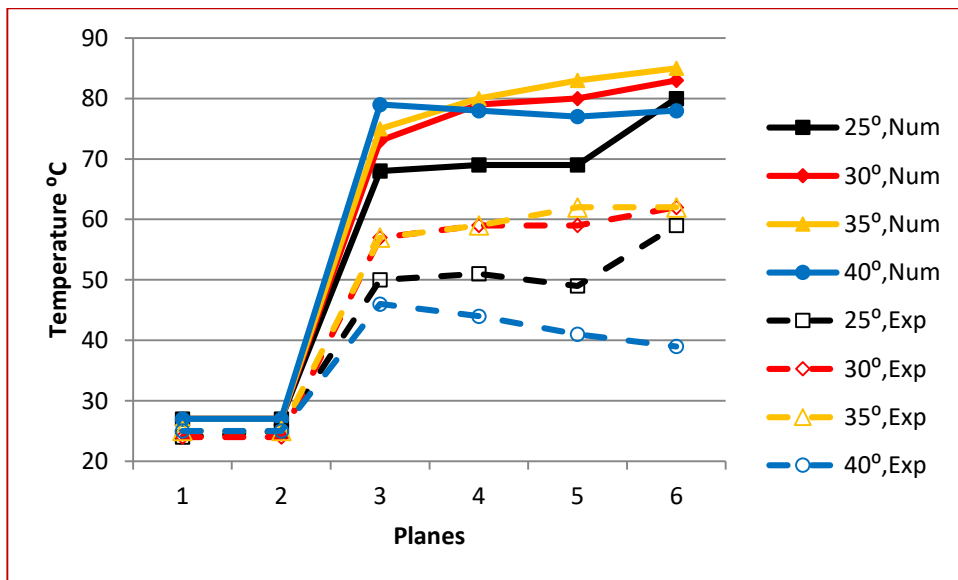
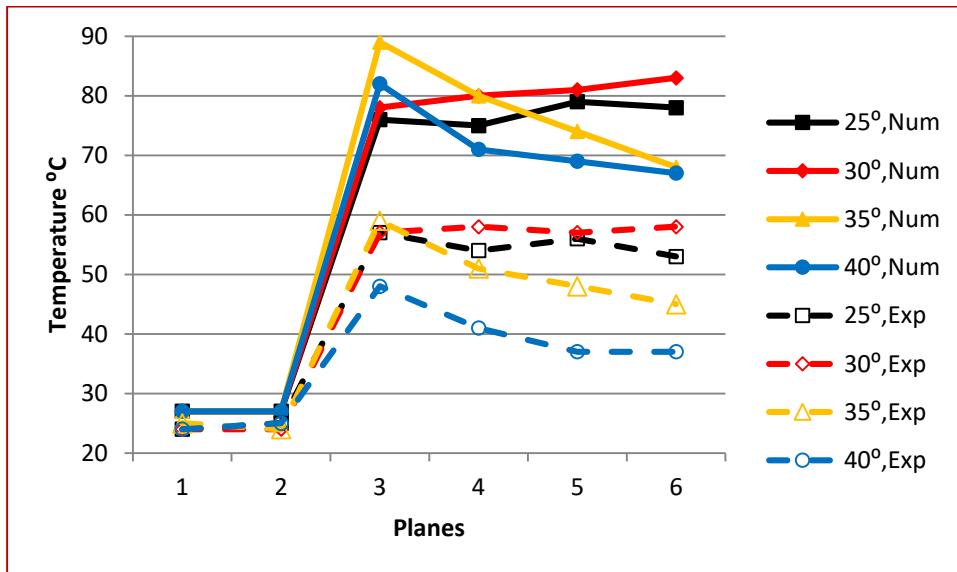


Figure 3.5 Profiles of midpoint temp. on planes in case B for  $VV=2.5\text{m/s}$



**Figure 3.6 Profiles of midpoint temp. on planes in case B for VV=3.0m/s**

For case B, as no hot fluid flows through the first two plane, temperature is constant. Increase of inclination angle provides lower midpoint temperatures on the planes. The decrease in the temperatures from third to fourth plane is owing to the linkage of the tunnels likewise in case A. Rising hot gases hitting on the ceiling and corners, so trends are affected. Contrary to case A, there is no significant increase in temperatures through the fan, decrements even are observed. This situation is due to the same reason of region between the tunnels. Air exhaust by fan affects the temperature distribution reversely. Even some fluctuations in trends of temperature for experimental results, numerical data is in a very good accordance with them.

### 3.1.2 Midpoint Temperature Trends for Different Ventilation Velocities

In this section midpoint temperature trends are presented for analogy on ventilation velocities in Figures 3.7-3.14 and same data in previous section as new figures are put forward to behold to the ventilation velocity effects in the same graphs for each inclination angle.



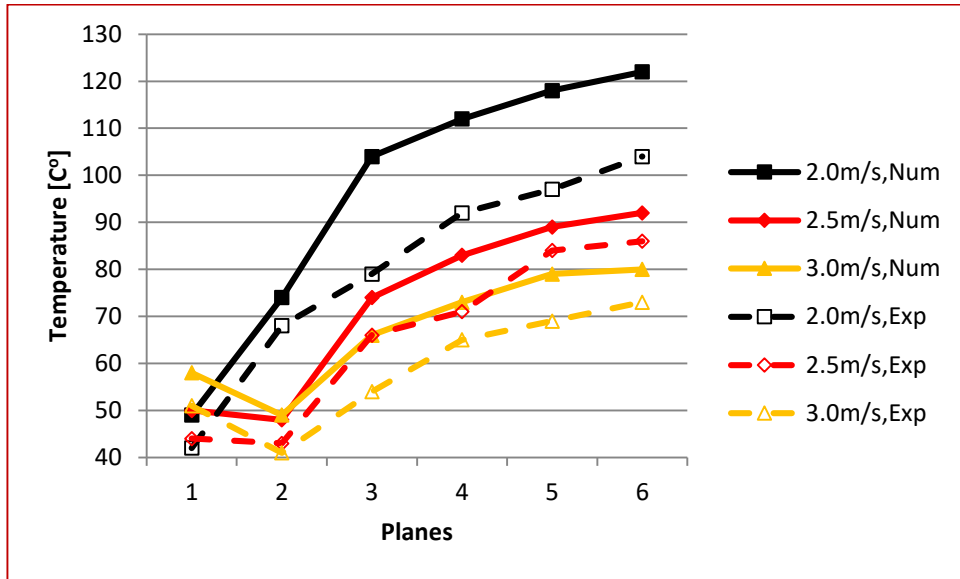


Figure 3.7 Profiles of midpoint temp. on planes in case A for  $\alpha=25^\circ$

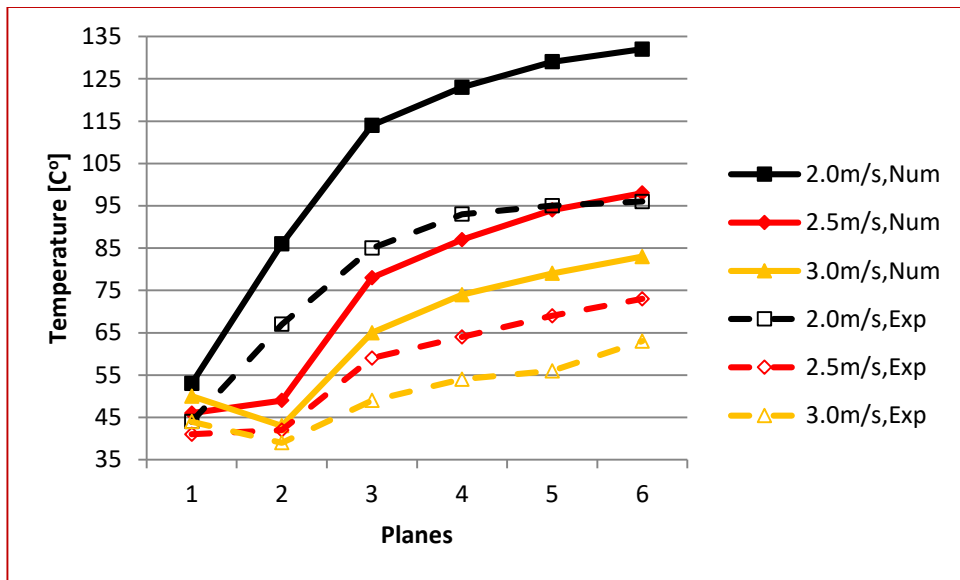
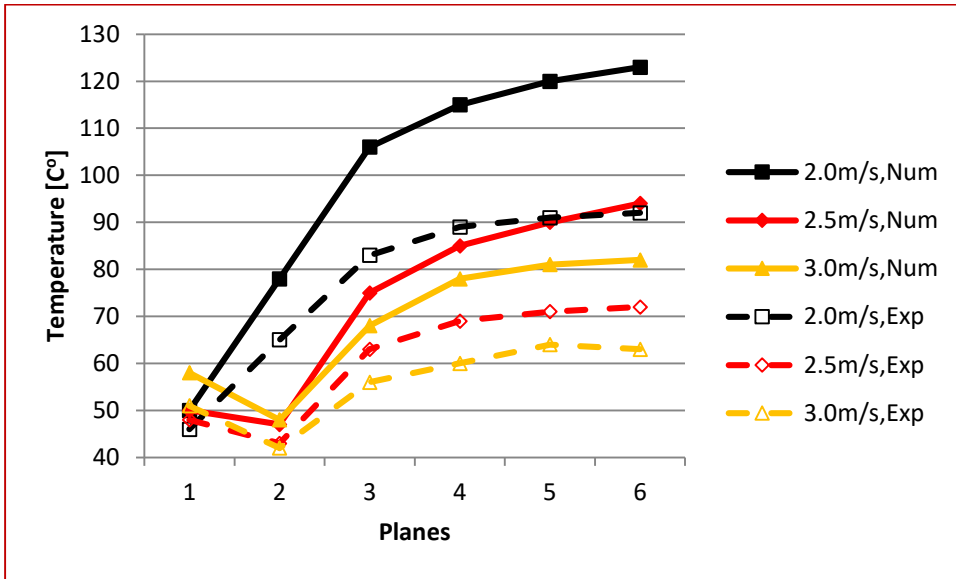
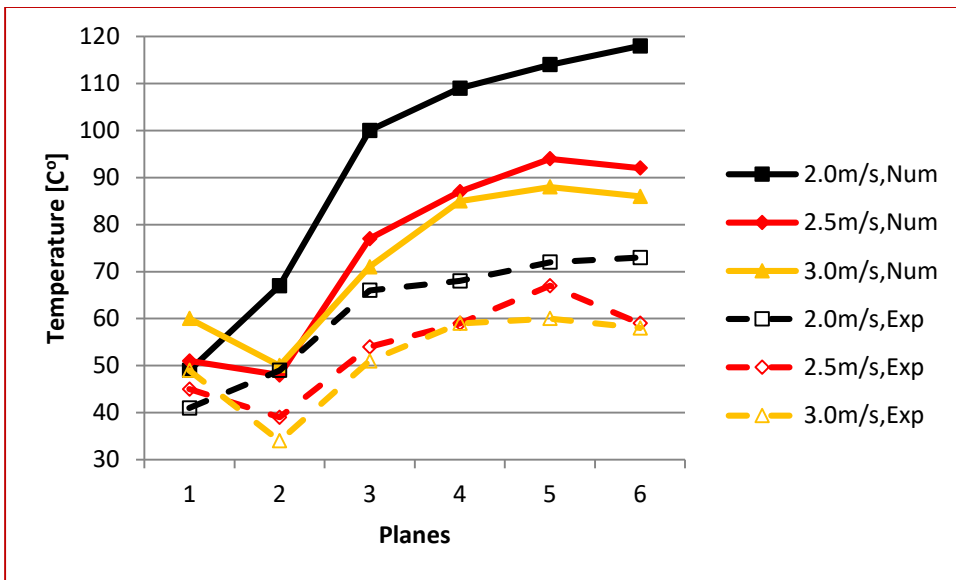


Figure 3.8 Profiles of midpoint temp. on planes in case A for  $\alpha=30^\circ$



**Figure 3.9 Profiles of midpoint temp. on planes in case A for  $\alpha=35^\circ$**



**Figure 3.10 Profiles of midpoint temp. on planes in case A for  $\alpha=40^\circ$**

For case A, results of midpoint temperatures on each plane clearly show that midpoint temperature levels decreases with the increase of VV. A great difference are distinguished between ventilation velocities of 2m/s and 3m/s from the the figures.

Likewise in the previous section, the increase in the temperatures from third to fourth plane is sharp for the temperature results due to the same reason. Experimental results have some undulations; however, trends are in a good agreement with numerical ones.

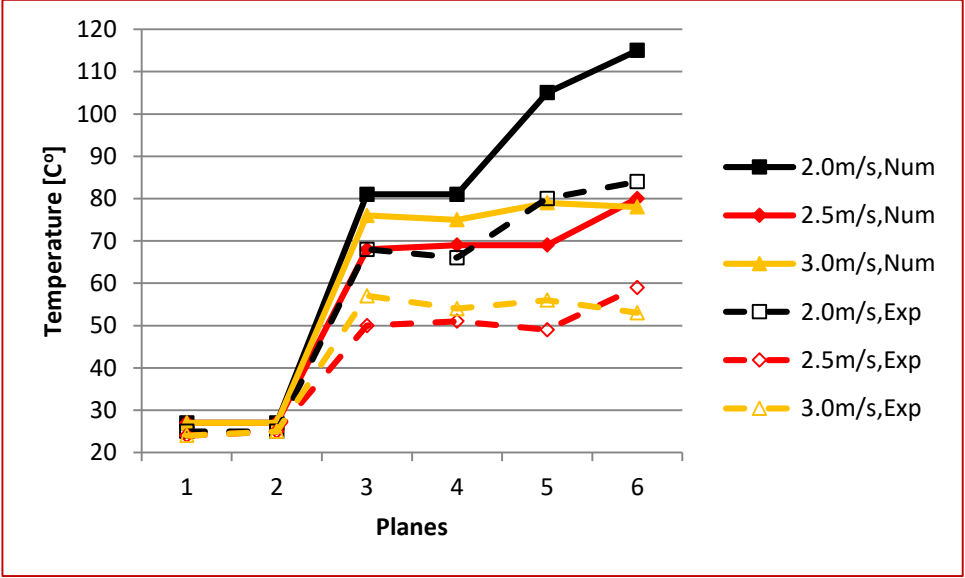


Figure 3.11 Profiles of midpoint temp. on planes in case B for  $\alpha=25^\circ$

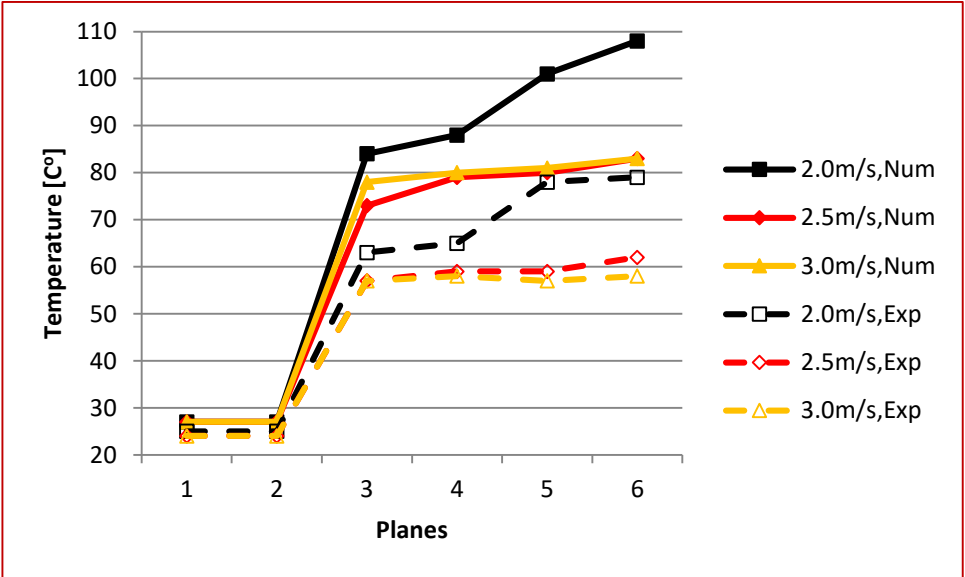
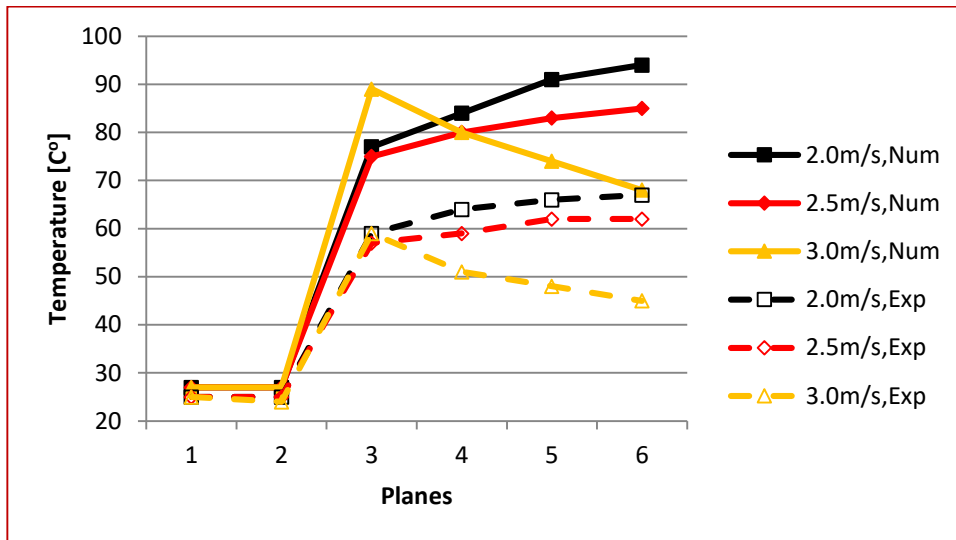
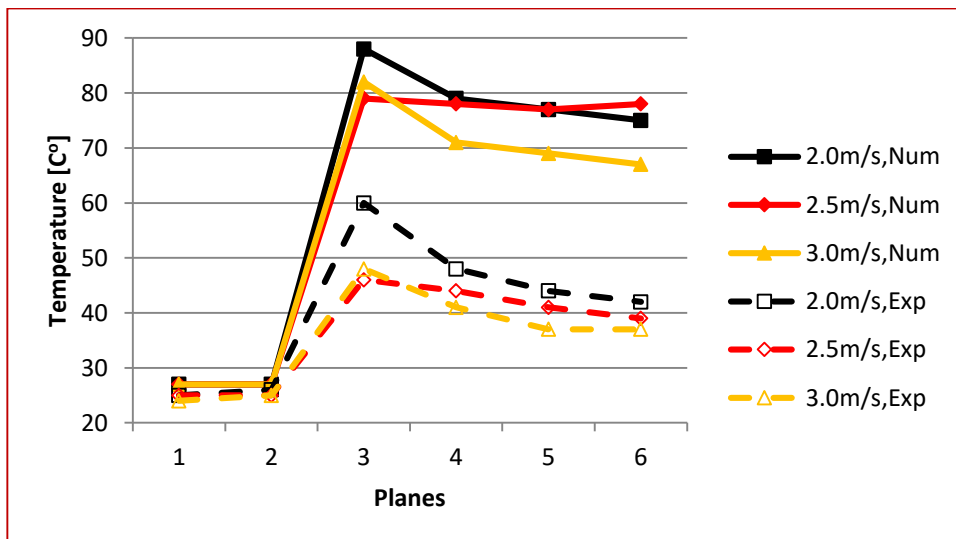


Figure 3.12 Profiles of midpoint temp. on planes in case B for  $\alpha=30^\circ$



**Figure 3.13 Profiles of midpoint temp. on planes in case B for  $\alpha=35^\circ$**



**Figure 3.14 Profiles of midpoint temp. on planes in case B for  $\alpha=40^\circ$**

For case B, midpoint temperatures decreases with the increase of VV as in case A. However, the effect is not great as the other case. The peak point is available on third plane for these figure, either. Some reason is valid once more. The consistency between the parts of the study is veridic yet.

### 3.2 Results of Maximum Temperature on Planes

Maximum temperature profiles for each plane are shown in this section. Results are presented for two main variables of ventilation velocity and inclination angle. The change in the maximum temperature results are given in Figures 3.15-28.

Comparing the results of the experimental and numerical results, it is clearly seen in Figures in section 3.1 that there is a pretty much perfect match-up of temperature trends between the two study.

#### 3.2.1 Maximum Temperature Trends for Different Inclination Angles

In this section maximum temperature trends are presented for analogy on inclination angles in Figures 3.15-3.20.

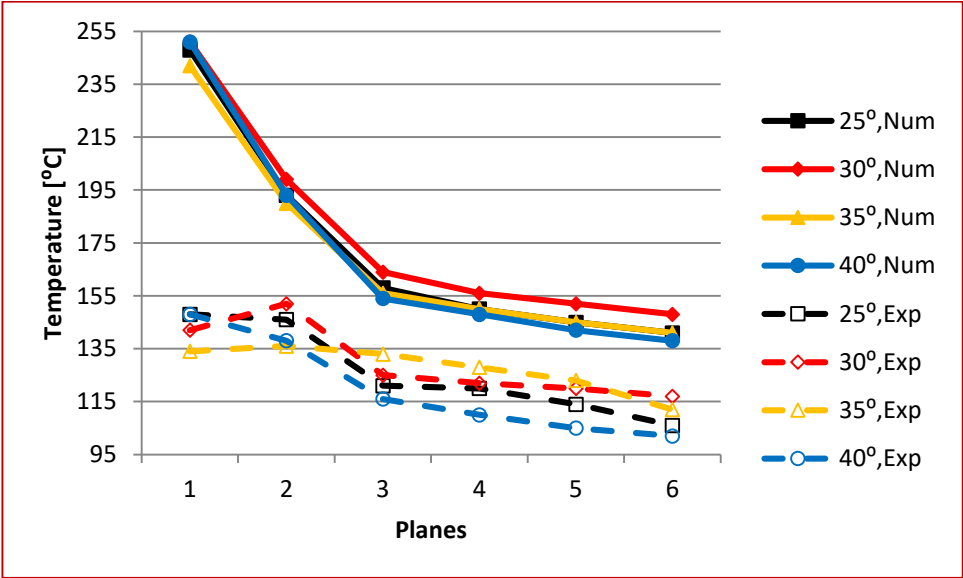
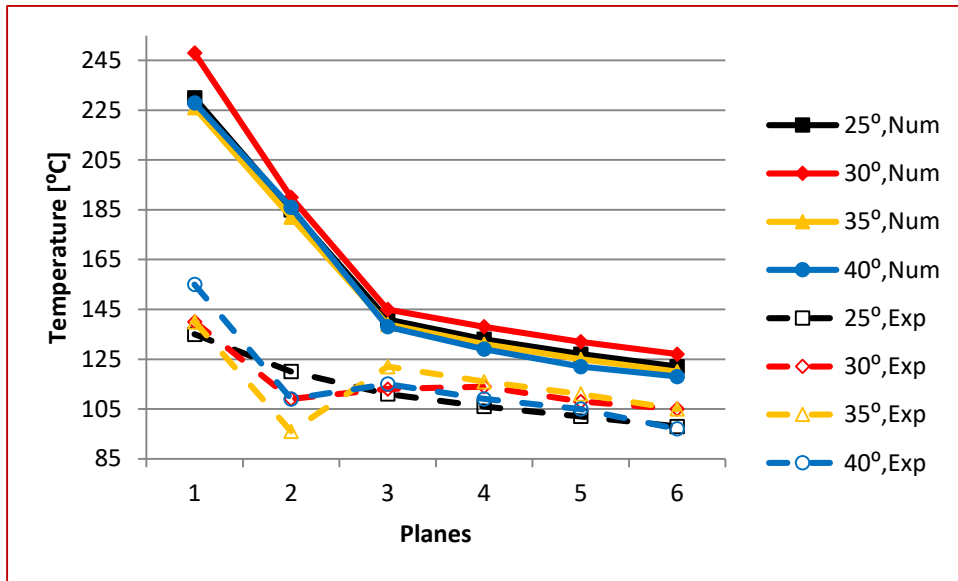
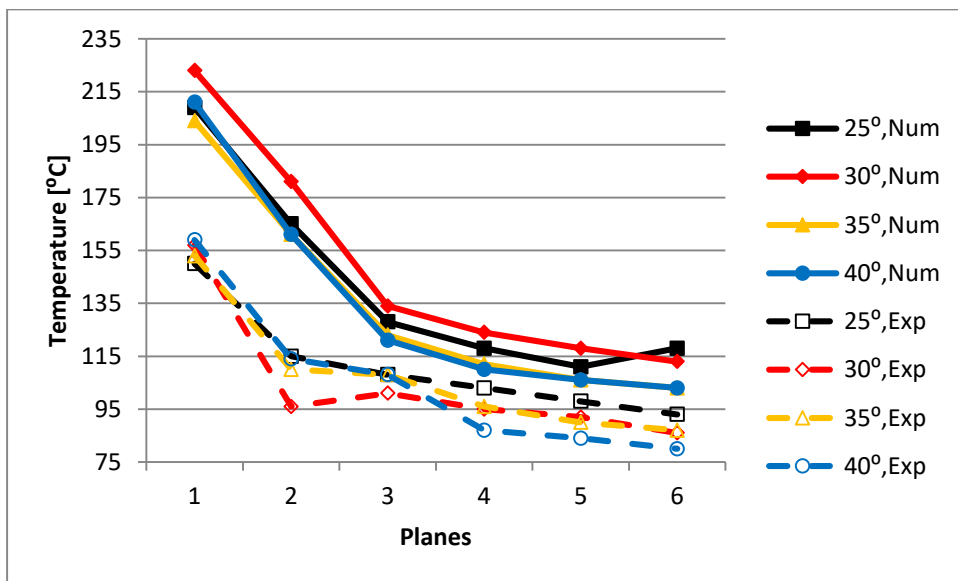


Figure 3.15 Profiles of maximum temp. on planes in case A for VV=2m/s



**Figure 3.16 Profiles of maximum temp. on planes in case A for VV=2.5m/s**



**Figure 3.17 Profiles of maximum temp. on planes in case A for VV=3m/s**

For case A, increase of inclination angle results in decrease in maximum temperatures on the planes. Unlike midpoint temperatures, maximum temperatures are continuously decreasing through the tunnel. This is because the fact that the transient region around

the linkage of the tunnels do not change the global temperature value. Experiments and numerical work reveals the results on the same manner.

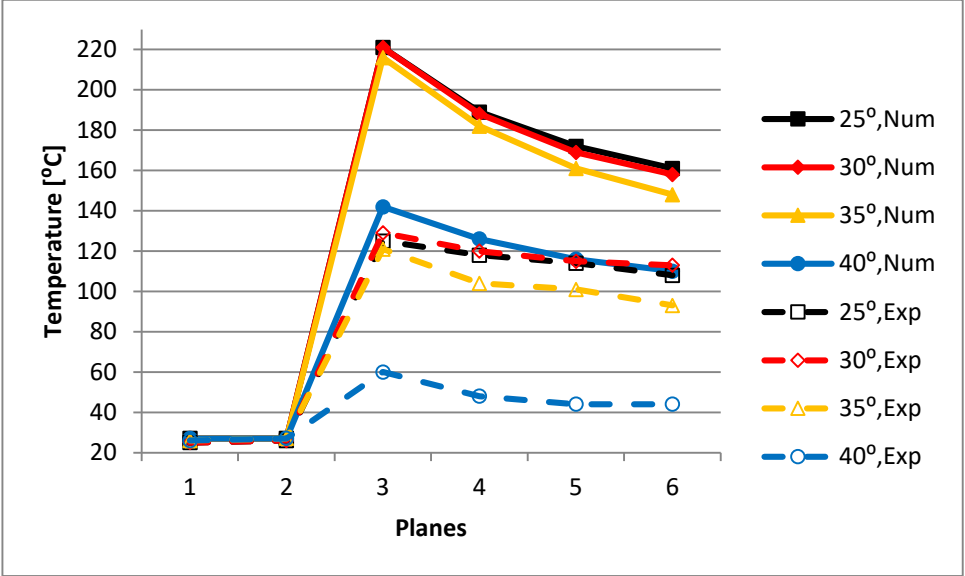


Figure 3.18 Profiles of maximum temp. on planes in case B for VV=2m/s

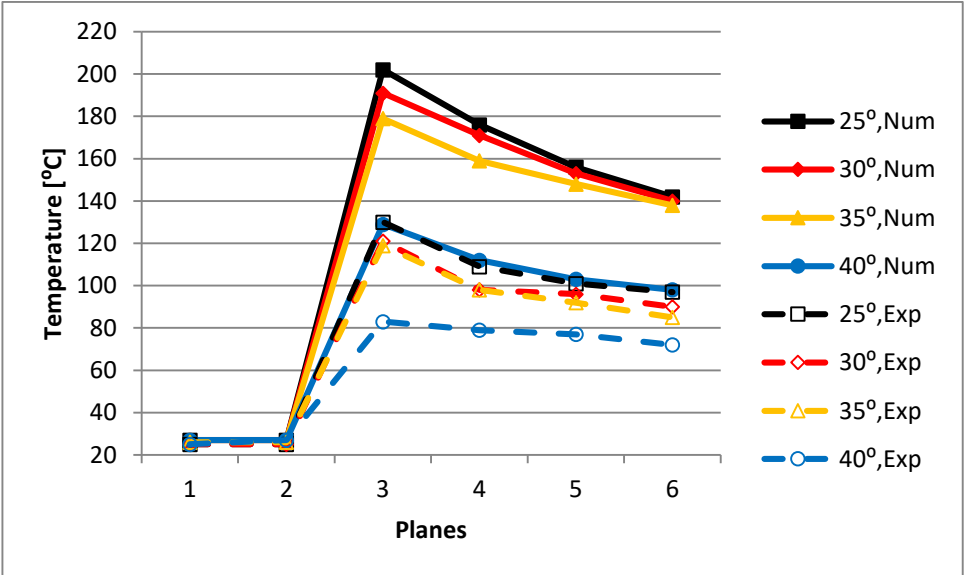
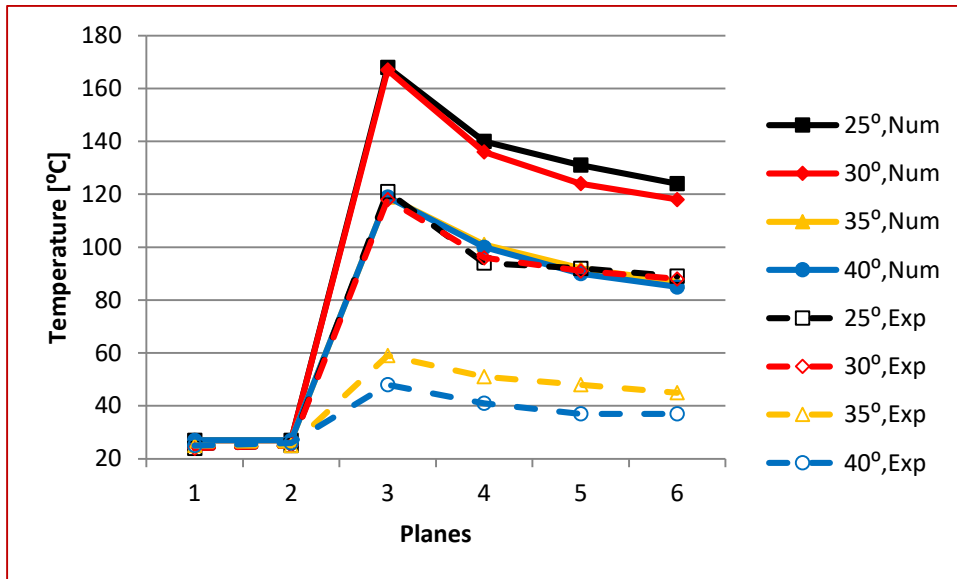


Figure 3.19 Profiles of maximum temp. on planes in case B for VV=2.5m/s



**Figure 3.20 Profiles of maximum temp. on planes in case B for VV=3m/s**

For case B, increase of inclination angle leads maximum temperatures to decrease as in case A. However, while angle increase does not make a big difference in case A, quite the contrary, maximum temperatures fall into a higher decrease and especially for inclination angle of 40 degrees, maximum temperatures significantly decrease. Likewise the other case, maximum temperatures are decreasing through the tunnel except the peak on the third planes. The reason of the situation is the fact that fire location is at the beginning of the inclined tunnel and first two planes are not affected by temperature as fluid flow is through the opposite direction of the tunnel. Results of the experimental study provides the conformity with the numerical one.

### 3.2.2 Maximum Temperature Trends for Different Ventilation Velocities

In this section maximum temperature trends are presented for analogy on ventilation velocities in Figures 3.21-3.28 and same data in previous section as new figures are put forward to behold to the ventilation velocity effects in the same graphs for each inclination angle.



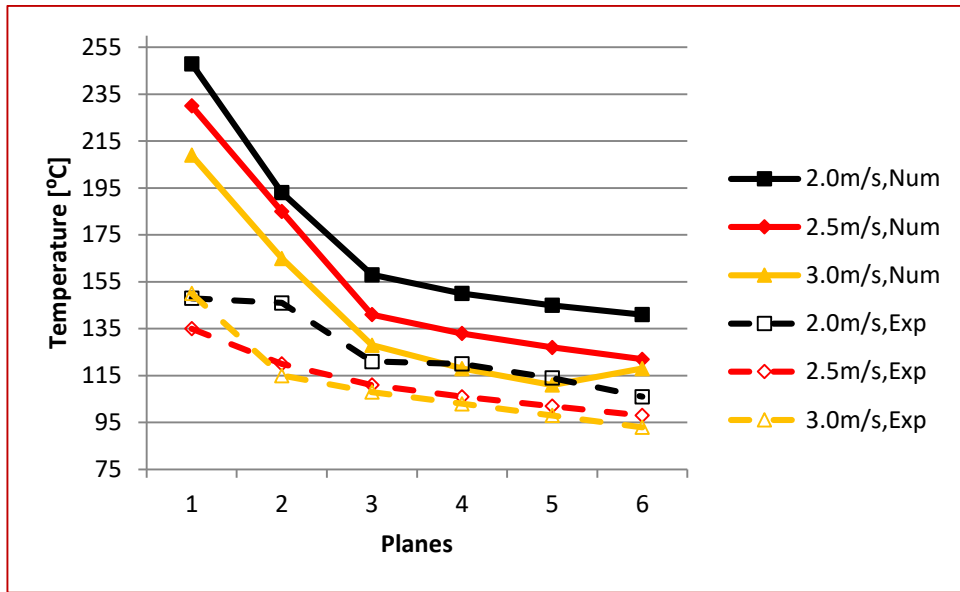


Figure 3.21 Profiles of maximum temp. on planes in case A for  $\alpha=25^\circ$

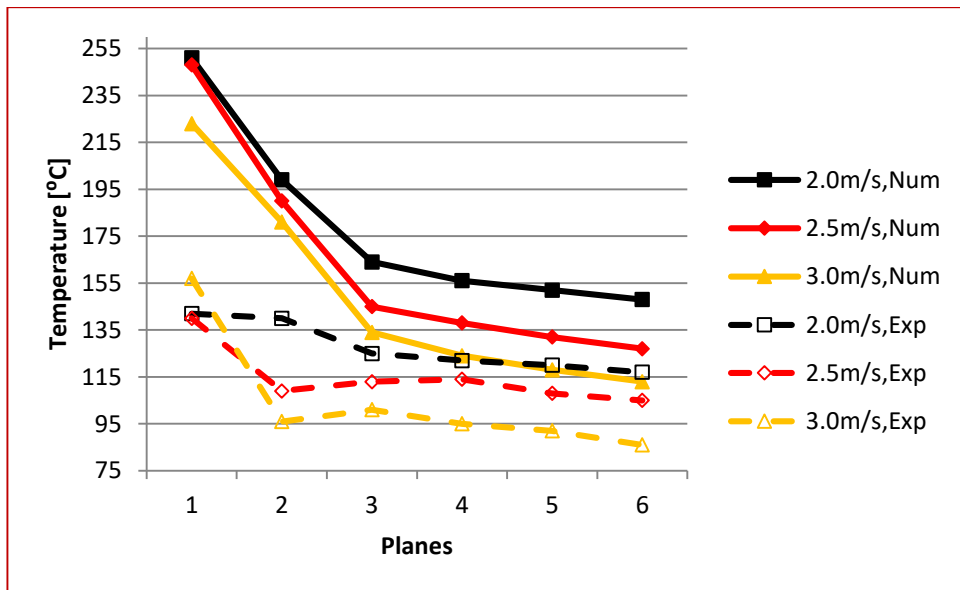


Figure 3.22 Profiles of maximum temp. on planes in case A for  $\alpha=30^\circ$

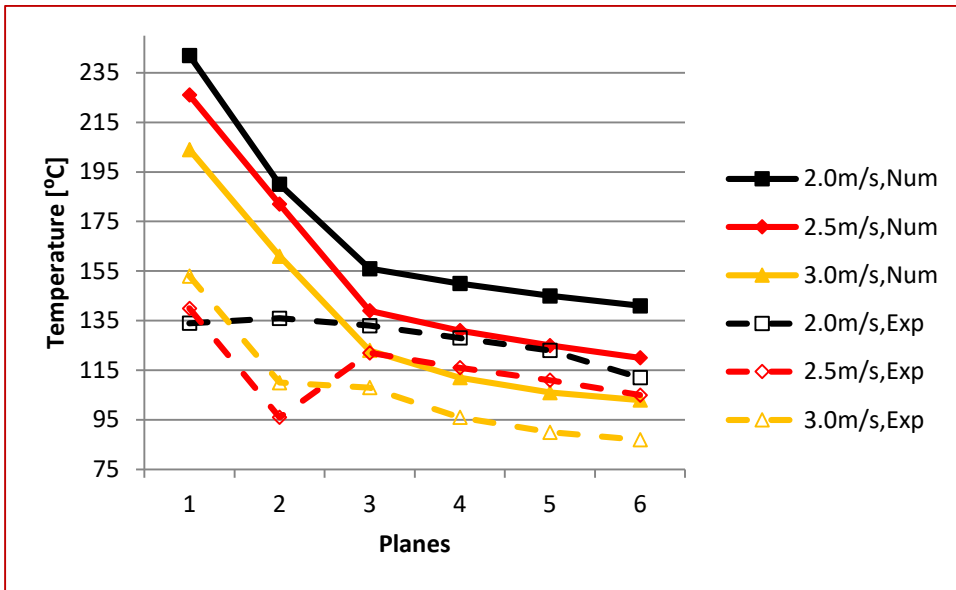


Figure 3.23 Profiles of maximum temp. on planes in case A for  $\alpha=35^\circ$

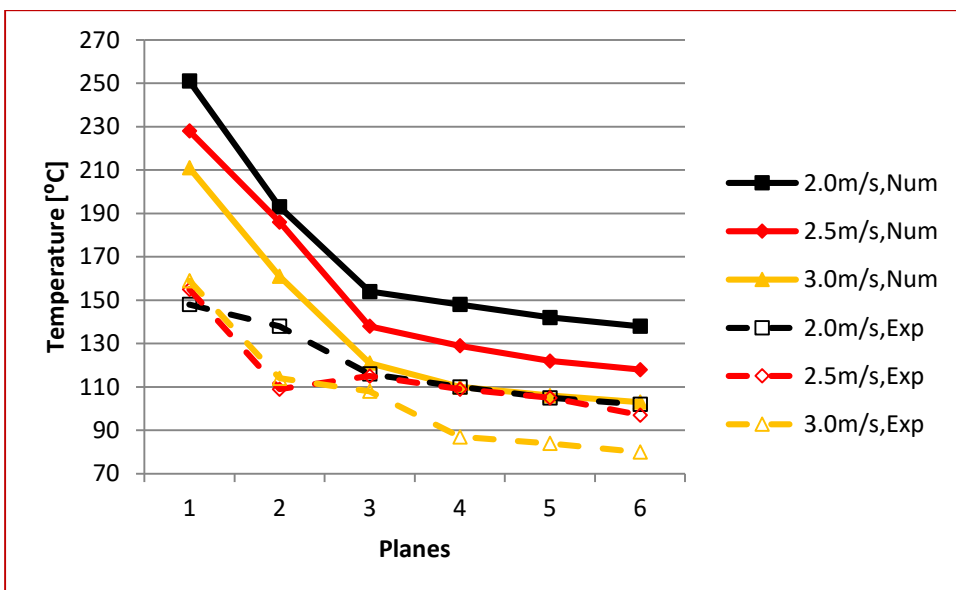


Figure 3.24 Profiles of maximum temp. on planes in case A for  $\alpha=40^\circ$

For case A, numerical and experimental results of maximum temperatures on each planes indicate that maximum temperature levels decreases with the increase of

ventilation velocity. Having regard to the results in previous section, trends shows that inclination angle effect on maximum temperature is more significant comparing to ventilation velocity. Even the fluctuations on the some experiment results, there is still a good accordance between the parts of the study.

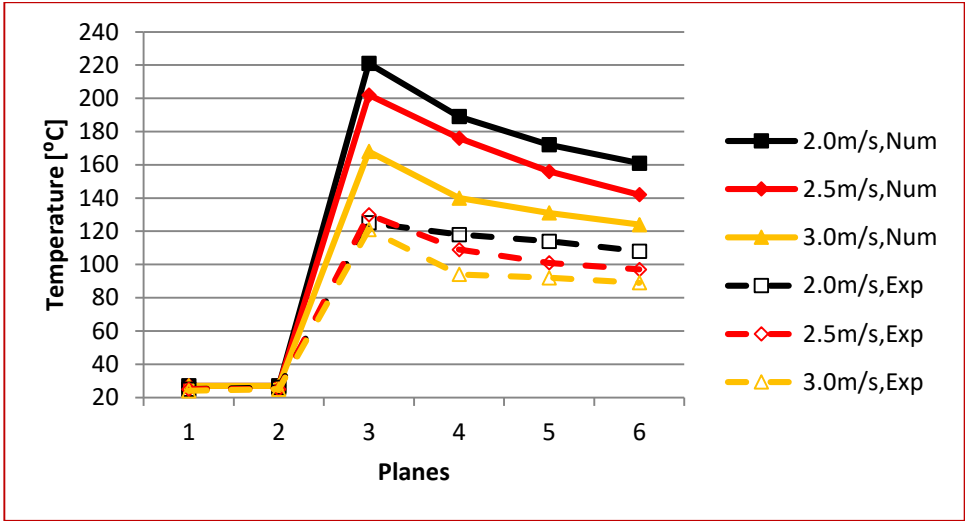


Figure 3.25 Profiles of maximum temp. on planes in case B for α=25°

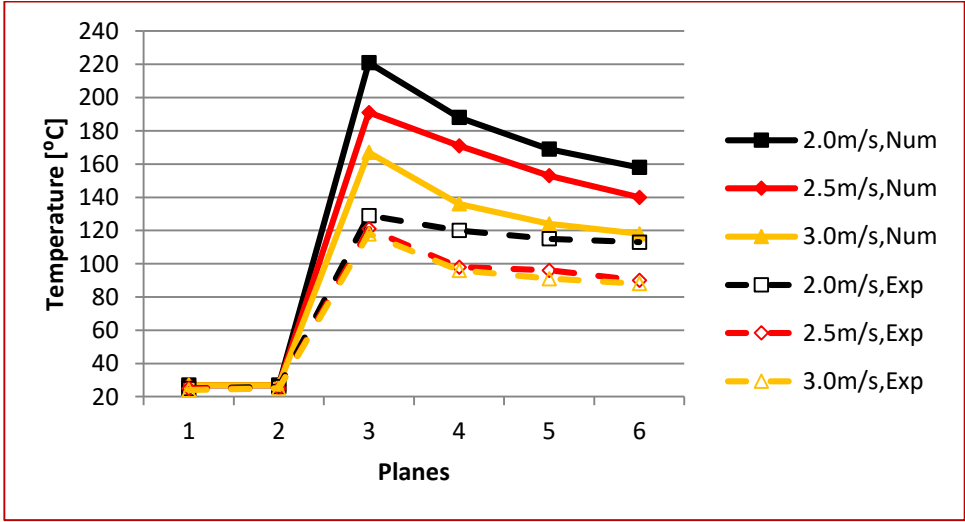


Figure 3.26 Profiles of maximum temp. on planes in case B for α=30°

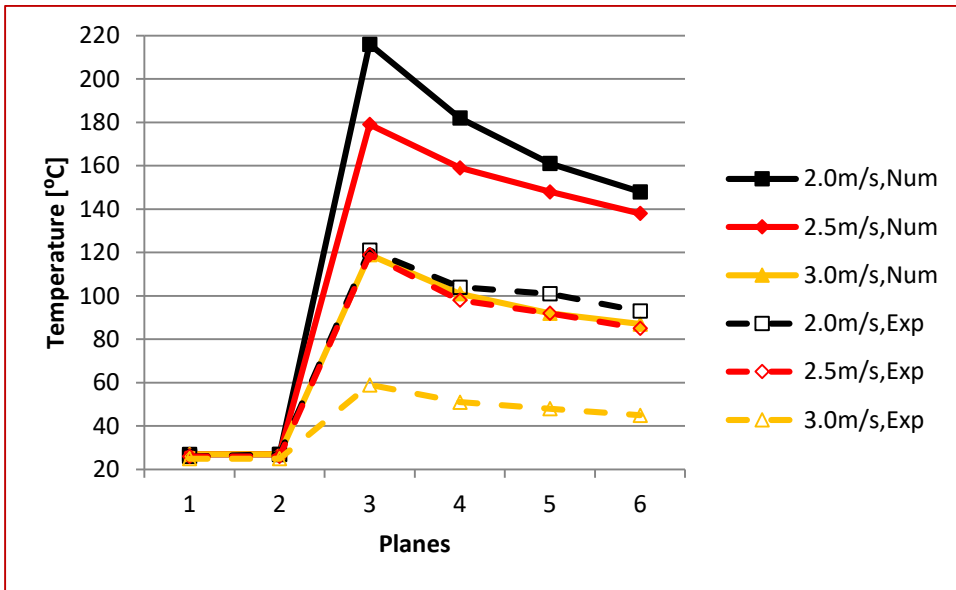


Figure 3.27 Profiles of maximum temp. on planes in case B for  $\alpha=35^\circ$

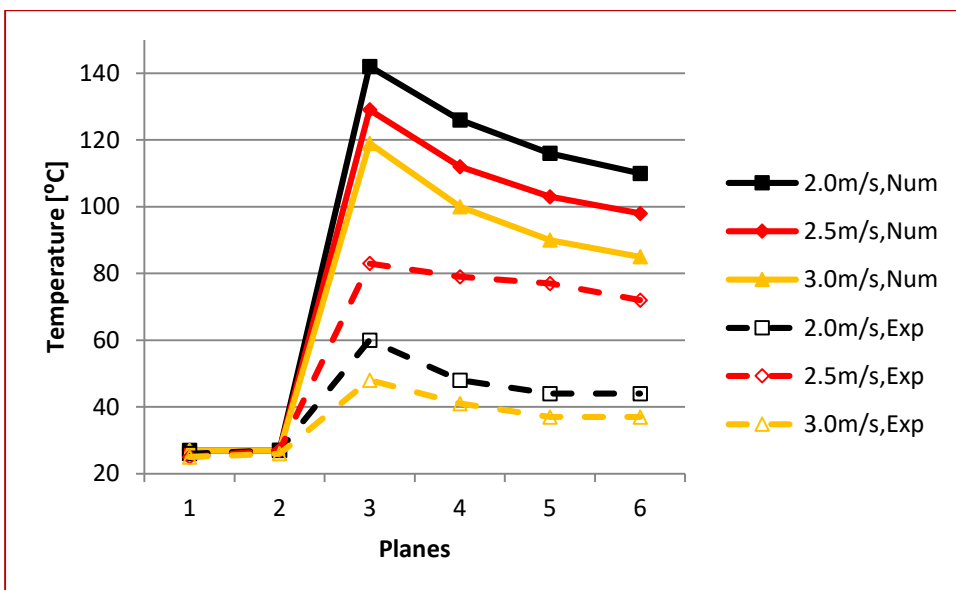


Figure 3.28 Profiles of maximum temp. on planes in case B for  $\alpha=40^\circ$

For case B, maximum temperatures decreasing with the increase of ventilation velocity as in case A. As in the midpoint temperature results, increase of ventilation

velocity does not affect on the decrease of the temperatures in case A. However, for case B, ventilation velocity effect on the maximum temperatures is significant. Peak of the values on third plane is the result of the same reason of fluid flow direction. Numerical and experimental conformity is satisfied.

### 3.3 Results of Numerical Midpoint Velocity on Planes

Numerical midpoint velocity profiles in case A are shown in this section. Velocity results are presented for only numerical work due to the limitations in experimental setup. Keeping ventilation velocity constant, the change in the x-velocity, which is the x- direction component of velocity according to the coordinate system in Figure 2.9, results are given in Figures 3.29-3.42.

#### 3.3.1 Midpoint Velocity Trends for Different Inclination Angles

In this section midpoint velocity trends are presented for analogy on inclination angles in Figures 3.29-3.34.

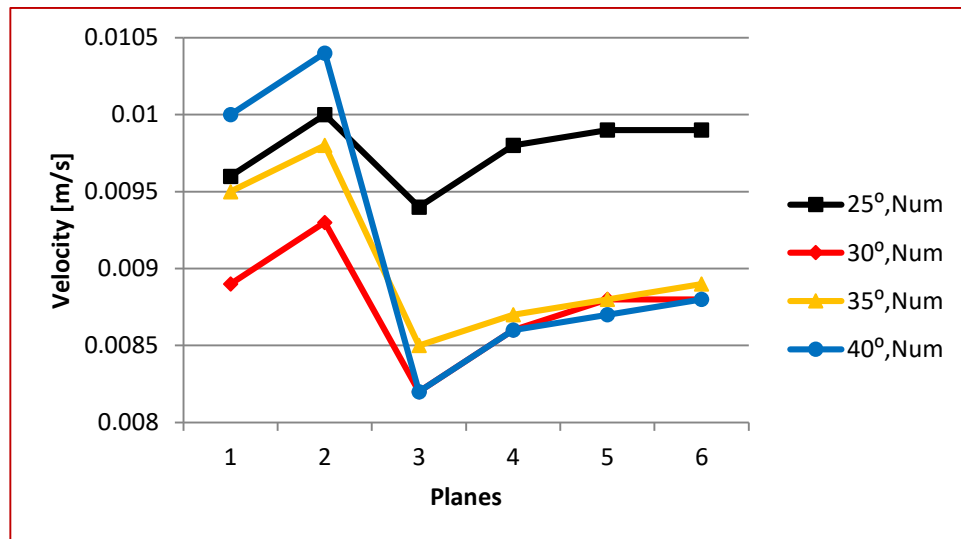
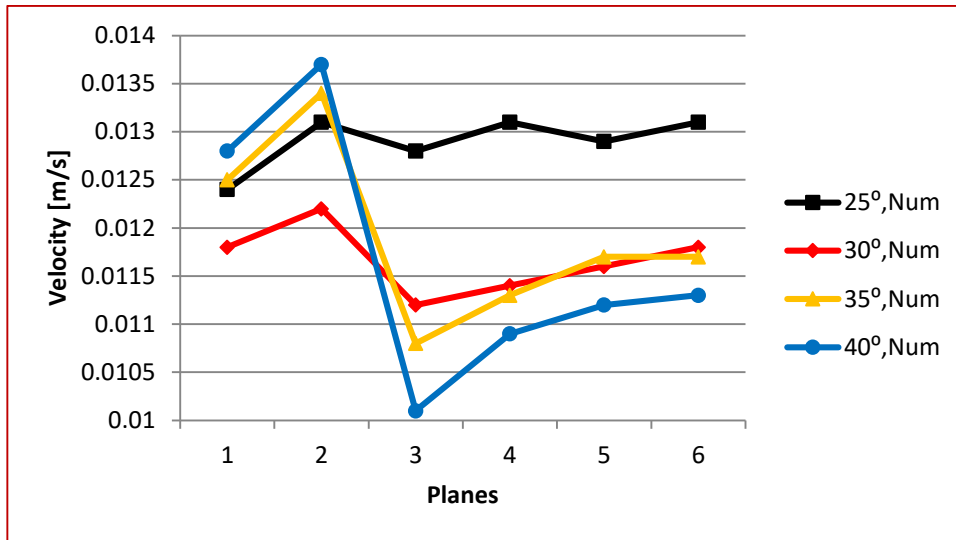
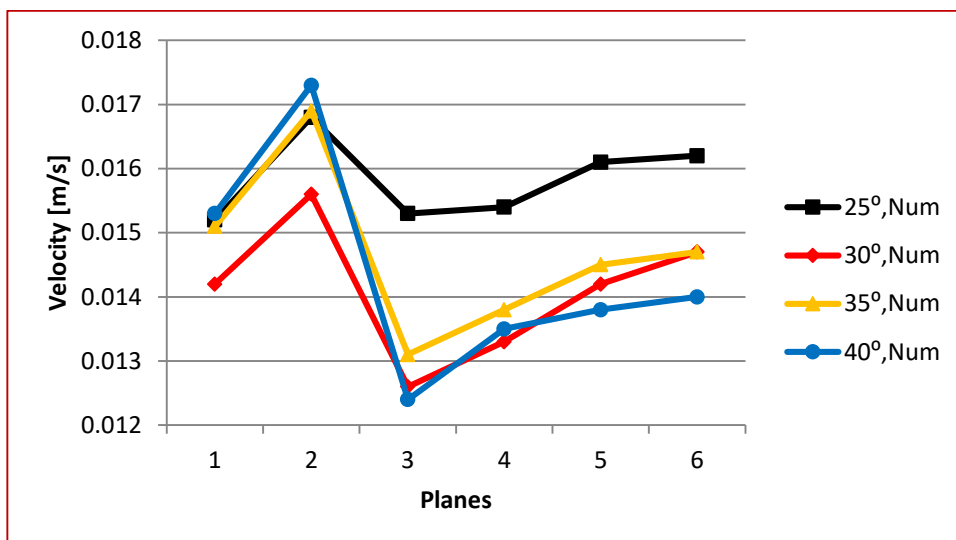


Figure 3.29 Numerical midpoint x-velocity profiles in case A for VV=2.0m/s



**Figure 3.30 Numerical midpoint x-velocity profiles in case A for VV=2.5m/s**



**Figure 3.31 Numerical midpoint x-velocity profiles in case A for VV=3.0m/s**

For case A, it is observed that increase of inclination angle results in decrease in midpoint x-velocities. The peak points on the third planes are due to transient region. Especially, velocity of the fluid is very sensitive to boundaries in case of change in direction of fluid particles. The situation results in sudden drops in this region.

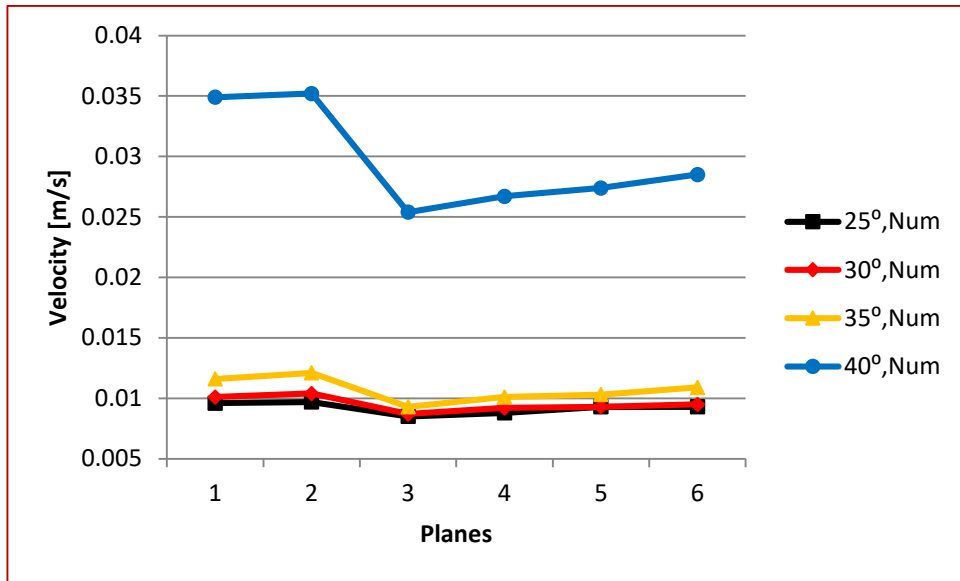


Figure 3.32 Numerical midpoint x-velocity profiles in case B for VV=2.0m/s

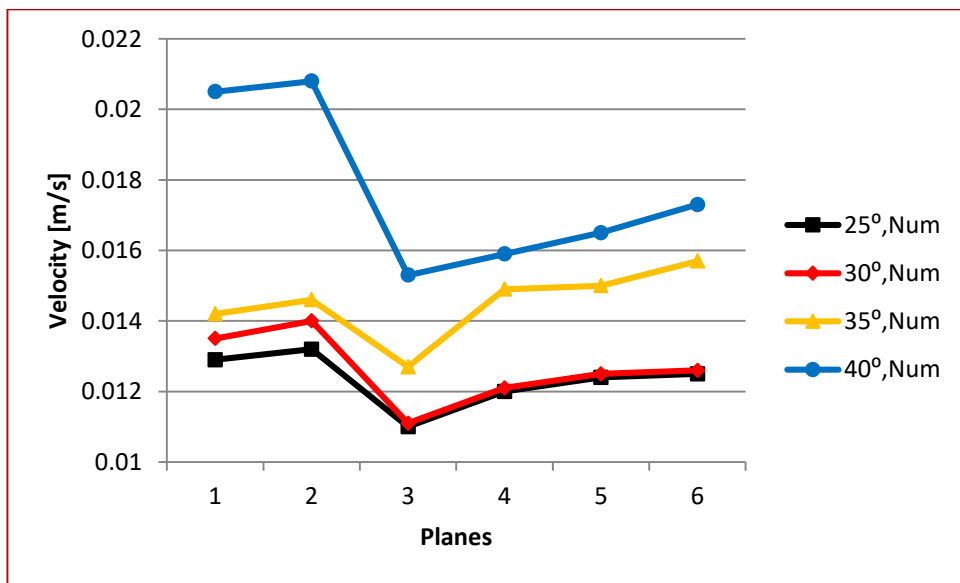
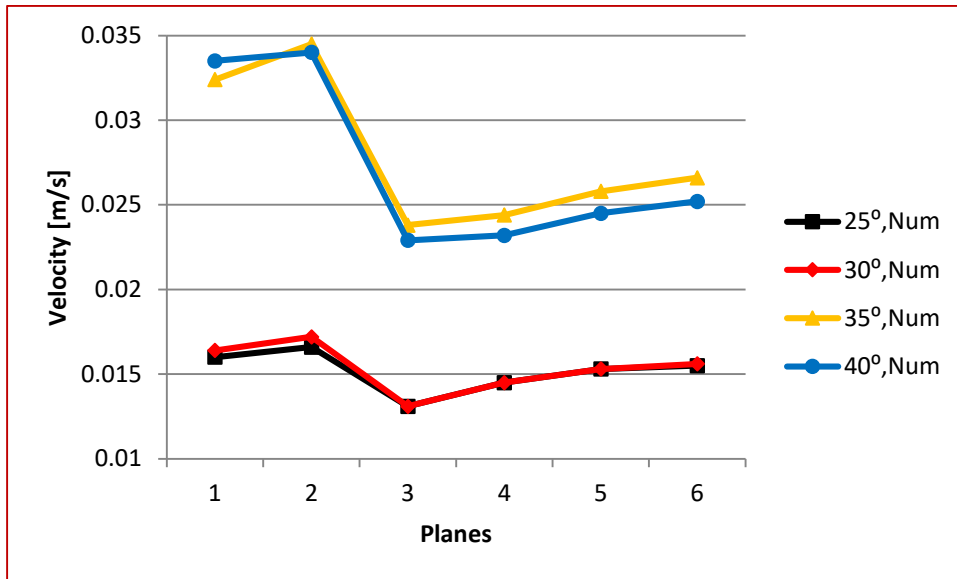


Figure 3.33 Numerical midpoint x-velocity profiles in case B for VV=2.5m/s



**Figure 3.34 Numerical midpoint x-velocity profiles in case B for VV=3.0m/s**

For case B, the increase of inclination angle leads the midpoint x-velocities to decrease. However, increase of the ventilation velocity reduces the differences in the x-velocities for different angles. X-velocity differences are so great between the inclination angle of 40° and others for ventilation velocity of 2m/s. The difference is decreasing with the increase of ventilation velocity and results are getting closer. This may be the results of sensitivity of fluid velocity to the transient region changes with the inclination angle. Furthermore, the backflow formation in lower inclination angles is easier for the same ventilation velocity, as revealed in Section 3.4. So the explanation of the trends may be concluded to the backflow formation and changes in the fluid flow directions can lower the x-velocities.

### 3.3.2 Midpoint Velocity Trends for Different Ventilation Velocities

In this section midpoint velocity trends are presented for analogy on ventilation velocities in Figures 3.35-3.42 and same data in previous section as new figures are put forward to behold to the ventilation velocity effects in the same graphs for each inclination angle.



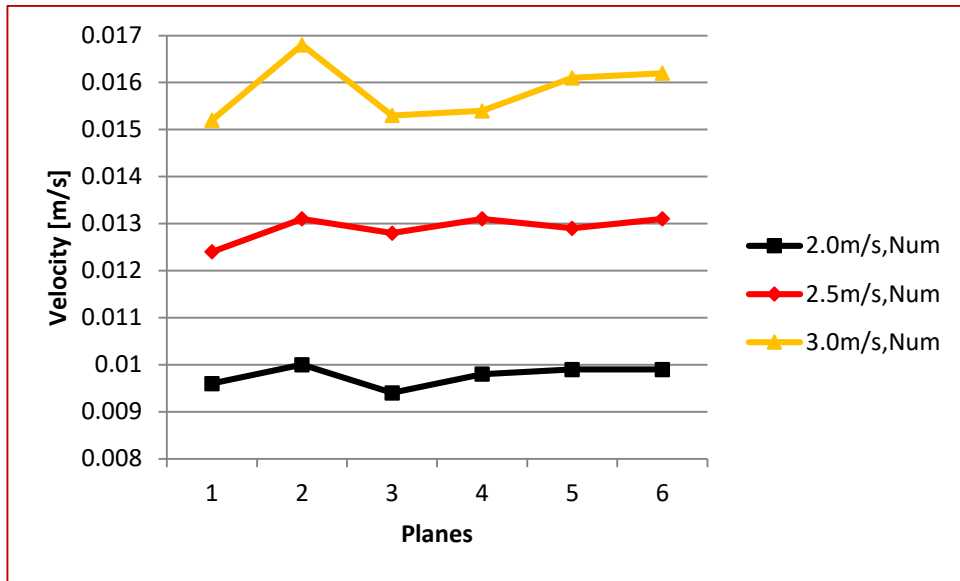


Figure 3.35 Numerical midpoint x-velocity profiles in case A for  $\alpha=25^\circ$

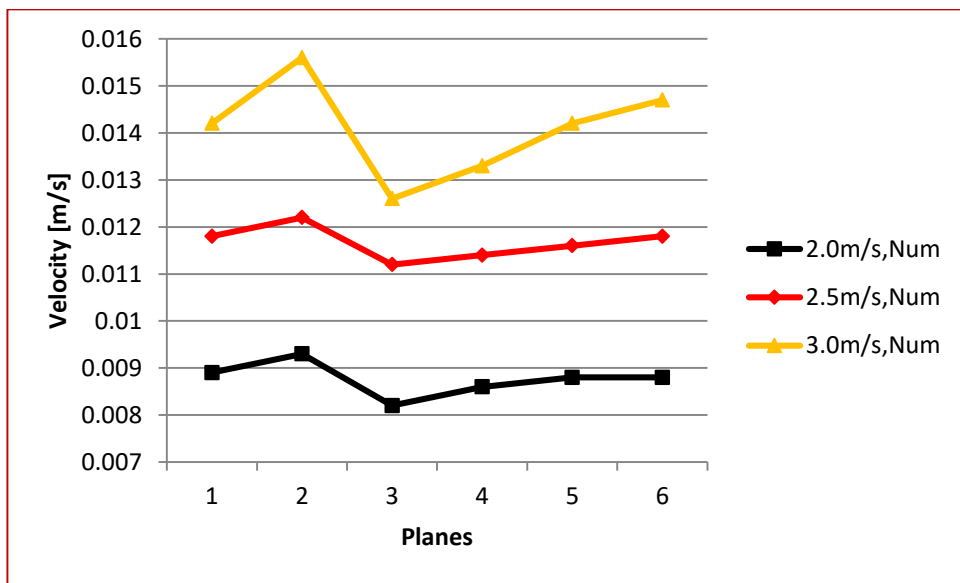


Figure 3.36 Numerical midpoint x-velocity profiles in case A for  $\alpha=30^\circ$

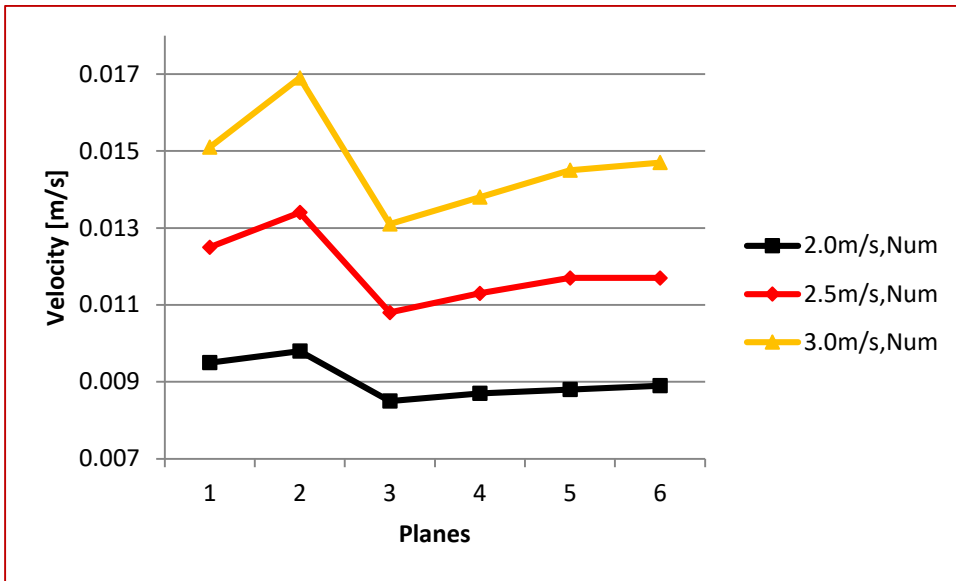


Figure 3.37 Numerical midpoint x-velocity profiles in case A for  $\alpha=35^\circ$

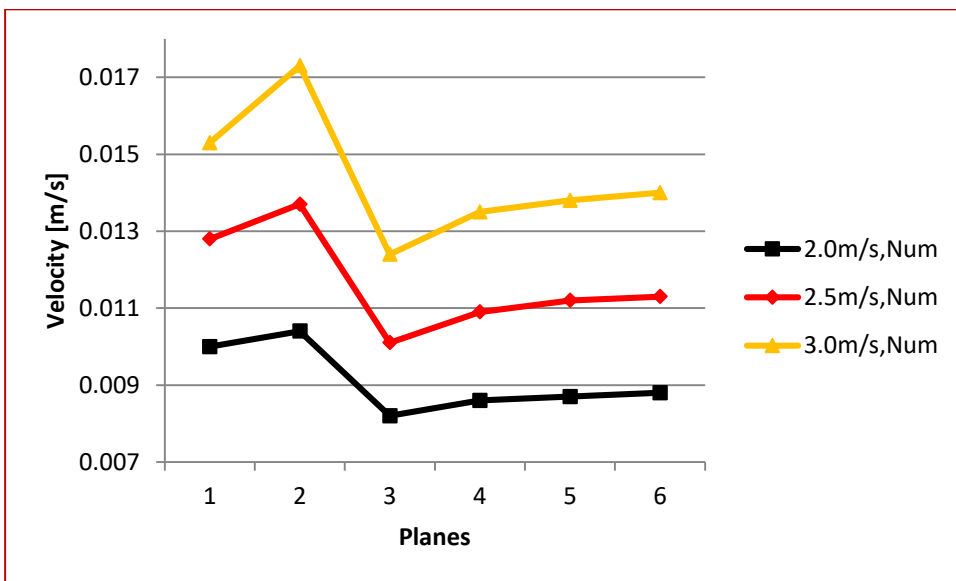


Figure 3.38 Numerical midpoint x-velocity profiles in case A for  $\alpha=40^\circ$

For case A, increase of ventilation velocities results in increase in the midpoint x-velocities. Transient region affect is increasing with the increase of inclination angle and sharper drops take place on third plane. Ventilation velocity affects positively the fluid flow through the tunnel as expected.

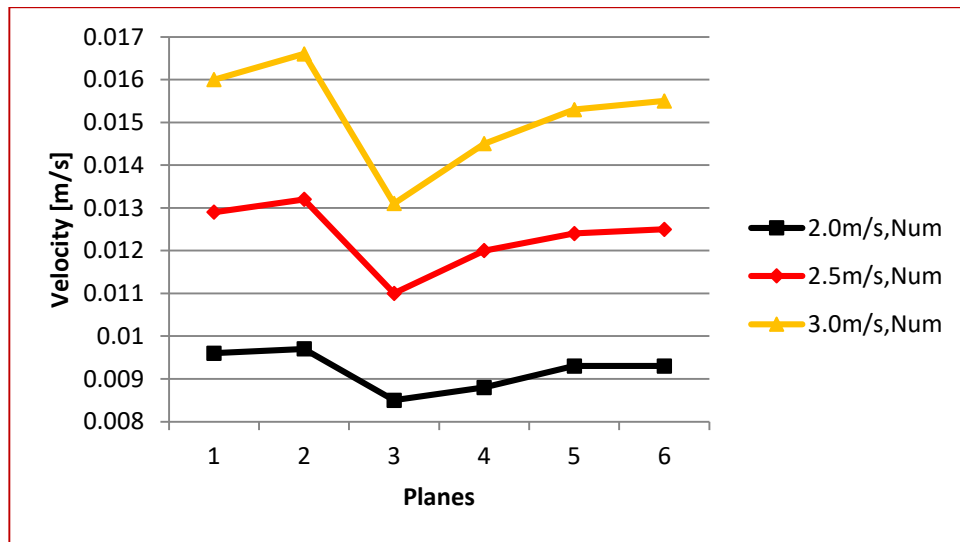


Figure 3.39 Numerical midpoint x-velocity profiles in case B for  $\alpha=25^\circ$

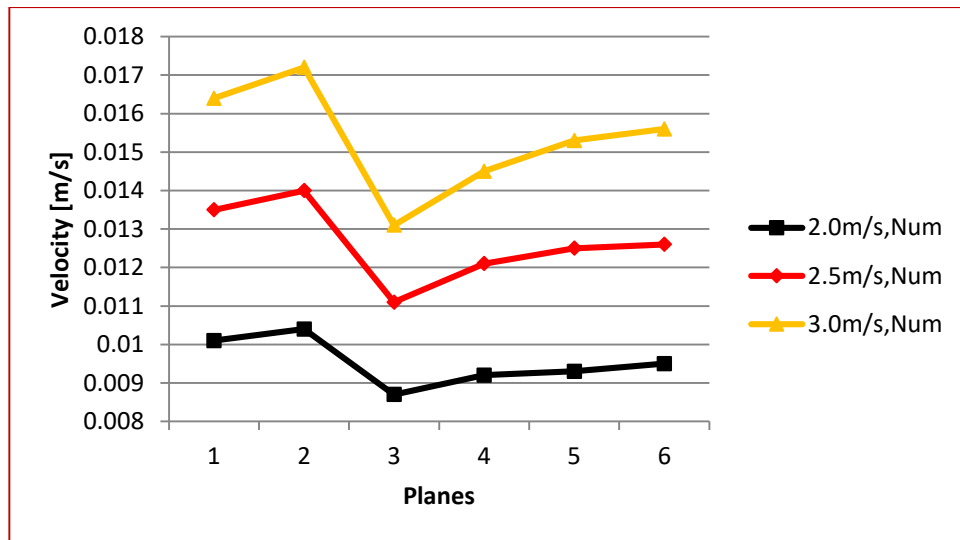


Figure 3.40 Numerical midpoint x-velocity profiles in case B for  $\alpha=30^\circ$

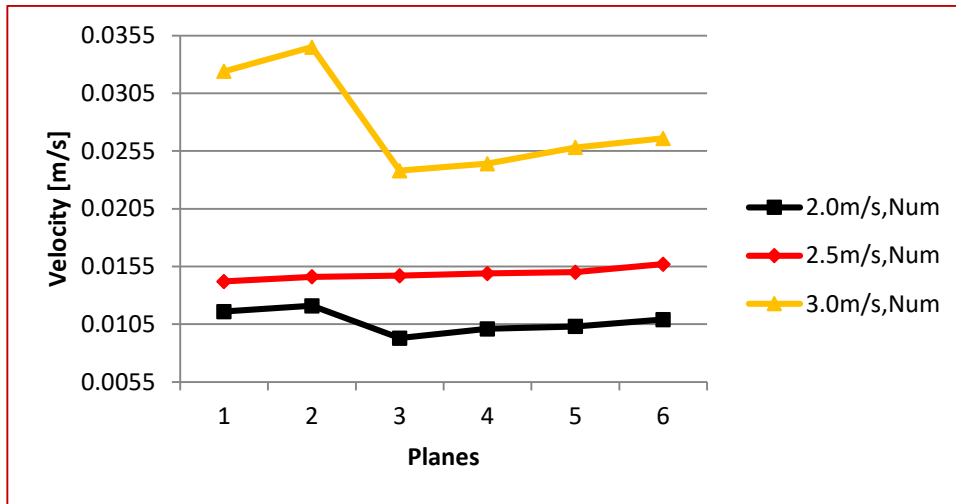


Figure 3.41 Numerical midpoint x-velocity profiles in case B for  $\alpha=35^\circ$

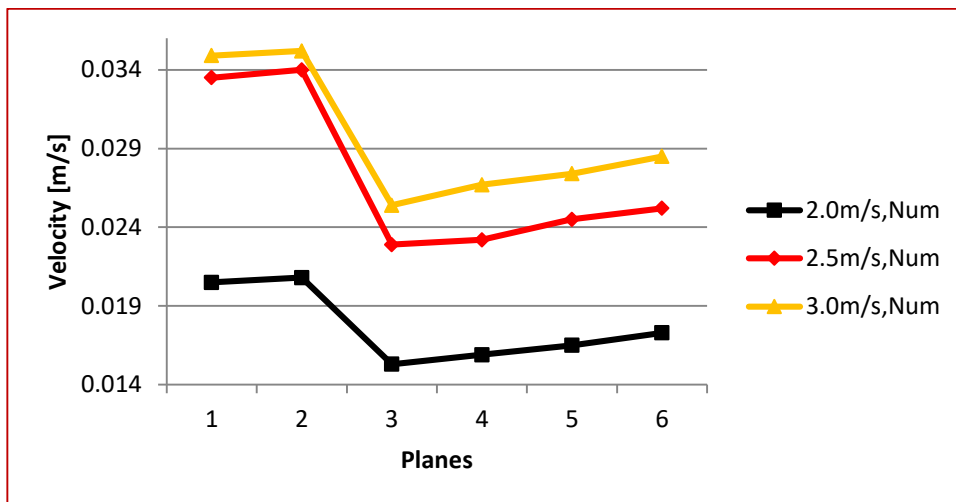


Figure 3.42 Numerical midpoint x-velocity profiles in case B for  $\alpha=40^\circ$

For case B, the effect on x-velocities is same with case A. However, for inclination angles of 35 and 40 degrees in case B, increase of ventilation velocity leads more effects on the increase of mid point velocities. For this reason it can be said that fire placement is an important criteria for the velocity of the flow inside of the tunnel in case of a fire. This situation can be linked to the backflow formation as in the previous section. Especially for case B, it is harder for the flow to build up its regime through

the tunnel, while in case A, it has more way exist through the tunnel until the problematic region of linkage, to get in to the steady regime. The same trends of x-velocities for 35 and 40 degrees is observed as in the previous section.

### 3.4 Numerical Streamline Results

Numerical streamline profiles are presented in this section. Back-layer formations in which conditions take placed and how to be hindered are discussed. For each ventilation velocity and for each inclination angles, resulted streamline profiles are given in Figures 3.43 and 3.44.

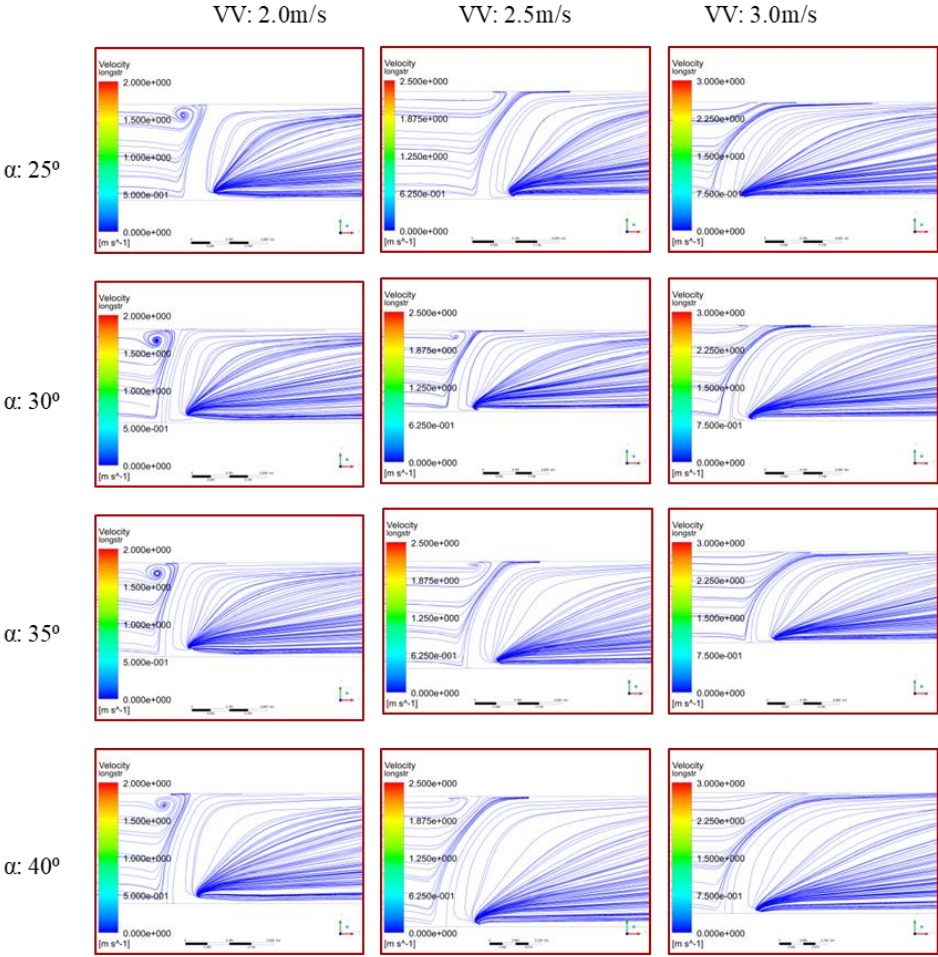
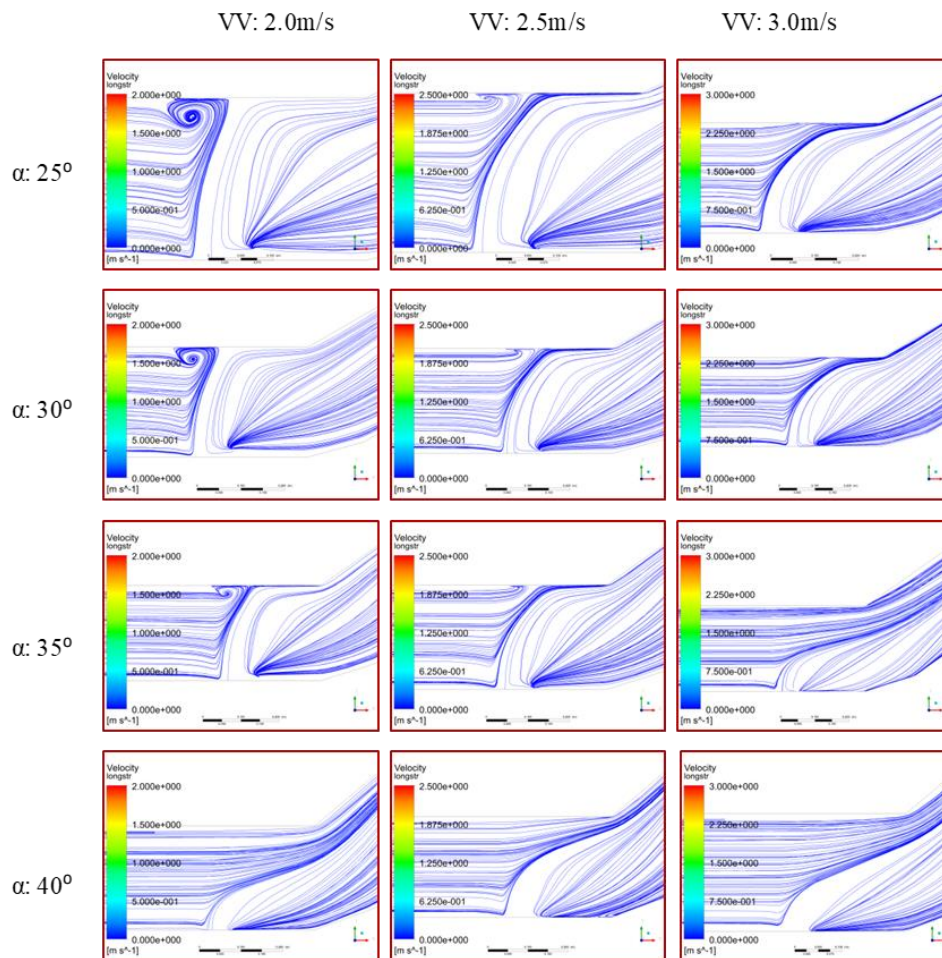


Figure 3.43 Numerical streamline results for case A



**Figure 3.44 Numerical streamline results for case B**

Even the aim of this thesis is the smoke flow visualization with the temperature profile investigation, unfortunately, it was not possible in this experimental setup to visualize the burned gases which are colorless. Also, it was not possible to burn a material like wood, coal etc. as not having suitable measurement instruments to stabilize the mass flow rate due to the impurities in such materials. Then, it was decided to visualize the trends of hot air patterns in numerical study. So after the very good match-up results, less-than-stellar, of numerical and experimental work, streamlines and velocity vectors were showed in numerical analyses. After program runs for every single case, streamline results were reached. Following the trials and investigations for meaningful velocities, velocities were decided to be as 2m/s, 2.5m/s

and 3m/s. It was deduced from the numerical results that increasing velocities with same inclination angle results in a decrease in the volume of backflows shown as vorticities in Figures 3.43 and 3.44. Moreover it is clearly seen that in Figures 3.43 and 3.44, increasing inclination angles with the same ventilation velocity also results in a decrease of in the volume of backflows. Furthermore, changing both velocity and inclination angle at the same time, as can be seen comparing cases of inclination angle of 25° and ventilation velocity of 2m/s and inclination angle of 30° and ventilation velocity of 2.5 m/s in Figure 3.44, backflows can be destroyed with slight adjustments rather than changing one of this properties in great amount. Besides, comparing case A and case B, it is fathom out that in case B hot air tends to create larger vorticities causing backflow as presented in Figures 3.43 and 3.44. However, as an important result, for inclination angle of 40° and ventilation velocity of 2.0m/s, it can be deduced comparing Figures 3.43 and 3.44 that for a fire existing closer to stairs, it is simpler to destroy the backflows. So fire placement is a very important criteria in terms of backflow formation.

**Table 3.1 Key Results**

<b>Results</b>	<b>Change</b>
Midpoint temperature	Maximum value of the midpoint temperature decreases with $\alpha$ by 35% in Figure 3.4
Maximum temperature	Maximum temperatures decreases with $\alpha$ by 36% in Figure 3.19
Midpoint velocity	Midpoint velocities decreases with $\alpha$ by 72% in Figure 3.32
Back flow	Backflow formation can be hindered with increase of VV or $\alpha$

### **3.5 Numerical Streamline Results for Lower Ventilation Velocity**

Analyses for lower velocities were also performed. Results show that temperature

outputs cannot be interpreted in a sensible way as fluid speed is very low, and there is no heat flux through the walls. The temperature does nearly not change much in the system. However, flow patterns looks very interesting for lower ventilation velocities. In numerical part, air inlet does not flow properly through the fan side when velocities are in lower ranges in case of the same inlet mass flow rates and vorticities show up. Cases of 0.1 m/s are presented in Figures 3.45 and 3.46.

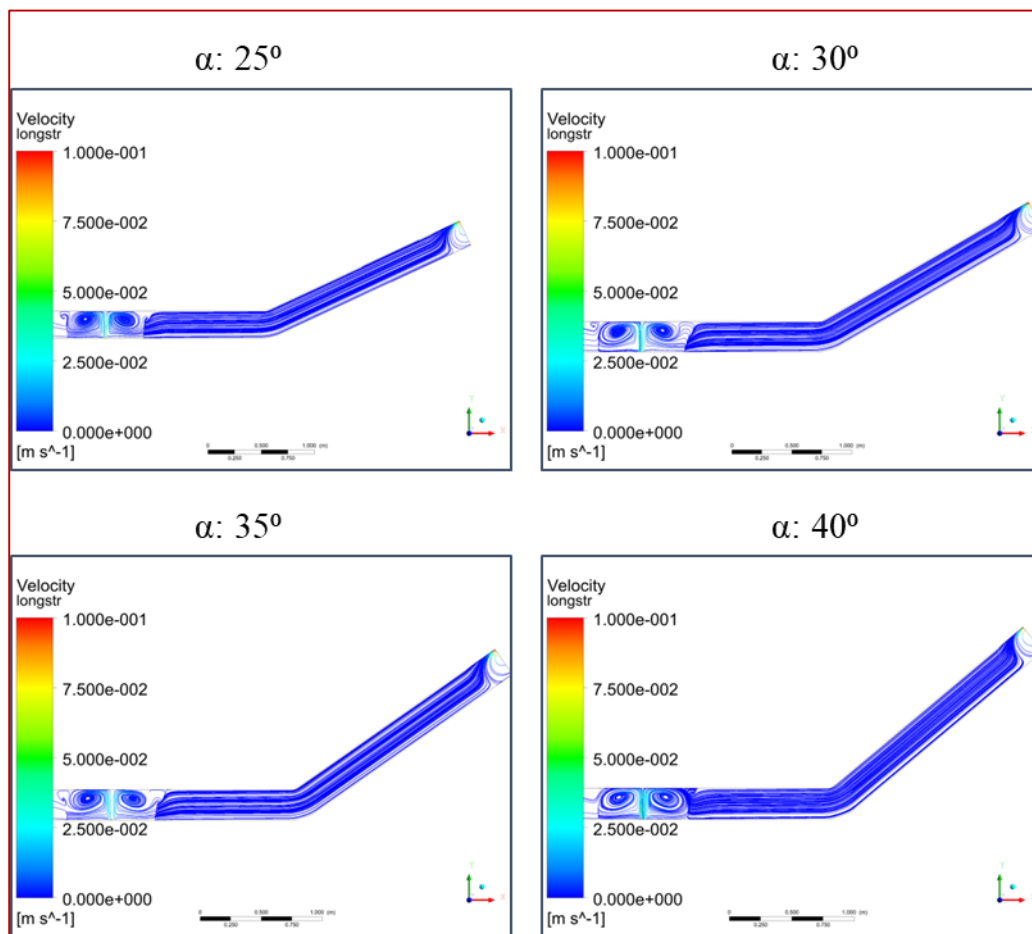
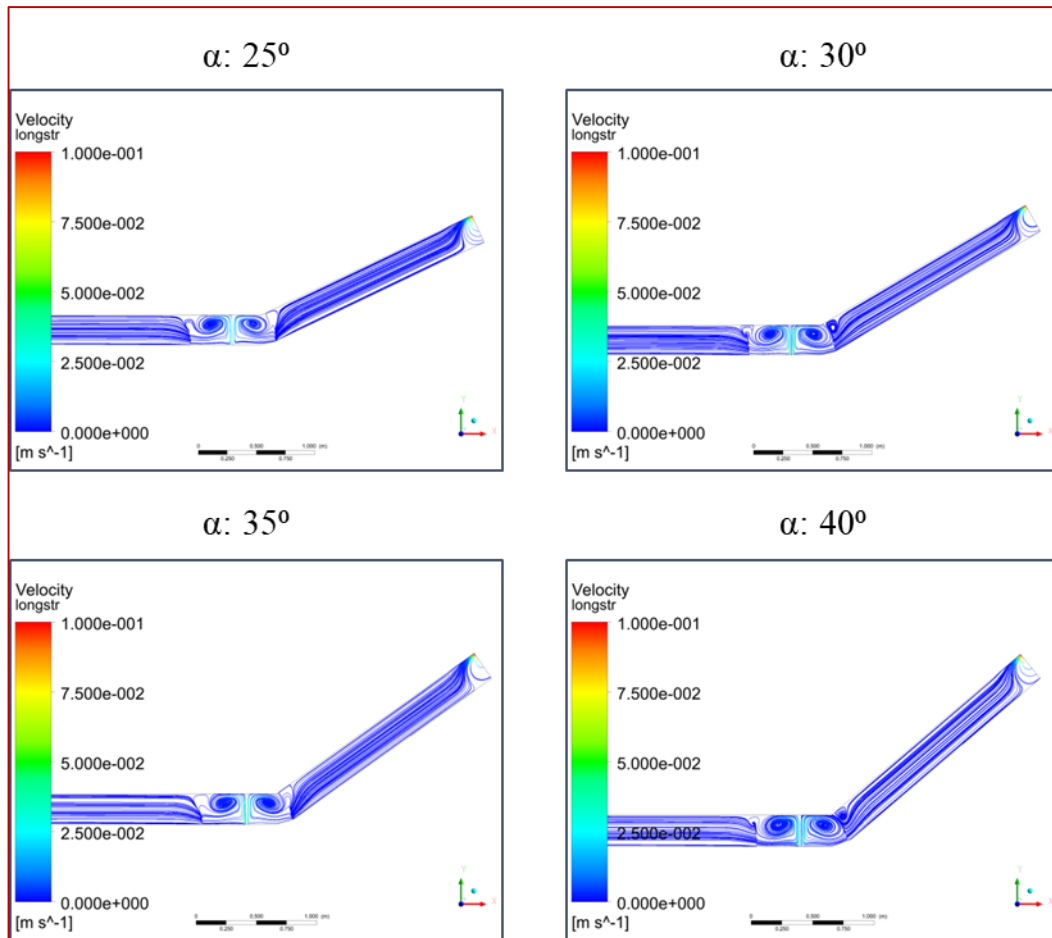


Figure 3.45 Numerical streamlines of  $VV= 0.1\text{m/s}$  for case A





**Figure 3.46 Numerical streamlines of  $VV= 0.1\text{m/s}$  for case B**

For lower ventilation velocities, lower inlet mass flow rate is required. Therefore, as mass flow of the inlet of the experimental system is not able to be regulated as required, lower ventilation velocities could not be investigated.

However an interesting results can be seen on the Figures 3.45 and 3.46. Besides the larger vorticities, other smaller vorticities stand at the ceiling. For both cases smaller vorticities occur and it is seen that inclination angle increase do not affect the intensity of their volumes.

This results are due to the decrease of the ventilation velocities. Comparing the main

study with higher ventilation velocities, lower velocities have tendency to affect the flow patterns in a very different way. Furthermore, while no smaller vorticities are observed one side of the fire location, one can occur on the other side. Besides, vorticity formations can be seen on the both sides. To sum up, another study with smaller ventilation velocities may bring on the understanding of the flow characteristics for different inclination angles.

## CHAPTER 4

### CONCLUSION

#### 4.1 Conclusions

Two different approaches were applied to the subject of flow visualization and determination of temperature distribution in inclined channels as experimental and numerical.

In experimental approach, a combined tunnel system including one horizontal and one inclined tunnel integrated to each other was constructed in a laboratory. After an about two months of work for setup constructions, experiment and numerical work matrix presented in Table 2.1 was created. Afterwards, trials in a couple of weeks were made to stabilize the setup and consistent data was taken.

In experimental study, experiment matrix was applied and results were taken. Data collections were gathered and controlled by making all the experiments again. In numerical approach, analyses on temperature and flow patterns for the exact fire case scenario of experimental study were performed, except wall boundary conditions explained in Section 2.4.

All the study were done constituting an original setup by means of including both horizontal and inclined tunnels as a whole and specifically focusing the inclination angles higher than 25 degrees.

Main conclusions are summarized as follows:

- Temperatures on the planes are strictly dependent on the all three parameters of inclination angle, fire placement and ventilation velocity.
- Inclination angle and ventilation velocities should be carefully chosen for optimization on the tunnels as midpoint temperatures on the positions that may represent the height of the heads of people, in a real subway, taking the stairs do not have a straight forward trend affected by these parameters.
- Fire location is another important parameter. Ventilation velocity, in case of a fire, should be controlled by velocity adjustable fans for different fire locations.
- Maximum temperatures in tunnels are easy to be overcome comparing to midpoint temperature control. Increase of inclination angle and/or increase of ventilation velocity lead the maximum temperatures decrease. However, fire locations should be taken into consideration for the adjustment to reach intended lower temperatures.
- Inclination angle effect on maximum temperature is more significant comparing to ventilation velocity.
- For midpoint x-velocities, increase of inclination angle and/or decreasing ventilation velocity lead the x-velocities decrease and these parameters should be adjusted not to disturb balance of people, for a real fire case, while they are rushing to the exit. X-velocities are either sensitive to fire location as temperature, and must be optimized according to the location of fire.
- In a fire case, hot gases flow nearby the ceiling and high temperature regions take place in heights in tunnel, shown on figures in Appendix A in detail.
- Over the region of fire taking place, hot gases create backflows that are to be hindered saving people in the tunnel from intoxication for a real scenario.
- By means of ventilation to discharge the released hot gases, backflows can be destroyed. There are two alternatives to avoid the backflows that are increasing ventilation velocity and increasing inclination angle or both.

- Increasing inclination angle looks way better solution due to the fact that discharge velocity may disturb people in tunnels for a real fire scenario. Moreover, as higher angles decrease the distance between the ground and tunnel basement, people would reach the safe atmosphere in a shorter time period.
- The region where the fire takes place is an important criterion for the flow velocity through the longitudinal direction of the tunnels.
- The most remarkable results are the drops in the temperatures and the x-velocities. Figure 3.14 shows that maximum value of the midpoint temperatures decreases to 35%, and Figure 3.19 reveals that total maximum temperatures on planes decreases by 36%, and moreover; Figure 3.32 represents that midpoint velocities decreases by 72%, with the change of the inclination angles from 25° to 40°.

All in all, ventilation velocity and inclination angle are very important parameters that affect the temperature and velocity distributions, and backflow formations in inclined tunnels.

#### **4.2 Recommendations for Future Work**

In future work, a better setup may be constructed with high resolution cameras capable of capturing high number of frames in second and flow patterns can be visualized in experimental study.

In the analyses, backflow formations were investigated in terms of variables of fire placement, inclination angle and ventilation velocity. For further analyses, a parameter to measure the backflow may be presented and changes of its characteristics can be discussed by means of that parameter.

This study was conducted to understand the effects of  $VV$  and  $\alpha$  on the temperatures, velocities and backflow formations. As this study do not give results for real subway tunnels in terms of ventilation velocities, a further study can be made for more realistic ventilation cases.

In this thesis, LPG was used as fuel as being suitable for measuring the flow rate and easy to be reached. Later on, a material that is possible to be found in subway stations may be burned to approach a better realistic case.

Besides, a new method called as water mist suppression system as indicated in [28] may be applied to an inclined tunnel to check the visibility inside in such a suppression scenario.

Moreover, as it is seen that new flow patterns are observed for ventilation velocity of 0.1m/s, new studies can be conducted for lower ventilation velocities to understand the flow characteristics for different inclination angles.

## REFERENCES

- [1] Korea Joongang Daily, <http://koreajoongangdaily.joins.com/news/>, last visited on February 2018.
- [2] Aradağ S., *Underground Transportation System Ventilation by Train Piston Effect*, M.S., Department of Mechanical Engineering, METU, 2002.
- [3] Eduardo Blanco Javier Cueto Joaquín Fernández Raúl Barrio, *Numerical Simulation of the Back-layer Critical Velocity in the Memorial Tunnel Test (MTFVTP)*, ASME Fluids Engineering Conference, August, Florida, USA, 2008.
- [4] Yang H., Jia L., Yang L., *Effect of Initial Velocity Field on Smoke Diffusion Characteristic in Subway Tunnel*, ASME Heat Transfer Summer Conference, July, San Francisco, California, USA, 2009.
- [5] Ji J., Wana H., Li K., Han J., Sun J., *A Numerical Study on Upstream Maximum Temperature in Inclined Urban Road Tunnel Fires*, International Journal of Heat and Mass Transfer, Vol 88, pp 516-526, 2015.
- [6] Kayılı S., *CFD Simulation of Fire and Ventilation in the Stations of Underground Transportation Systems*, M.S., Department of Mechanical Engineering, METU, 2005.
- [7] Musluoğlu E., *A Theoretical Analysis of Fire Development and Flame Spread in Underground Trains*, Ph.D. , Department of Mechanical Engineering, METU, 2009.
- [8] Yazıcı Ö., *Metro İstasyonları ve Tünellerinde Yangın ve Tedbirlerinin Analizi*, Yüksek Lisans Tezi, Makine Mühendisliği Anabilim Dalı, Gebze Yüksek Teknoloji Enstitüsü, 2013.
- [9] Altay M., *Tünel Yangınlarının Modellenmesi ve Etkin Parametrelerin Modellemedeki Gerçekçiliğinin İncelenmesi*, Yüksek Lisans Tezi, Makine Mühendisliği Anabilim Dalı, Bursa Teknik Üniversitesi, 2016.

- [10] Yüzücü İ., *Yangın Simülasyon Sonuçlarına Bağlı Olarak Tahliye Senaryolarının Geliştirilmesi*, Yüksek Lisans Tezi, Makine Mühendisliği Anabilim Dalı, Sakarya Üniversitesi,2017.
- [11] Wu Y., Stoddard J.P, James P., Atkinson J.T., *Effect of Slope on Control of Smoke Flow in Tunnel Fires*, Fire Safety Science-Proceedings Of The Fifth International Symposium,pp 1225-1236, 1997.
- [12] Wu Y., Bakar M.Z.A., *Control of smoke flow in tunnel fires using longitudinal ventilation systems - a study of the critical velocity*, Fire Safety Journal,Vol. 35, pp 363-390, 2000.
- [13] Tsai K.C, Lee Y.P., Lee S.K, *Critical Ventilation Velocity for Tunnel Fires Occurring near Tunnel Exits*, Fire Safety Journal, Vol. 46, pp 556-557, 2011.
- [14] Tanaka F., Kato M., Majima S., Kawabata N., Kikumoto T., Yamada M., *On the Smoke Propagation of a Fire in a Tunnel with Concentrated Exhaust Ventilation*, ASME-JSME-KSME Joint Fluids Engineering Conference, July, Hamamatsu, Shizuoka, Japan, 2011.
- [15] Kayılı S., *Effect of Vehicles' Blockage on Heat Release Rate in Case of Tunnel Fire*, Ph.D. , Department of Mechanical Engineering, METU, 2009.
- [16] Yamalı T.U., *An Experimental Study on the Pool Fire Burning Characteristics of N-Heptane and Ethanol in the Tunnels*, M.S., Department of Mechanical Engineering, METU, 2015
- [17] Shafee S., Yamalı U., Yozgatligil A., *Experimental Investigation on the Mass Loss Rates of Thin-Layered n-Heptane Pool Fires in Longitudinally Ventilated Reduced Scale Tunnel*, Combustion Science and Technology, Vol 189:11, pp 1907-1923, 2017.
- [18] Shafee S., Yozgatligil A., *An Experimental Study On The Burning Rates Of Interacting Fires In Tunnels*, Fire Safety Journal, Vol 96, pp 115-123, 2018.
- [19] Kayılı S., Yozgatligil A., Eralp C., *An experimental study on the effects of blockage ratio and ventilation velocity on the heat release rate of tunnel fires*, Journal of Fire Sciences , Vol 29(6), pp 555-575, 2011.



- [20] Kayili S., Yozgatligil A., Eralp C., *Effect of Ventilation and Geometrical Parameters of the Burning Object on the Heat Release Rate in Tunnel Fires*, Combustion Science and Technology, Vol 184:2, pp 165-177, 2012.
- [21] Çelik A., *Experimental and Numerical Studies on Fire in Tunnels*, M.S., Department of Mechanical Engineering, METU, 2011.
- [22] Wu Y., Xing H.J., Atkinson G., *Interaction of Fire Plume with Inclined Surface*, Fire Safety Journal, Vol. 35, pp 391-403, 2000.
- [23] Vauquelin O., Wu Y., *Influence of Tunnel Width on Longitudinal Smoke Control*, Fire Safety Journal, Vol. 41, pp 420-426, 2006.
- [24] Hu L.H., Fong N.K., Yang L.Z., Chow W.K., Li Y.Z., Huo R., *Modeling Fire Induced Smoke Spread and Carbon Monoxide Transportation in a Long Channel: Fire Dynamics Simulator Comparisons with Measured Data*, Journal of Hazardous Materials, Vol. 140, pp 293-298, 2007.
- [25] Zhang J., Zhou X., Xu Q., Yang L., *The Inclination Effect on CO Generation and Smoke Movement in an Inclined Tunnel Fire*, Tunnelling and Underground Space Technology, Vol. 29, pp 78-84, 2012.
- [26] Hu L.H., Huo R., Chow W.K., *Studies on Buoyancy-Driven Back-Layering Flow in Tunnel Fires*, Experimental Thermal and Fluid Science, Vol. 32, pp 1468-1483, 2008.
- [27] Chow W.K., Wong K.Y., Chung W.Y., *Longitudinal Ventilation for Smoke Control in a Tilted Tunnel by Scale Modeling*, Tunnelling and Underground Space Technology, Vol 25, pp 122-128, 2010.
- [28] Balık G., *Karayolu Tünellerinde Su Sisi Söndürme Sistemi*, 11. Ulusal Tesisat Mühendisliği Kongresi, Nisan, İzmir, 2013



## APPENDIX A

### CONTOUR RESULTS OF CFD

#### CASE A

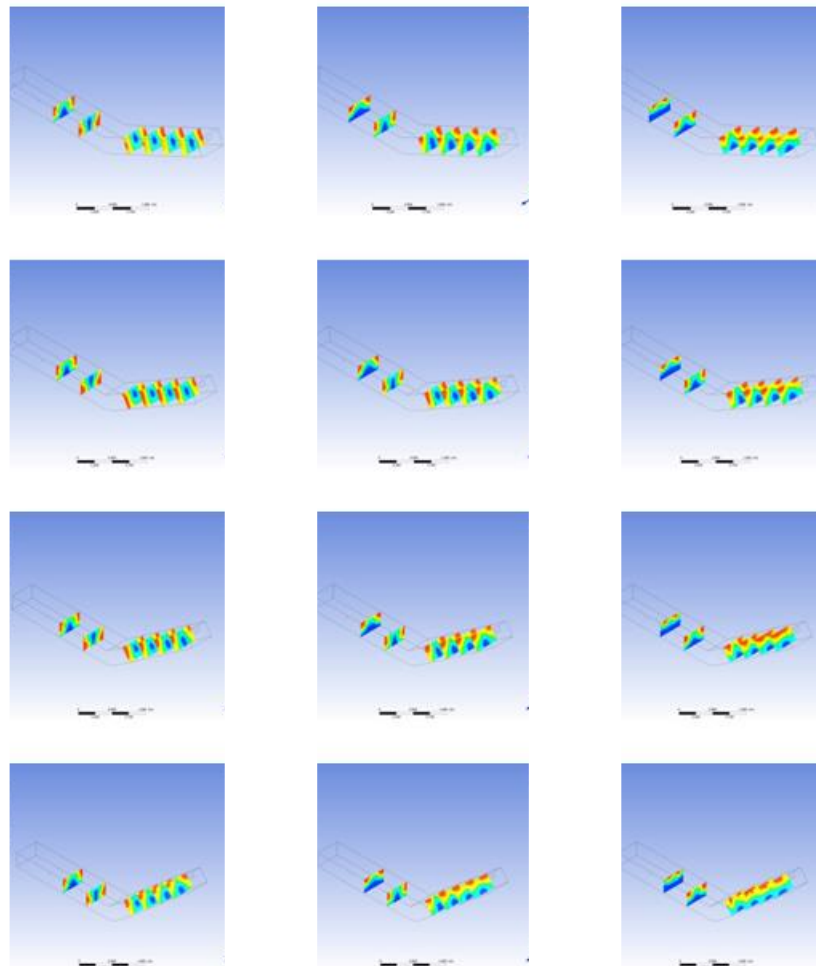


**Figure A.1** Temperature contours for case A

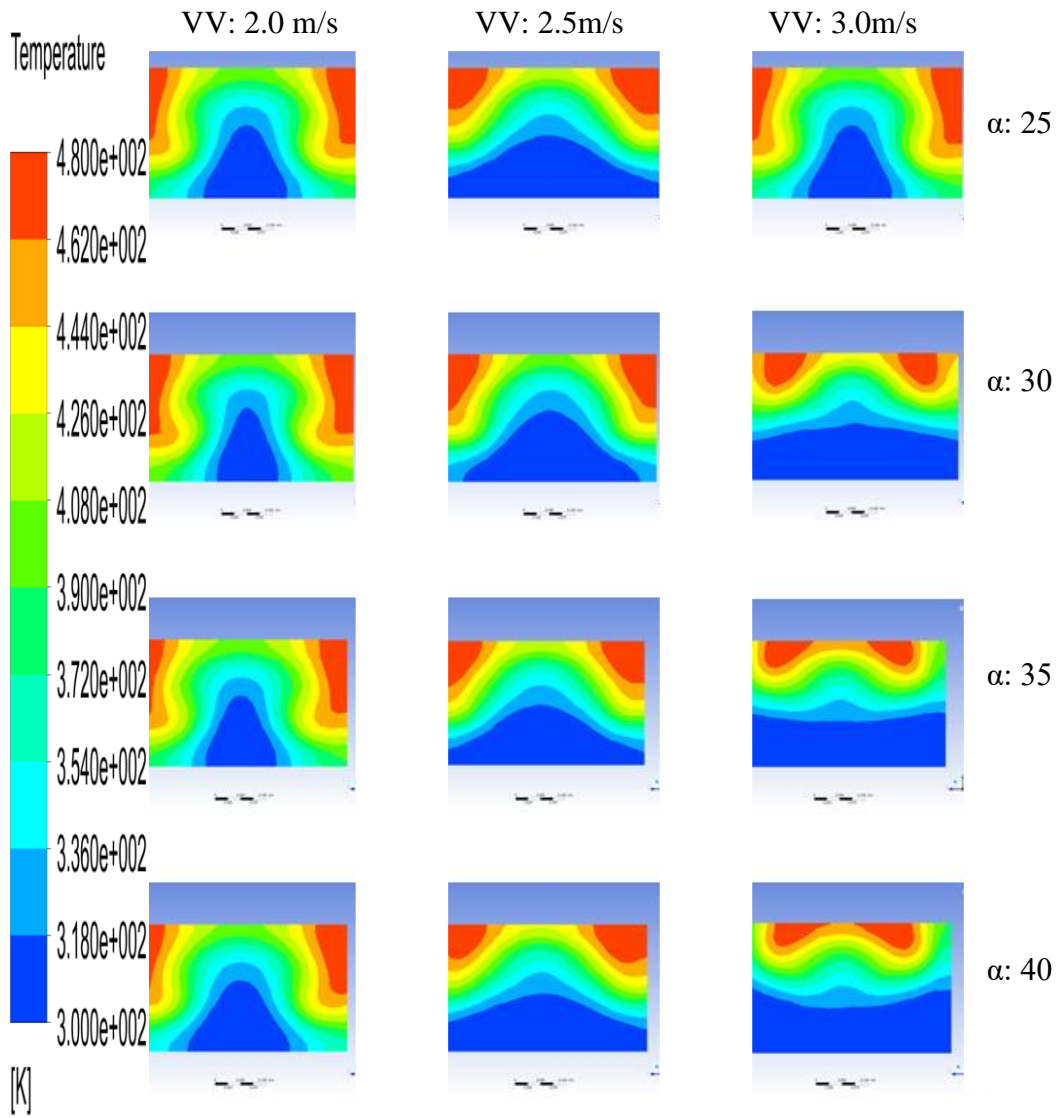


**Figure A.2 Temperature contours on plane horz1 for case A**

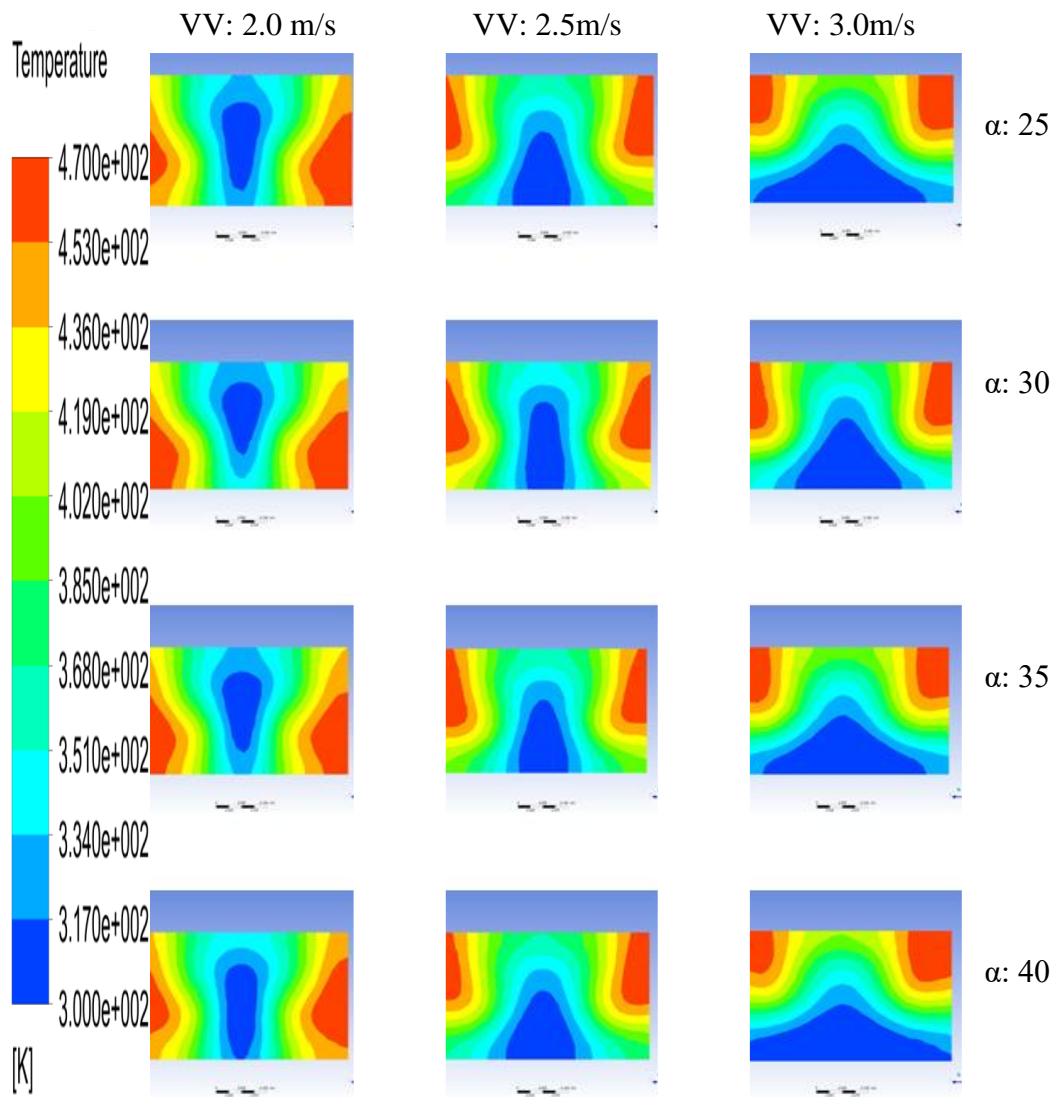


**Figure A.3 Temperature contours on plane horz2 for case A**

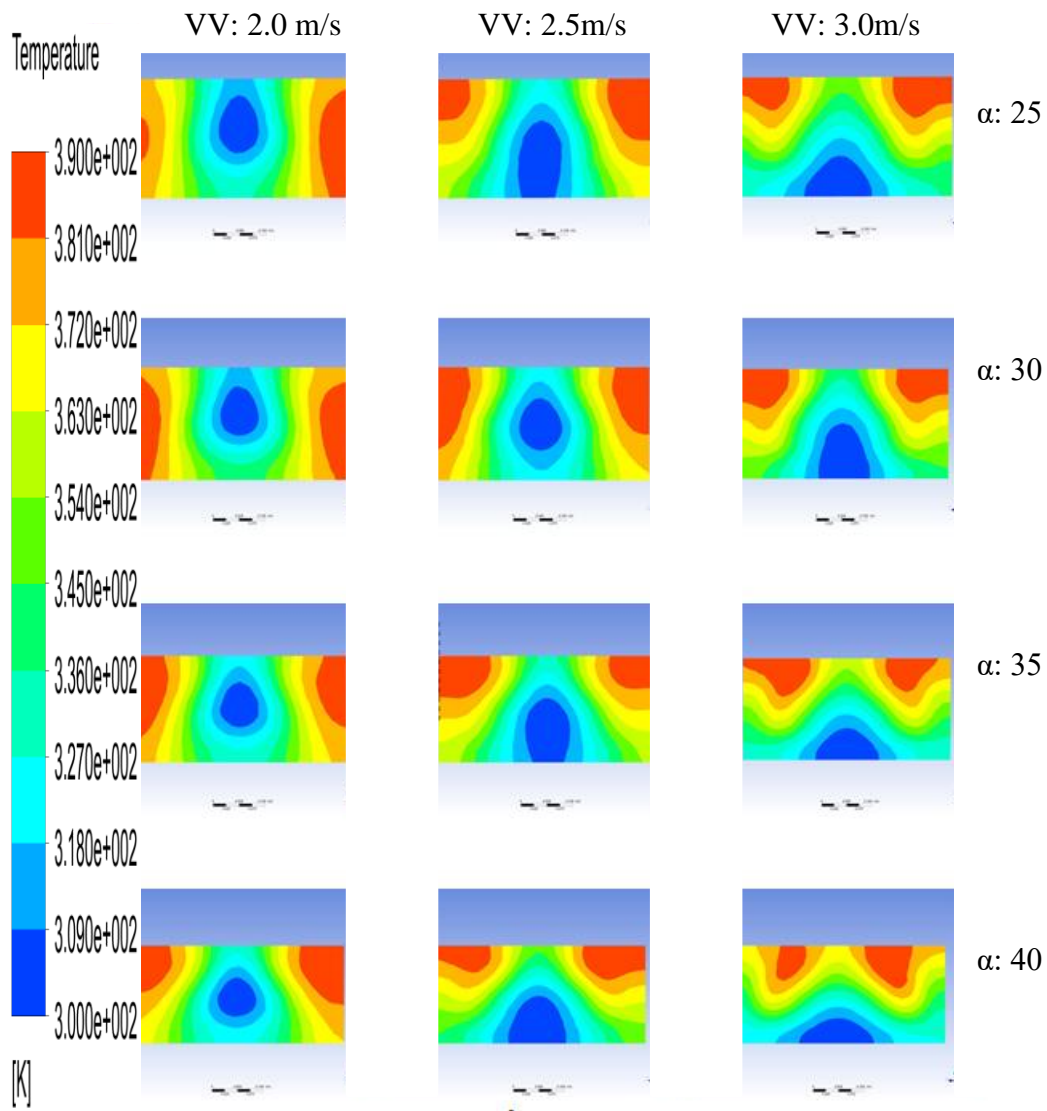


**Figure A.4 Temperature contours on plane inc1 for case A**

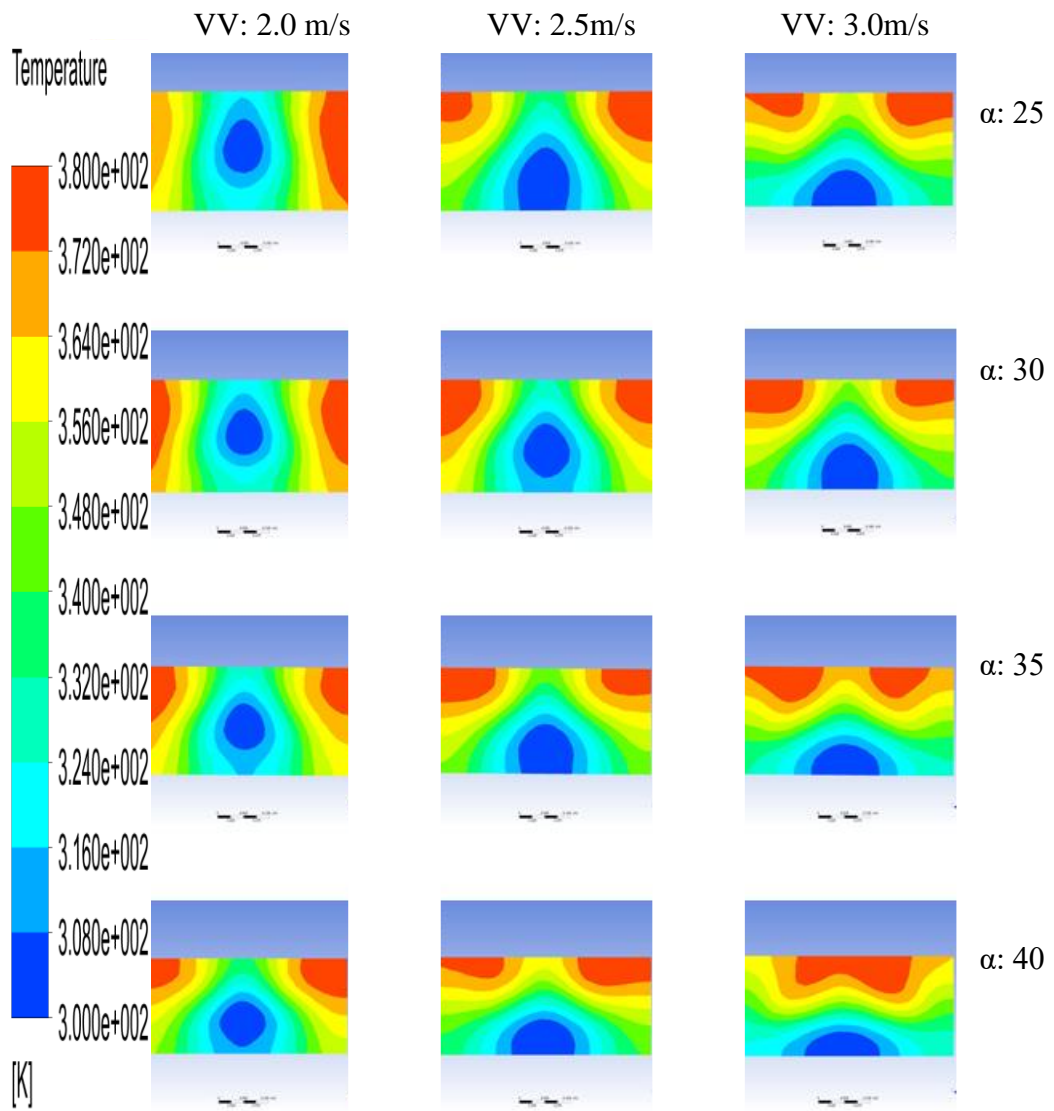


**Figure A.5 Temperature contours on plane inc2 for case A**

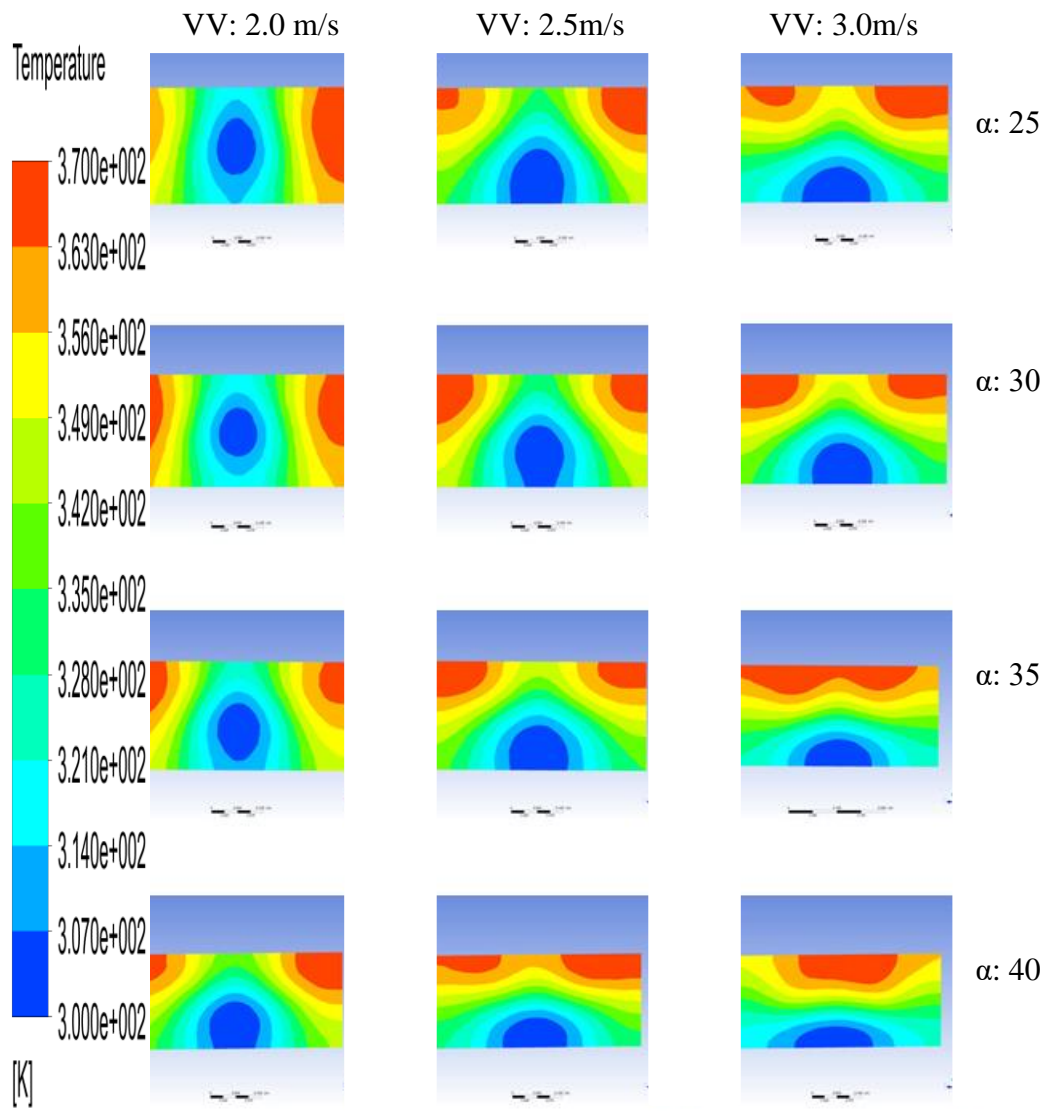


**Figure A.6 Temperature contours on plane inc3 for case A**



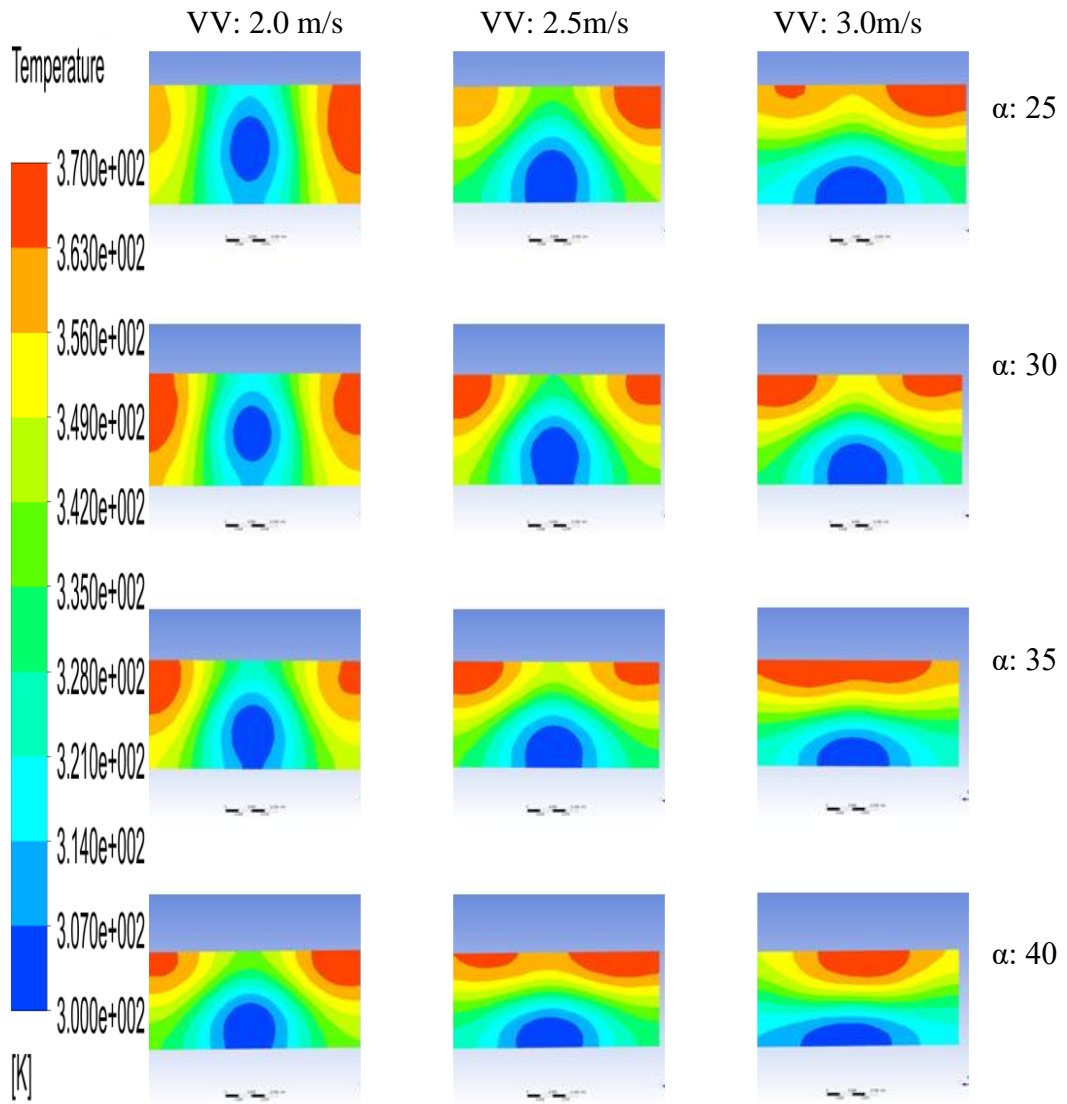


**Figure A.7 Temperature contours on plane inc4 for case A**

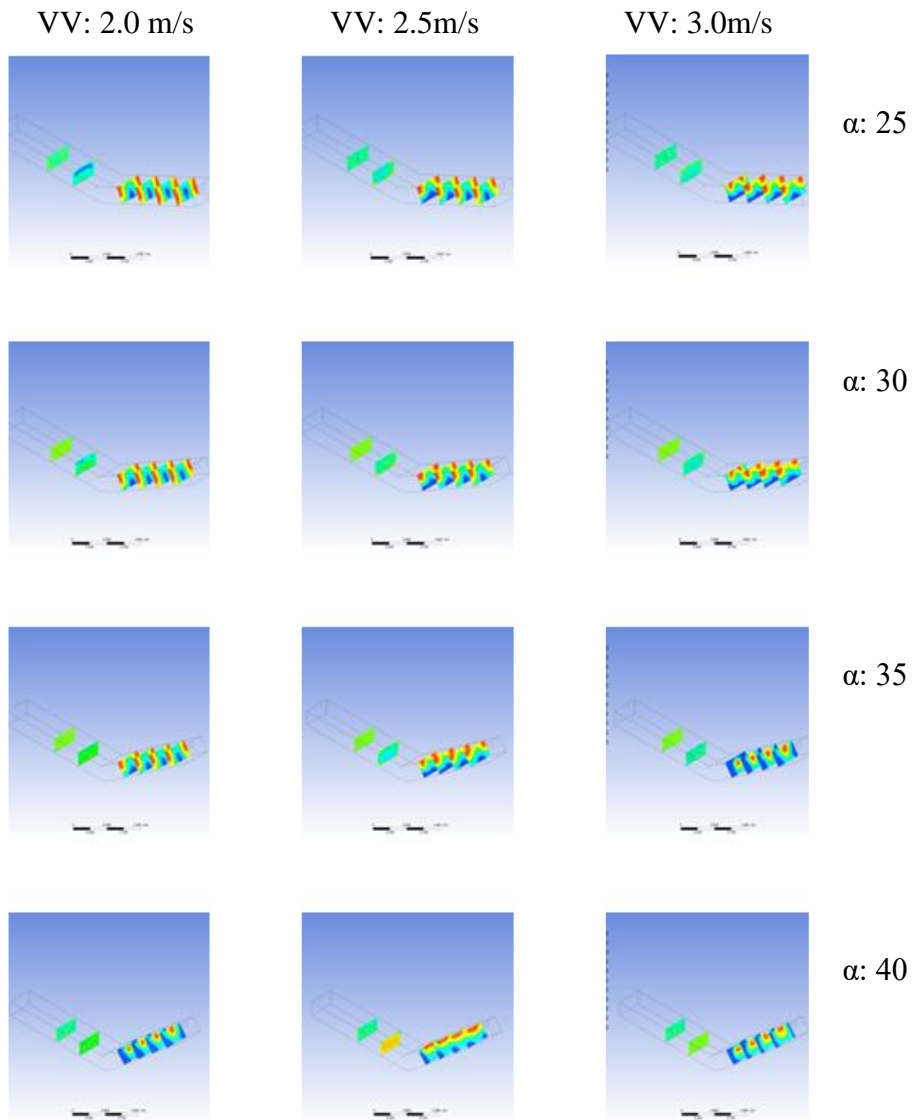


**Figure A.8 Temperature contours for case B**

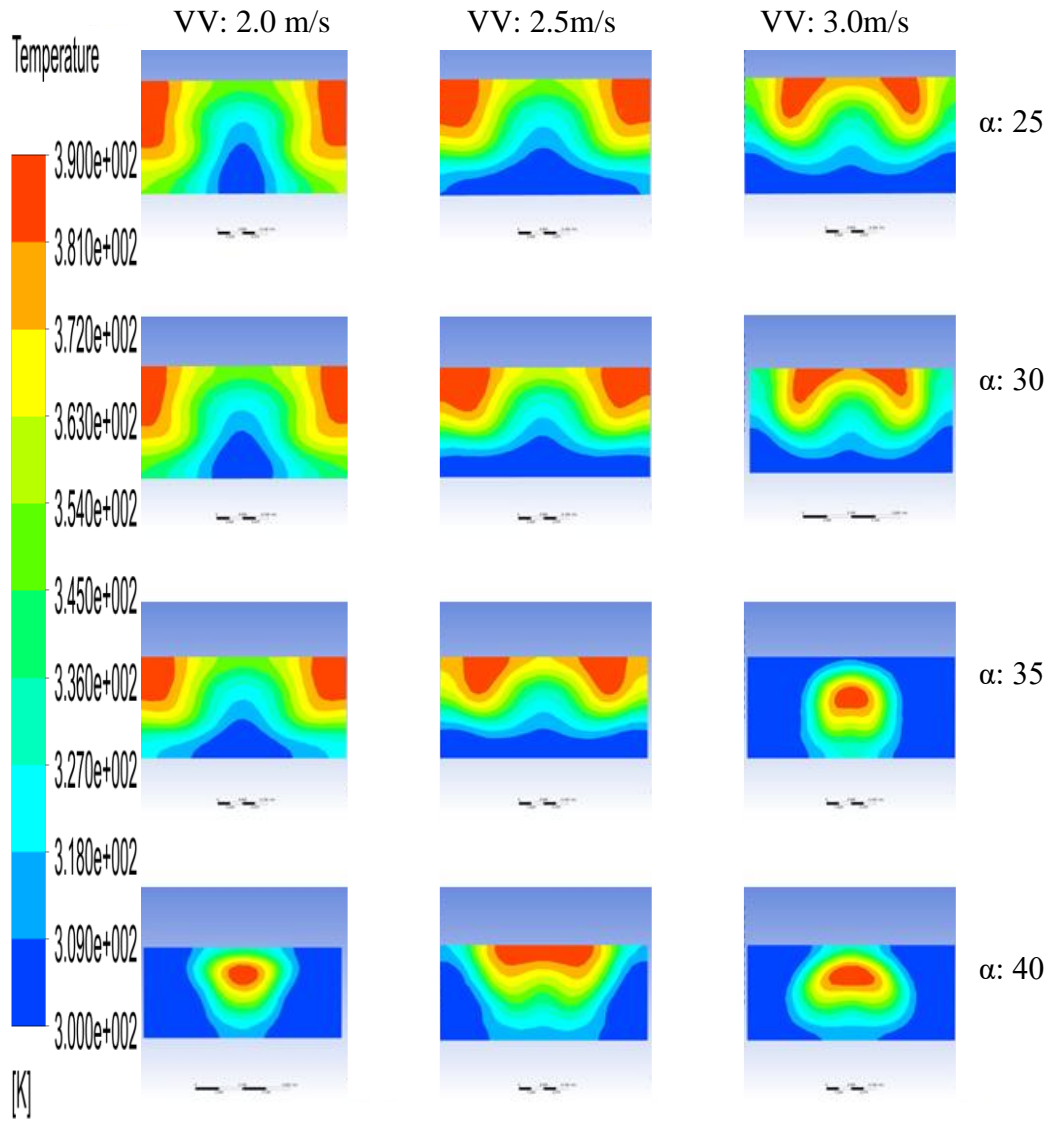


**Figure A.9** Temperature contours on plane incl1 for case B

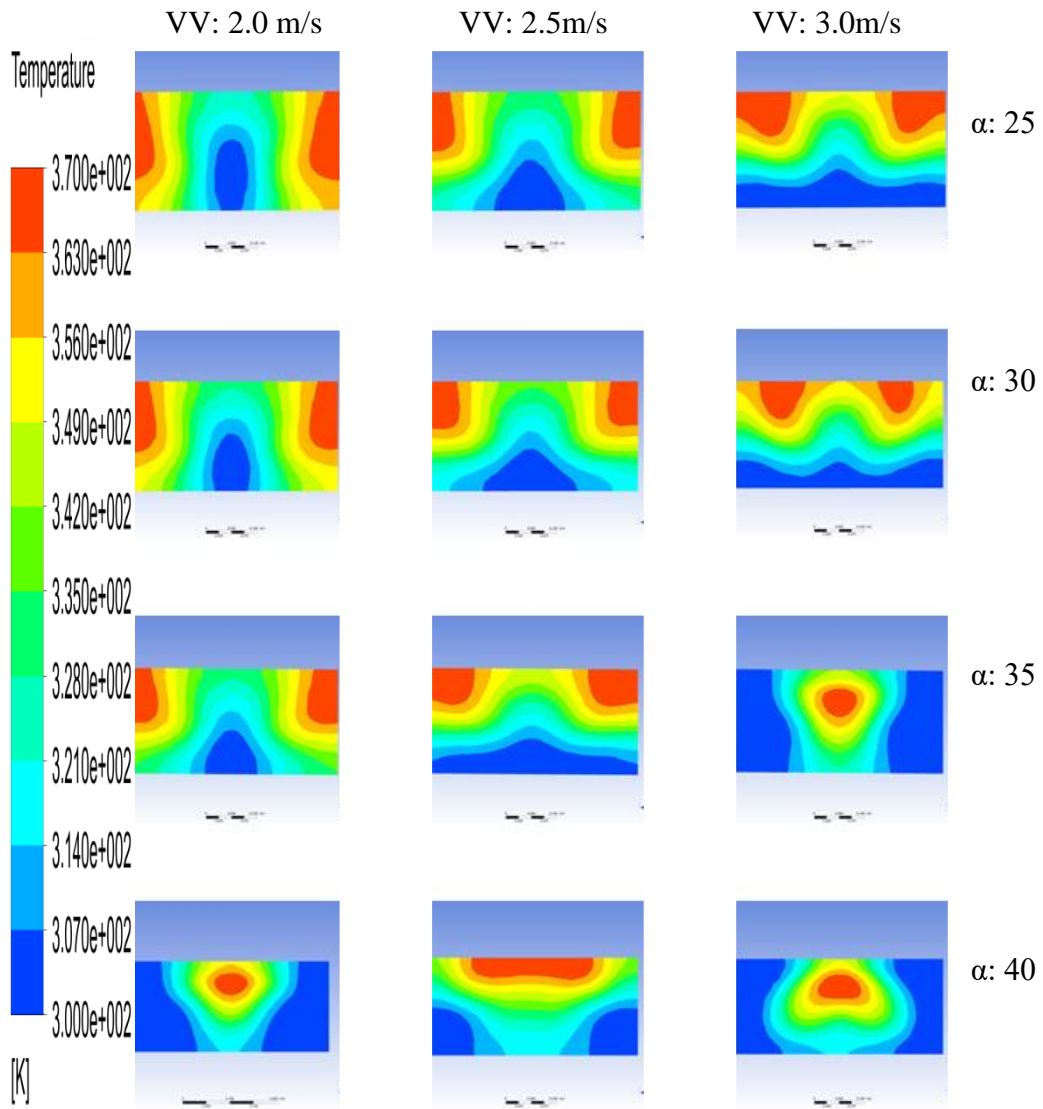


**Figure A.10 Temperature contours on plane inc2 for case B**

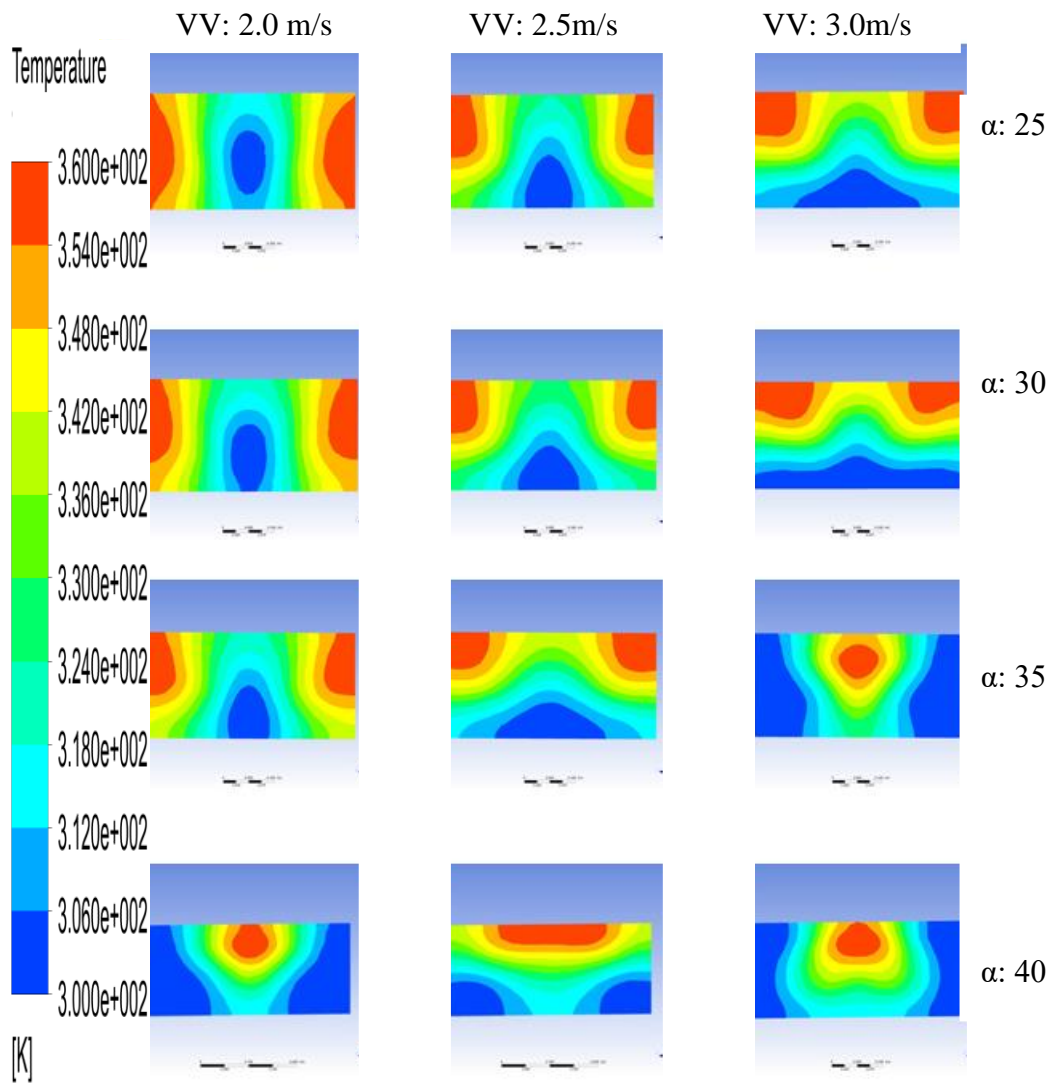


**Figure A.11 Temperature contours on plane inc3 for case B**

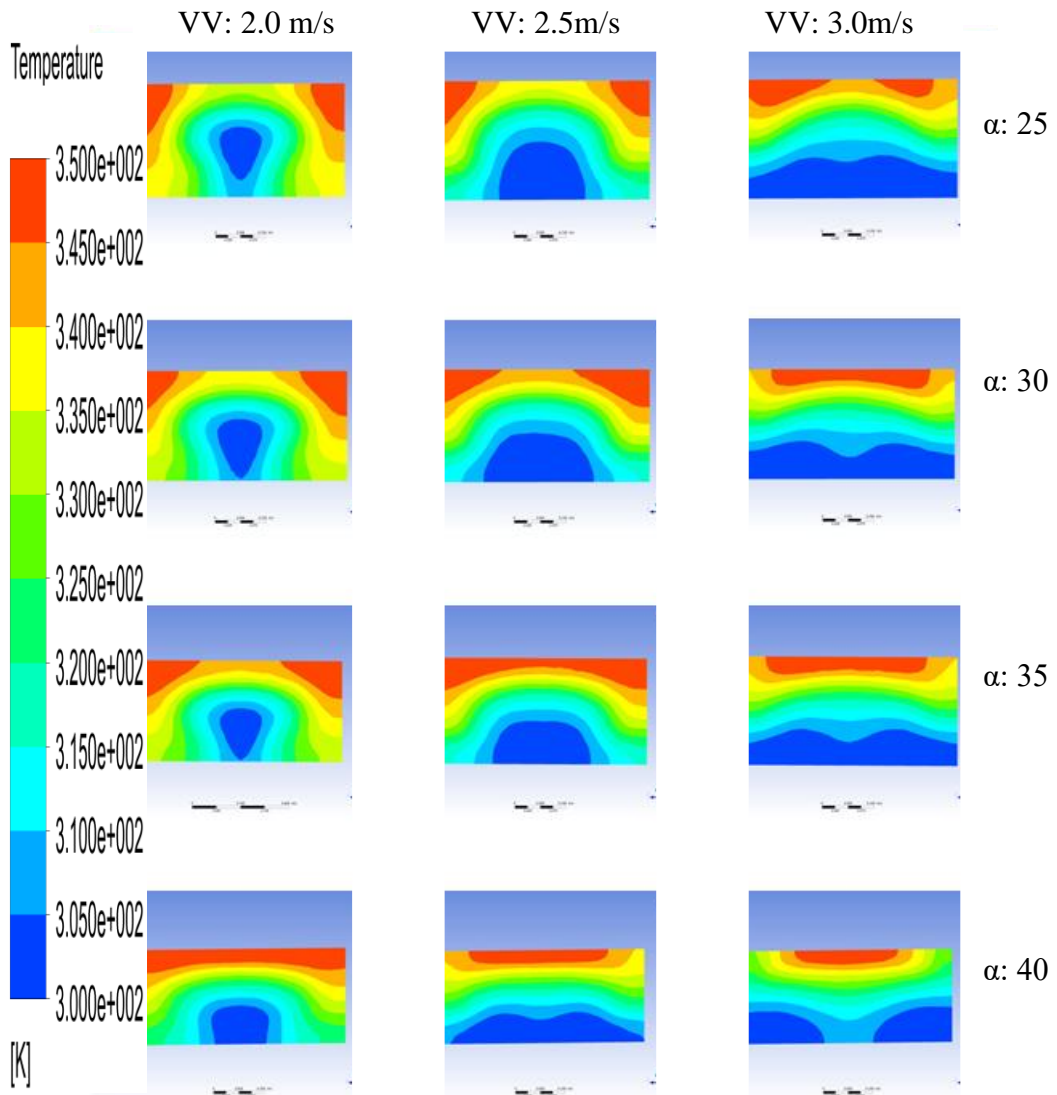


**Figure A.12 Temperature contours on plane inc4 for case B**

## APPENDIX B

### DATA TAKEN IN STUDIES

25° 2.0m/s	horz1 <table border="1" style="width: 100%; border-collapse: collapse;"> <tr><td>148</td><td>42</td><td>144</td></tr> <tr><td>126</td><td></td><td>121</td></tr> </table>	148	42	144	126		121	horz2 <table border="1" style="width: 100%; border-collapse: collapse;"> <tr><td>114</td><td>68</td><td>110</td></tr> <tr><td>146</td><td></td><td>141</td></tr> </table>	114	68	110	146		141	inc1 <table border="1" style="width: 100%; border-collapse: collapse;"> <tr><td>121</td><td>79</td><td>118</td></tr> <tr><td>116</td><td></td><td>113</td></tr> </table>	121	79	118	116		113	inc2 <table border="1" style="width: 100%; border-collapse: collapse;"> <tr><td>120</td><td>92</td><td>117</td></tr> <tr><td>113</td><td></td><td>110</td></tr> </table>	120	92	117	113		110	inc3 <table border="1" style="width: 100%; border-collapse: collapse;"> <tr><td>114</td><td>97</td><td>111</td></tr> <tr><td>112</td><td></td><td>108</td></tr> </table>	114	97	111	112		108	inc4 <table border="1" style="width: 100%; border-collapse: collapse;"> <tr><td>106</td><td>104</td><td>102</td></tr> <tr><td>102</td><td></td><td>99</td></tr> </table>	106	104	102	102		99
148	42	144																																								
126		121																																								
114	68	110																																								
146		141																																								
121	79	118																																								
116		113																																								
120	92	117																																								
113		110																																								
114	97	111																																								
112		108																																								
106	104	102																																								
102		99																																								
25° 2.5m/s	horz1 <table border="1" style="width: 100%; border-collapse: collapse;"> <tr><td>153</td><td>44</td><td>149</td></tr> <tr><td>37</td><td></td><td>33</td></tr> </table>	153	44	149	37		33	horz2 <table border="1" style="width: 100%; border-collapse: collapse;"> <tr><td>106</td><td>43</td><td>103</td></tr> <tr><td>96</td><td></td><td>95</td></tr> </table>	106	43	103	96		95	inc1 <table border="1" style="width: 100%; border-collapse: collapse;"> <tr><td>114</td><td>66</td><td>111</td></tr> <tr><td>91</td><td></td><td>87</td></tr> </table>	114	66	111	91		87	inc2 <table border="1" style="width: 100%; border-collapse: collapse;"> <tr><td>108</td><td>71</td><td>106</td></tr> <tr><td>90</td><td></td><td>89</td></tr> </table>	108	71	106	90		89	inc3 <table border="1" style="width: 100%; border-collapse: collapse;"> <tr><td>103</td><td>84</td><td>102</td></tr> <tr><td>93</td><td></td><td>90</td></tr> </table>	103	84	102	93		90	inc4 <table border="1" style="width: 100%; border-collapse: collapse;"> <tr><td>99</td><td>86</td><td>98</td></tr> <tr><td>92</td><td></td><td>91</td></tr> </table>	99	86	98	92		91
153	44	149																																								
37		33																																								
106	43	103																																								
96		95																																								
114	66	111																																								
91		87																																								
108	71	106																																								
90		89																																								
103	84	102																																								
93		90																																								
99	86	98																																								
92		91																																								
25° 3.0m/s	horz1 <table border="1" style="width: 100%; border-collapse: collapse;"> <tr><td>150</td><td>51</td><td>146</td></tr> <tr><td>28</td><td></td><td>28</td></tr> </table>	150	51	146	28		28	horz2 <table border="1" style="width: 100%; border-collapse: collapse;"> <tr><td>115</td><td>41</td><td>112</td></tr> <tr><td>50</td><td></td><td>48</td></tr> </table>	115	41	112	50		48	inc1 <table border="1" style="width: 100%; border-collapse: collapse;"> <tr><td>108</td><td>54</td><td>106</td></tr> <tr><td>59</td><td></td><td>59</td></tr> </table>	108	54	106	59		59	inc2 <table border="1" style="width: 100%; border-collapse: collapse;"> <tr><td>103</td><td>65</td><td>102</td></tr> <tr><td>55</td><td></td><td>54</td></tr> </table>	103	65	102	55		54	inc3 <table border="1" style="width: 100%; border-collapse: collapse;"> <tr><td>98</td><td>69</td><td>96</td></tr> <tr><td>53</td><td></td><td>53</td></tr> </table>	98	69	96	53		53	inc4 <table border="1" style="width: 100%; border-collapse: collapse;"> <tr><td>93</td><td>73</td><td>90</td></tr> <tr><td>57</td><td></td><td>56</td></tr> </table>	93	73	90	57		56
150	51	146																																								
28		28																																								
115	41	112																																								
50		48																																								
108	54	106																																								
59		59																																								
103	65	102																																								
55		54																																								
98	69	96																																								
53		53																																								
93	73	90																																								
57		56																																								

**Figure B.1 Temperature results of experiments for case A with  $\alpha=25^\circ$**

30° 2.0m/s	horz1 <table border="1" style="width: 100%; border-collapse: collapse;"> <tr><td>142</td><td>44</td><td>139</td></tr> <tr><td>129</td><td></td><td>127</td></tr> </table>	142	44	139	129		127	horz2 <table border="1" style="width: 100%; border-collapse: collapse;"> <tr><td>116</td><td>67</td><td>114</td></tr> <tr><td>152</td><td></td><td>148</td></tr> </table>	116	67	114	152		148	inc1 <table border="1" style="width: 100%; border-collapse: collapse;"> <tr><td>125</td><td>85</td><td>123</td></tr> <tr><td>117</td><td></td><td>115</td></tr> </table>	125	85	123	117		115	inc2 <table border="1" style="width: 100%; border-collapse: collapse;"> <tr><td>122</td><td>93</td><td>120</td></tr> <tr><td>113</td><td></td><td>112</td></tr> </table>	122	93	120	113		112	inc3 <table border="1" style="width: 100%; border-collapse: collapse;"> <tr><td>120</td><td>95</td><td>119</td></tr> <tr><td>110</td><td></td><td>108</td></tr> </table>	120	95	119	110		108	inc4 <table border="1" style="width: 100%; border-collapse: collapse;"> <tr><td>117</td><td>96</td><td>114</td></tr> <tr><td>107</td><td></td><td>107</td></tr> </table>	117	96	114	107		107
142	44	139																																								
129		127																																								
116	67	114																																								
152		148																																								
125	85	123																																								
117		115																																								
122	93	120																																								
113		112																																								
120	95	119																																								
110		108																																								
117	96	114																																								
107		107																																								
30° 2.5m/s	horz1 <table border="1" style="width: 100%; border-collapse: collapse;"> <tr><td>140</td><td>41</td><td>136</td></tr> <tr><td>37</td><td></td><td>37</td></tr> </table>	140	41	136	37		37	horz2 <table border="1" style="width: 100%; border-collapse: collapse;"> <tr><td>102</td><td>42</td><td>100</td></tr> <tr><td>109</td><td></td><td>106</td></tr> </table>	102	42	100	109		106	inc1 <table border="1" style="width: 100%; border-collapse: collapse;"> <tr><td>113</td><td>59</td><td>112</td></tr> <tr><td>98</td><td></td><td>97</td></tr> </table>	113	59	112	98		97	inc2 <table border="1" style="width: 100%; border-collapse: collapse;"> <tr><td>114</td><td>64</td><td>113</td></tr> <tr><td>98</td><td></td><td>96</td></tr> </table>	114	64	113	98		96	inc3 <table border="1" style="width: 100%; border-collapse: collapse;"> <tr><td>108</td><td>69</td><td>106</td></tr> <tr><td>96</td><td></td><td>95</td></tr> </table>	108	69	106	96		95	inc4 <table border="1" style="width: 100%; border-collapse: collapse;"> <tr><td>105</td><td>73</td><td>104</td></tr> <tr><td>95</td><td></td><td>94</td></tr> </table>	105	73	104	95		94
140	41	136																																								
37		37																																								
102	42	100																																								
109		106																																								
113	59	112																																								
98		97																																								
114	64	113																																								
98		96																																								
108	69	106																																								
96		95																																								
105	73	104																																								
95		94																																								
30° 3.0m/s	horz1 <table border="1" style="width: 100%; border-collapse: collapse;"> <tr><td>157</td><td>44</td><td>153</td></tr> <tr><td>28</td><td></td><td>28</td></tr> </table>	157	44	153	28		28	horz2 <table border="1" style="width: 100%; border-collapse: collapse;"> <tr><td>96</td><td>39</td><td>94</td></tr> <tr><td>56</td><td></td><td>55</td></tr> </table>	96	39	94	56		55	inc1 <table border="1" style="width: 100%; border-collapse: collapse;"> <tr><td>101</td><td>49</td><td>99</td></tr> <tr><td>76</td><td></td><td>76</td></tr> </table>	101	49	99	76		76	inc2 <table border="1" style="width: 100%; border-collapse: collapse;"> <tr><td>95</td><td>54</td><td>93</td></tr> <tr><td>72</td><td></td><td>70</td></tr> </table>	95	54	93	72		70	inc3 <table border="1" style="width: 100%; border-collapse: collapse;"> <tr><td>92</td><td>56</td><td>91</td></tr> <tr><td>70</td><td></td><td>68</td></tr> </table>	92	56	91	70		68	inc4 <table border="1" style="width: 100%; border-collapse: collapse;"> <tr><td>86</td><td>63</td><td>85</td></tr> <tr><td>68</td><td></td><td>66</td></tr> </table>	86	63	85	68		66
157	44	153																																								
28		28																																								
96	39	94																																								
56		55																																								
101	49	99																																								
76		76																																								
95	54	93																																								
72		70																																								
92	56	91																																								
70		68																																								
86	63	85																																								
68		66																																								

**Figure B.2 Temperature results of experiments for case A with  $\alpha=30^\circ$**

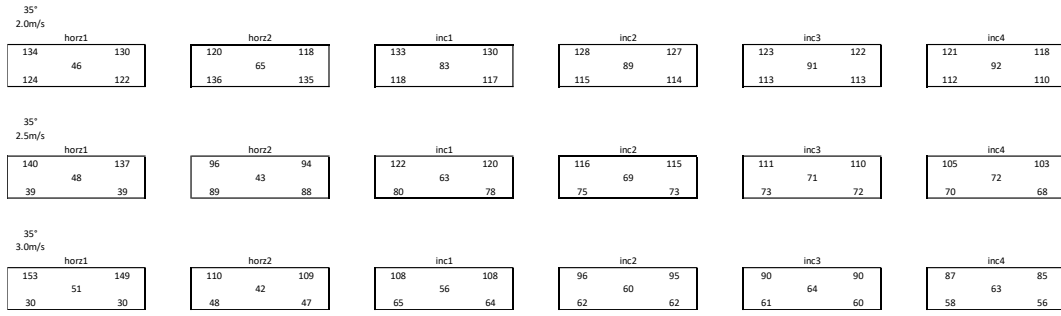


**Figure B.3 Temperature results of experiments for case A with  $\alpha=35^\circ$**

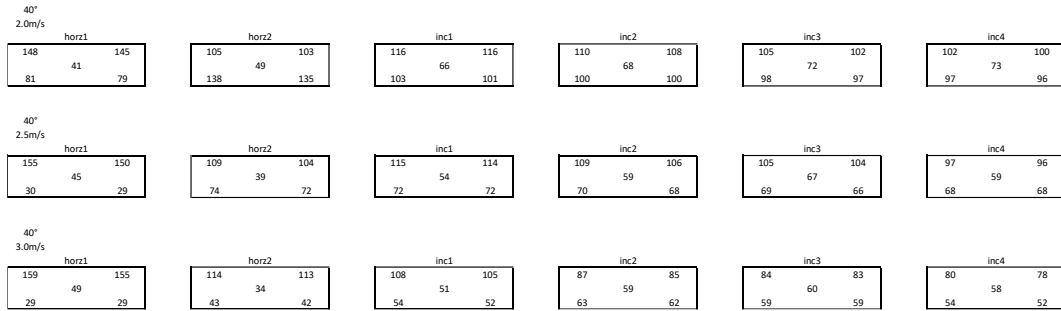


**Figure B.4 Temperature results of experiments for case A with  $\alpha=40^\circ$**

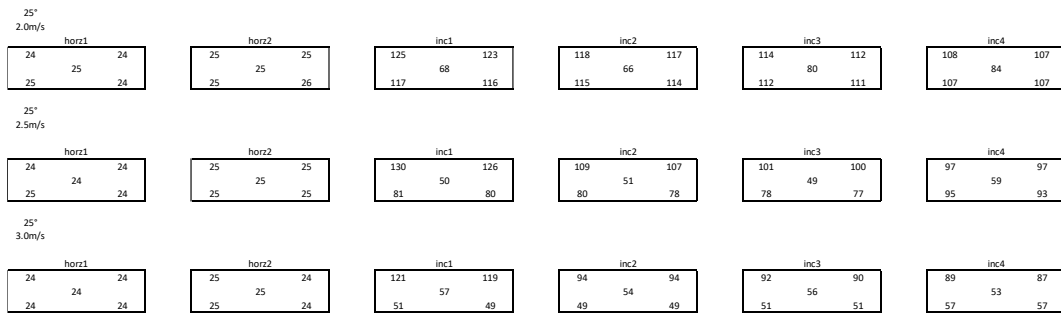


**Figure B.5 Temperature results of experiments for case B with  $\alpha=25^\circ$**



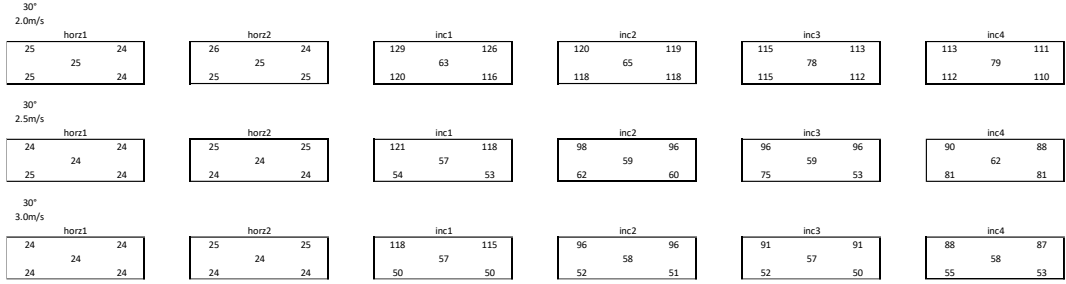


**Figure B.6 Temperature results of experiments for case B with  $\alpha=30^\circ$**

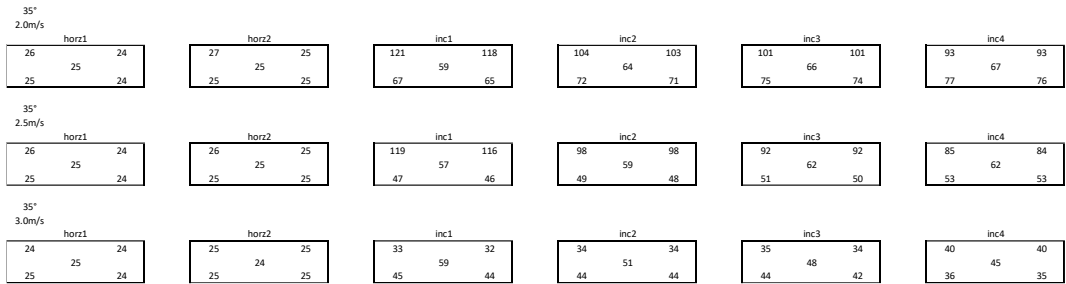


**Figure B.7 Temperature results of experiments for case B with  $\alpha=35^\circ$**

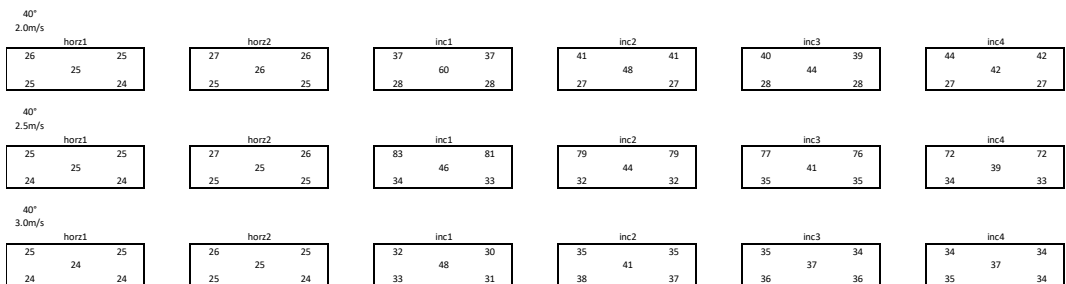


**Figure B.8 Temperature results of experiments for case B with  $\alpha=40^\circ$**

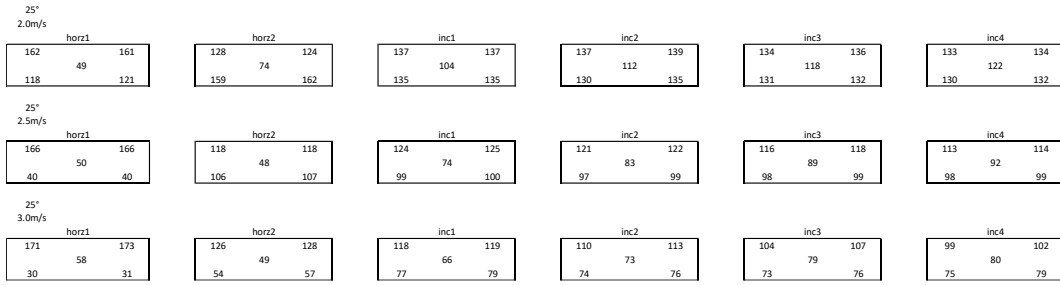


**Figure B.9 Temperature results of numerical work for case A with  $\alpha=25^\circ$**

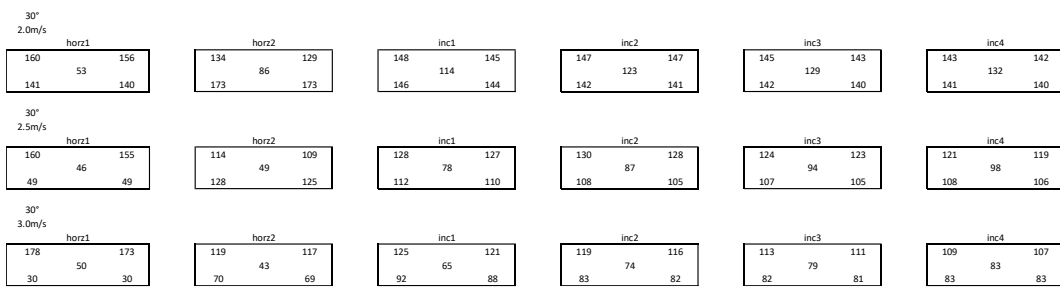


**Figure B.10 Temperature results of numerical work for case A with  $\alpha=30^\circ$**

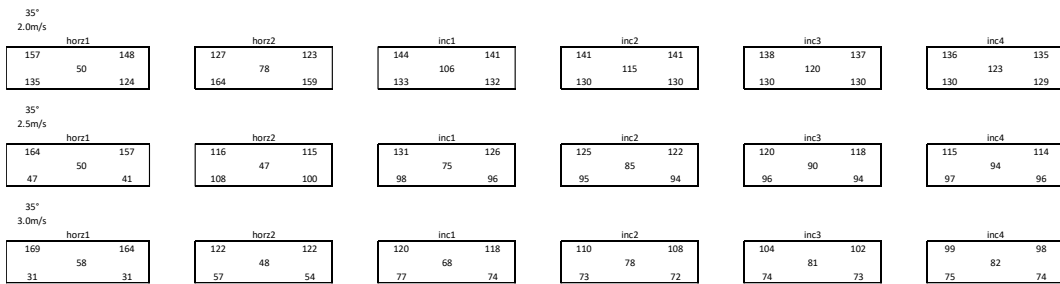


**Figure B.11 Temperature results of numerical work for case A with  $\alpha=35^\circ$**

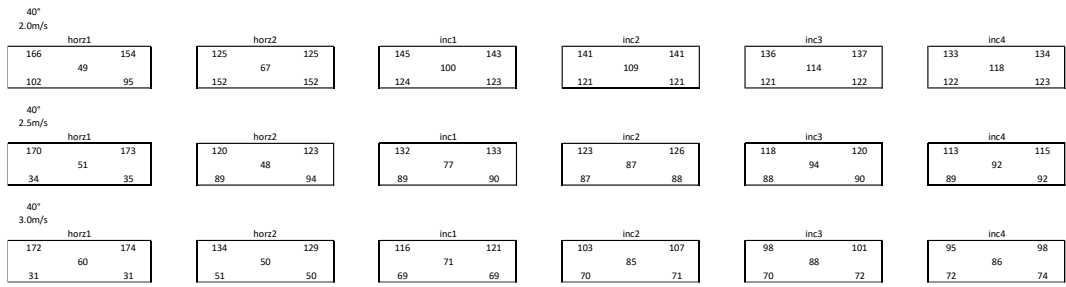


**Figure B.12 Temperature results of numerical work for case A with  $\alpha=40^\circ$**

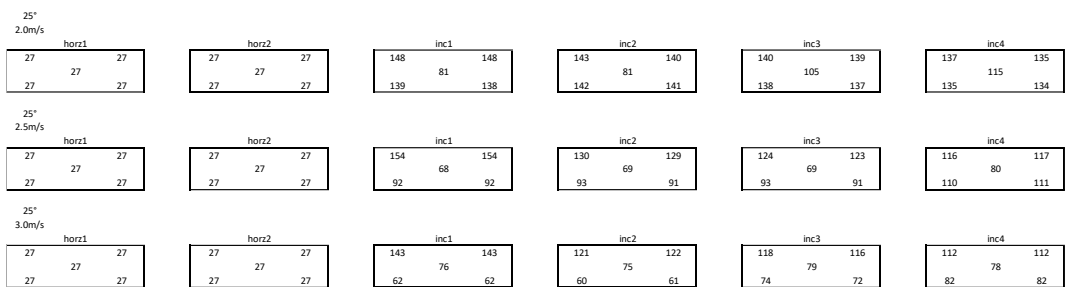


**Figure B.13 Temperature results of numerical work for case B with  $\alpha=25^\circ$**

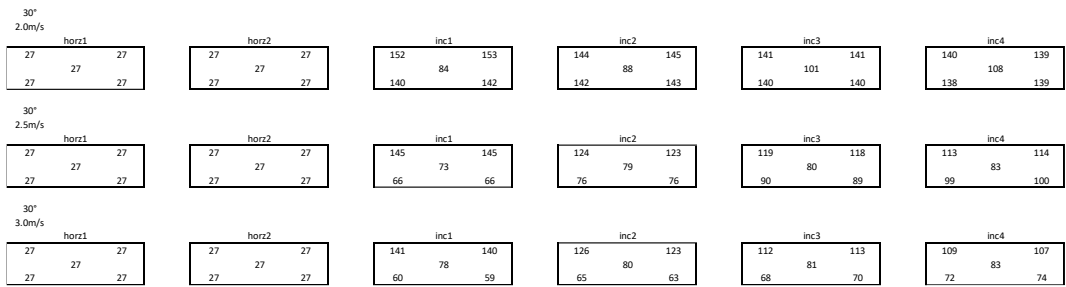


**Figure B.14 Temperature results of numerical work for case B with  $\alpha=30^\circ$**

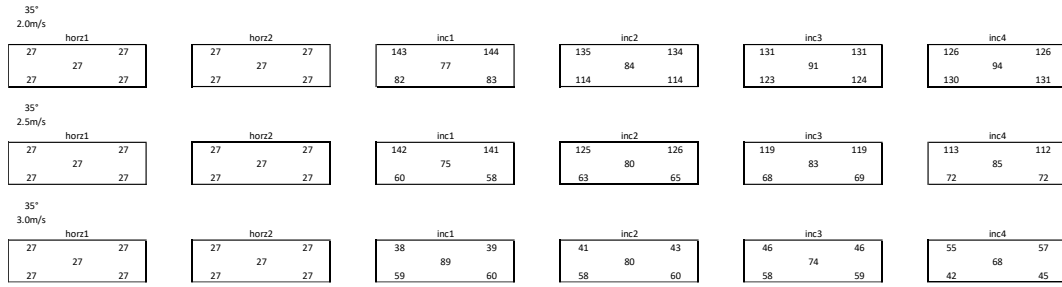


**Figure B.15 Temperature results of numerical work for case B with  $\alpha=35^\circ$**

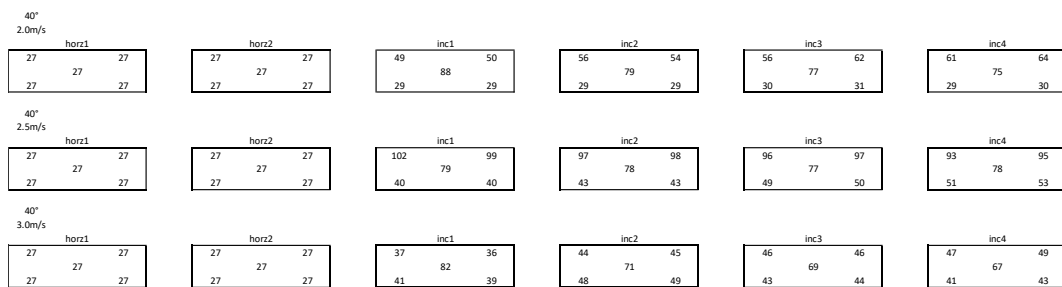


**Figure B.16 Temperature results of numerical work for case B with  $\alpha=40^\circ$**

## APPENDIX C

### BOUNDARY CONDITIONS AND CFD SETTINGS

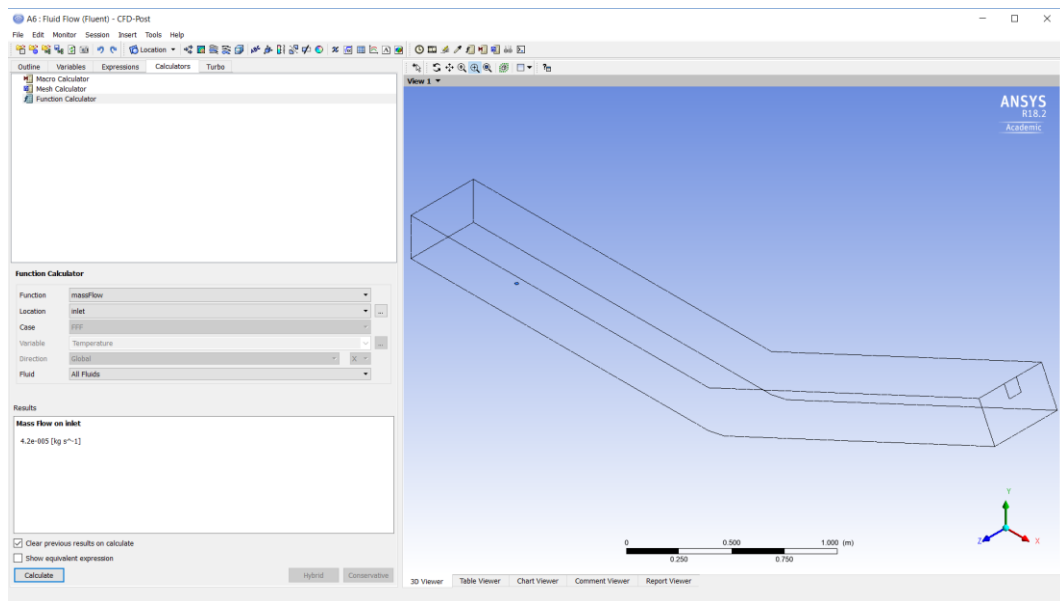
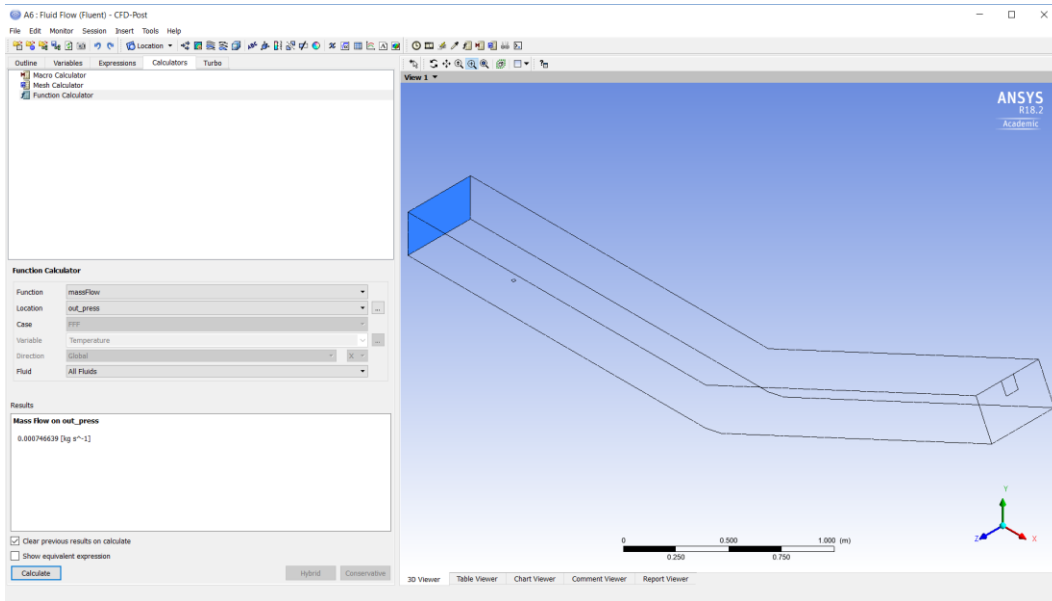
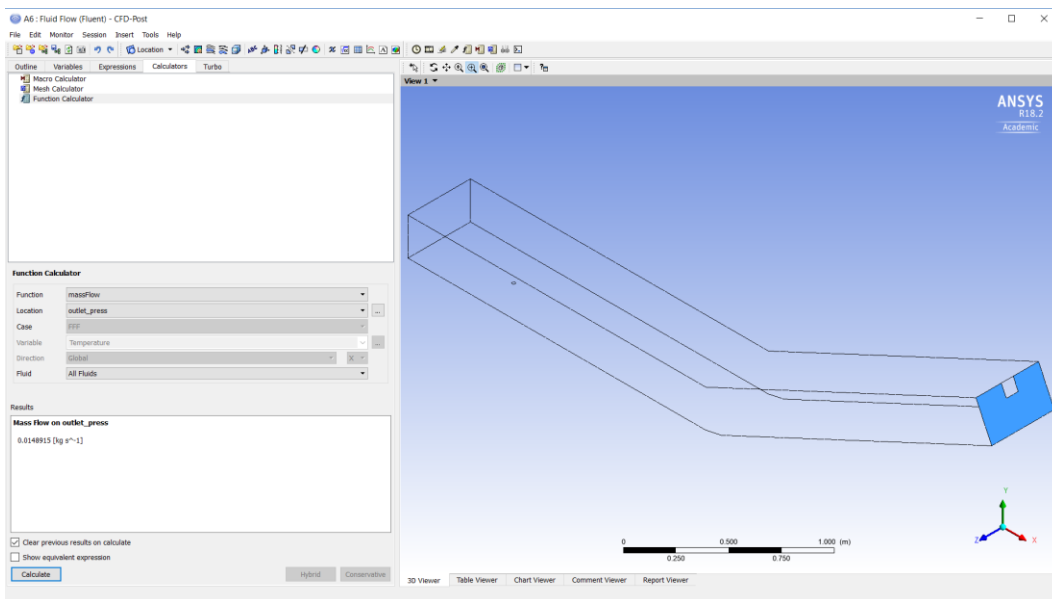


Figure C.1 Mass flow rate into the system through inlet



**Figure C.2 Mass flow rate into the system through the beginning of the horizontal part**



**Figure C.3 Mass flow rate into the system through the end of the inclined part**

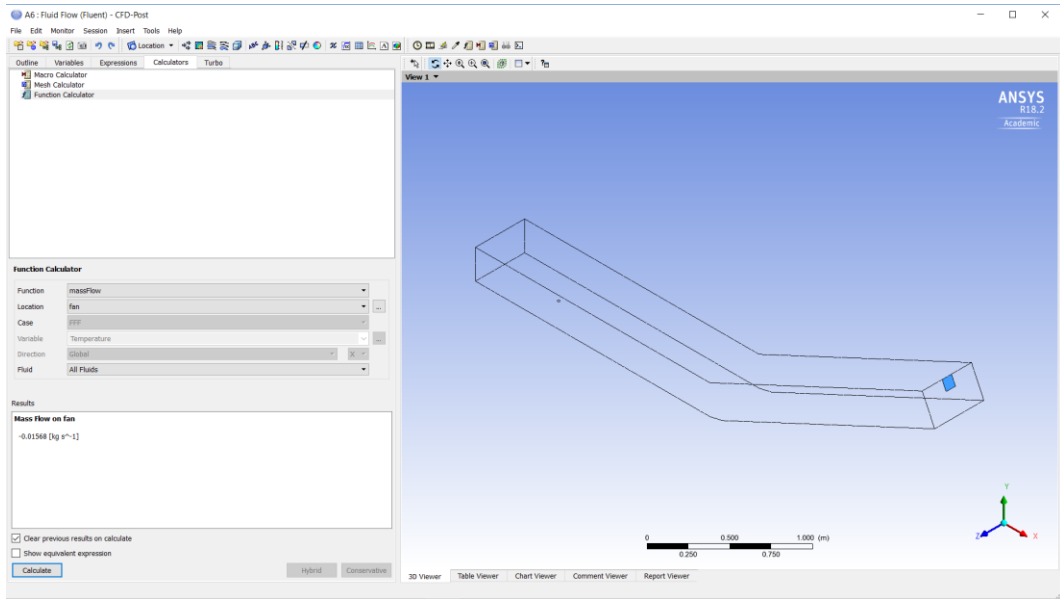


**Figure C.4 Mass flow rate leaving the system through the fan**

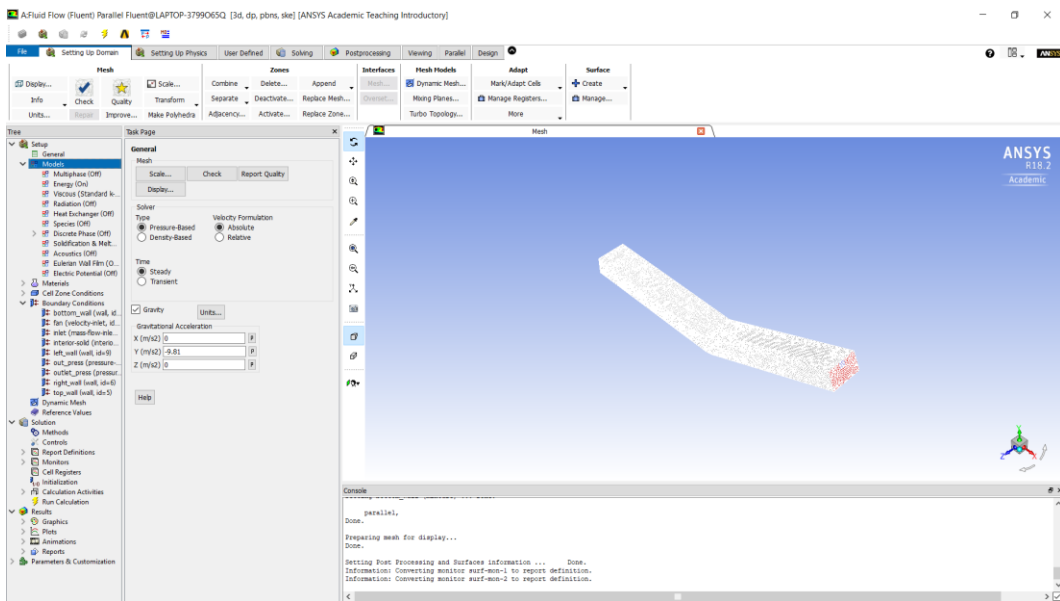


**Figure C.5 General setup for numerical analyses**

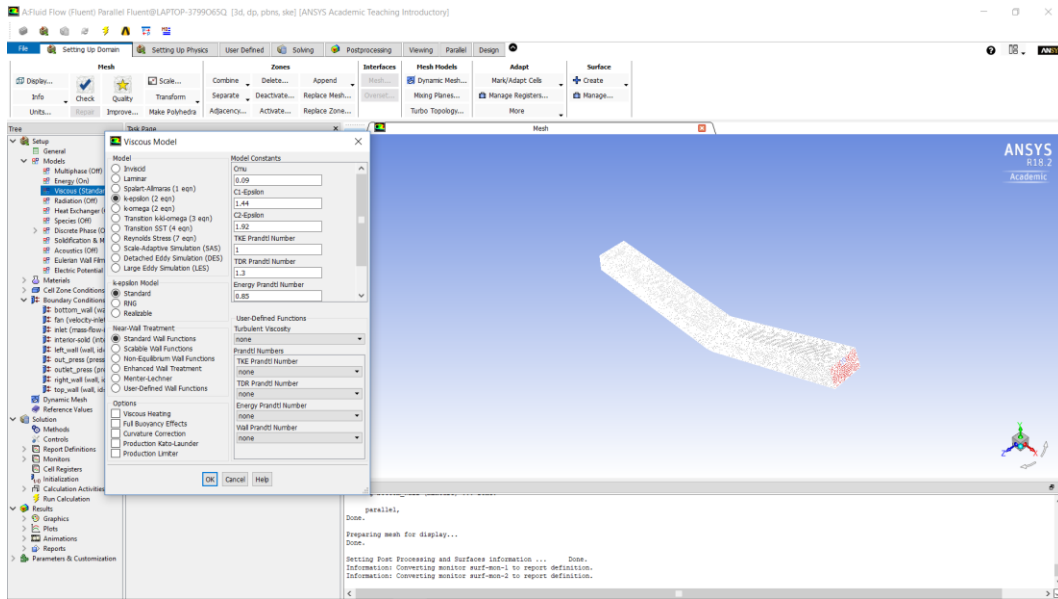


**Figure C.6 Turbulent model for numerical analyses**

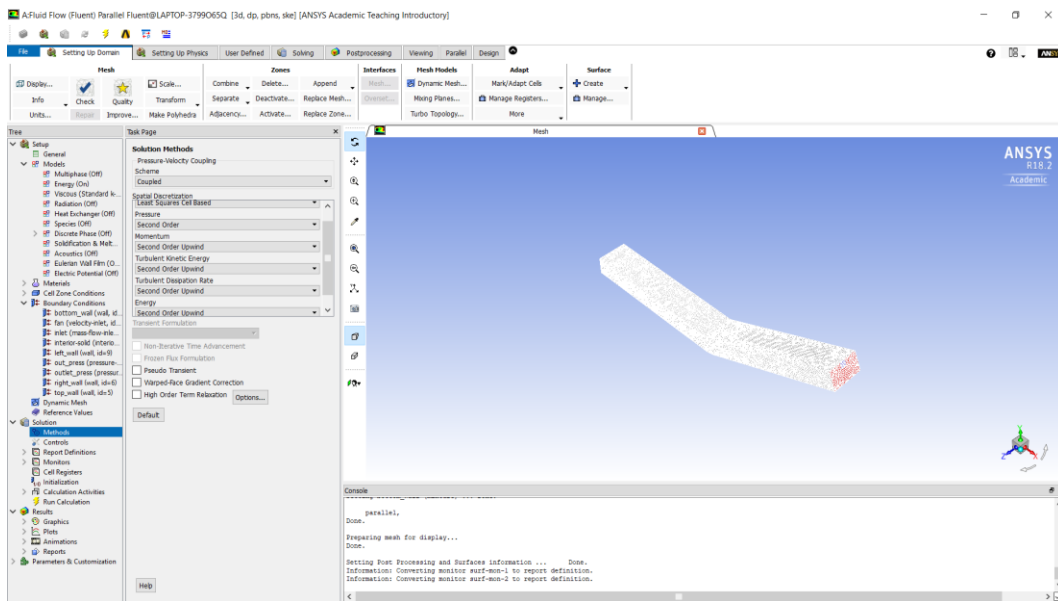


**Figure C.7 Solution methods for numerical analyses**